

**Flow Dynamics and Management Options
in a Stressed Carbonate Aquifer System,
The Western Aquifer Basin,
Palestine**

Dissertation
zur Erlangung des Doktorgrades
der Mathematisch-Naturwissenschaftlichen Fakultäten
der Georg-August-Universität zu Göttingen

vorgelegt von

Muath Jamil Abusaada

aus Illar-Tulkarem

Göttingen 2011

D 7

Referentin/Referent: **Prof. Dr. Martin Sauter**

Korreferentin/Korreferent: **Prof. Dr. Thomas Ptak**

Tag der mündlichen Prüfung: **27-06-2011**

TABLE OF CONTENTS

ACKNOWLEDGEMENT	7
ABSTRACT	9
ZUSAMMENFASSUNG	11
الخلاصة	13
LIST OF FIGURES	15
LIST OF TABLES	19
LIST OF ABBREVIATIONS	21
CHAPTER 1: INTRODUCTION TO THE WESTERN AQUIFER BASIN	25
1.1 Introduction.....	25
1.2 Trans-boundary Groundwater Resources.....	26
1.2.1 Western Aquifer Basin, the Case Study.....	26
1.2.2 Eastern Aquifer Basin.....	32
1.2.3 North-Eastern Aquifer Basin.....	32
1.3 Objective of the Study.....	33
1.4 Methodology.....	35
1.5 Previous Studies.....	36
1.6 Gaps in Previous Studies and Uniqueness of this Study.....	37
1.7 Data Acquisition.....	38
1.8 Beneficiaries of the Study.....	39
CHAPTER 2: CONCEPTUAL REVIEW OF THE WAB	43
2.1 Introduction.....	43
2.2 Geology and Hydrogeology of the WAB.....	44
2.3 Boundaries.....	47
2.3.1 Northern Boundary.....	47
2.3.2 Eastern Boundary.....	48
2.3.3 Southern Boundary.....	49
2.3.4 Western Boundary.....	51

2.4	Intra-aquifer Hydrological Connections	51
2.5	Natural Aquifer Outlets	53
2.6	Pumping and Injection	54
2.7	Recharge	56
2.8	Water Level.....	57
2.9	Flow Directions.....	57
2.10	Physical Properties.....	59
2.11	Salinity and Salinization Process.....	59
2.11.1	Northern Area	60
2.11.2	Central Area	62
2.11.3	Southern Area	64
CHAPTER 3: RAINFALL ANALYSIS AND ESTIMATION OF GROUNDWATER		
RECHARGE.....		69
3.1	Introduction.....	69
3.2	The previous recharge estimation technique	70
3.3	Rainfall over the WAB	71
3.4	Recharge Estimation Technique	75
3.5	Inflow and Outflow.....	78
3.6	Storage Coefficient	79
3.7	Recharge Equation.....	84
3.8	Annual Recharge versus Monthly Rainfall.....	86
3.9	Conclusion of the Recharge Estimation.....	91
CHAPTER 4: GROUNDWATER FLOW DYNAMICS UNDER PRE-DEVELOPMENT		
CONDITIONS		97
4.1	Introduction.....	97
4.2	Numerical Model Software	98
4.3	Model Geometry.....	98
4.4	Recharge	102
4.5	Water level	105
4.6	Natural Outflow of the WAB.....	107
4.7	Model Calibration	107
4.8	Hydraulic Properties of the WAB	111

4.9	Sensitivity Analysis	112
4.10	Conclusion of the pre-development model	114
CHAPTER 5: GROUNDWATER FLOW DYNAMICS UNDER TRANSIENT		
CONDITIONS		
		119
5.1	Introduction	119
5.2	The WAB outflows	120
5.3	The WAB Inflows	120
5.3.1	Natural Recharge	121
5.3.2	Artificial recharge and Sea Water Intrusion	122
5.4	Water level	123
5.5	Physical properties of the WAB	124
5.6	Calibration Methodology	124
5.7	Model Validation	125
5.8	Model Simulation Results	126
5.9	Conclusion Of The Transient Flow Model	131
CHAPTER 6: SUSTAINABILITY OF THE WAB UNDER DIFFERENT SCENARIOS		
		141
6.1	Introduction	141
6.2	Water Evaluation and Planning System (WEAP)	141
6.3	WEAP-MODFLOW Coupling	143
6.4	Scenarios Development	144
6.4.1	Climatic Scenarios	144
6.4.1.1	Normal Rainfall Scenarios (NRS)	145
6.4.1.2	Reduced Rainfall Scenarios (RRS)	146
6.4.2	Pumping Scenarios	147
6.4.2.1	Moving Average Scenarios	147
6.4.2.2	Aquifer Yield Scenarios	148
6.4.2.3	Related Pumping Scenarios	148
6.4.3	Management Scenario	149
6.5	Scenarios Evaluation and Analysis	151
6.5.1	Results under Normal Rainfall Scenario	154
6.5.2	Results under Reduction Rainfall Scenario	158
6.5.3	Results under Management Scenario	159

6.6	Conclusions.....	160
CHAPTER 7: SUMMARY AND FUTURE OUTLOOK.....		165
7.1	Introduction.....	165
7.2	Rainfall-Recharge Variations.....	166
7.3	The WAB responses under inflow and Outflow variations	167
7.4	Sustainability of the WAb under different Future Management Options	169
7.5	Suggestions for Further Research.....	169
LIST OF REFERENCES		173

ACKNOWLEDGEMENT

First and foremost, I would like to express my deepest thanks and gratitude to my supervisor Prof. Dr. Martin Sauter, Head of the Applied Geology Department, University of Gottingen. It has been an honour to be one of his Ph.D. students. I am especially grateful for his guidance, support, fruitful suggestions, motivation and his independence oriented supervision that has given me more insight into the field of scientific research.

I am grateful to the staff, colleagues and friends of the Department of Applied Geology in Gottingen University, Prof. Dr. Thomas Ptak, Prof. Dr. Ekkehard Holzbecher, Prof. Dr. Chicgoua Noubactep, Dr. Tobias Geyer, Dr. Tobias Licha, Dr. Ing. Bernd Rusteberg, Dr. William Alkhoury, Dipl. Geol. Torsten Lange, Eng. Mohammad Aziz Rahman, Dipl. Geol. Sebastian Schmidt, Dipl. Geol. Joanna Doummar, Ms Beka Peters Kewitz and Eng. Hartmut Düker. I am deeply indebted to them for their inspiring guidance, time-to-time discussions, constant encouragement and generous support throughout this research work.

Special thanks and gratitude to my brother and friend Dr. William Alkhoury, who always provided me with an extensive support during my stay in Germany, solving administrative problems, fruitful suggestions, motivations and always encouraging me with his brilliant smile.

I wish to express my gratitude to my beloved parents for their continuous support and encouragement. My deepest gratitude and love for their dedication and the many years of support during my undergraduate studies that provided the foundation for this work. My gratitude is also extended to my brothers and sisters who stood by me with their love and support.

No words in all world's languages can express my deepest thanks to my wife Fatima and my children Lujain and Hazem for their understanding and love during the past years. They have lost a lot due to my research abroad. Without their encouragement and understanding it would have been impossible for me to finish this work.

My thanks and appreciation also goes to Prof. Dr. Katja Tielborger, Dr. Cornelia Claus, Mr. Christopher Bonsi, Ms. Barbara Jaeger and Ms. Daniela Schloz from University of Tubingen and coordination team of GLOWA Jordan River project. Dr. Klaus Schelkes, Dr. Jobst Massmann, Dr. Johannes Wolfer and Dr. Mathias Toll from Federal Institute for Geosciences and Natural Resources (BGR). Dr. Anan Jayyousi from An-Najah National University. Eng. Deeb Abdelghafour, Eng. Adel Yasin from Palestinian Water Authority. Eng. Issam Nofel from Ministry of Agriculture, Eng. Yousef Abuasad, Eng. Isam Isa and Eng. Mohammed Abu Baker from Palestinian Metreological Department and Mr. Clemens Messerschmid, Mr. Markus Huber and Mr. Nidal Attallah for providing support, data and useful suggestions.

I would also like to thank the Palestinian Hydrology Group (PHG) for their support and inspiration for giving me the opportunity to persist my studies. Special thanks to Eng. Subha Ghannam for her grate help in revising the English of my thesis and for her grate suggestions for improvement my work.

Last and not least, I would like to thank the management board of GLOWA Jordan River (III), University of Tubingen, for their financial and administrative supports. This project is part of a larger research initiative launched by the German Federal Ministry of Education and Research under the title “Global Change in the Hydrological Cycle”.

Muath Abu Sadah

ABSTRACT

Sustainable management of trans-boundary groundwater aquifers is usually difficult due to the complexity of natural and man-made systems. Therefore, sustainable management of trans-boundary water resources is urgently needed. The Western Aquifer Basin (WAB), in the West Bank and Israel, was depicted as a case study. The aquifer inflow is dominated by the rainfall over the replenishment areas with an estimated annual average 373 Million m^3/yr during the period 1951-2006. The analysis of the recharge-rainfall relation confirmed that the annual recharge volumes are directly correlated to the monthly rainfall, where the highest recharge to rainfall ratio occurred whenever the majority of the annual rainfall comes during November, December, January and February. Accordingly, an empirical equation was developed which relates the annual recharge with monthly amounts of rainfall over the replenishment areas of the aquifer. The annual recharge values were then spatially and monthly distributed based on the distribution of rainfall, land use, aquifer geometry and outcropping formations.

The WAB, an area extending over 6250 km^2 , was simulated by a three-layer model using MODFLOW-2000. The model was calibrated during the period 1951-2000 and validated during 2000-2007 in monthly time steps. As a result, the model provides significant information about the aquifer's physical properties, flow dynamics, and aquifer water balance. The water balance shows that an average of 62% of the natural recharge directly replenishes the upper sub-aquifer and 11% of the total aquifer outflow flows from the lower towards the upper sub-aquifer.

This transient flow model of the WAB was extended in time, to 2034/2035, in order to evaluate the impact of a combination of different rainfall and pumping scenarios. The results showed a comparison between different scenarios in both water levels and springs' discharges under different climate and pumping conditions. Accordingly two pumping scenarios were recommended to maintain the water level and the springs' ability to continue discharging. These scenarios are (1) pumping 85% of the historical aquifer yield under the no change in rainfall scenario (i.e. 310 Mm^3/yr) and (2) 85% of the 7 year moving average of the aquifer recharge (254 Mm^3/yr) under the possible reduction in rainfall as expected by regional climate model.

ZUSAMMENFASSUNG: GRUNDWASSERDYNAMIK UND OPTIONEN ZUR BEWIRTSCHAFTUNG DES BEANSPRUCHTEN KARBONAT-AQUIFER-SYSTEMS DES WESTERN-AQUIFER-BASINS, PALÄSTINA

Die nachhaltige Bewirtschaftung von grenzüberschreitenden Grundwasserleitern ist üblicherweise schwierig. Diese Schwierigkeiten resultieren aus der Komplexität von natürlichen und anthropogenen Faktoren. Somit ist in jedem Einzelfall die Erarbeitung eines Konzepts erforderlich. In dieser Arbeit wurde das Westliche Aquifer Becken (Western Aquifer Basin - WAB) zwischen West Bank und Israel, welches sich über 6250 km² erstreckt, näher untersucht. Die Grundwasserneubildung erfolgt hauptsächlich über die Infiltration von Niederschlagswasser in den Ausstrichbereichen des Grundwasserleiters. Schätzungsweise betrug die jährliche durchschnittliche Grundwasserneubildung 373 Million m³ zwischen 1951 und 2006. Der Aquifer wird natürlich durch zwei große Quellen drainiert. Jedoch wird gegenwärtig der Großteil des Wassers durch einige hundert Pumpbrunnen entnommen. Die Analyse des Zusammenhanges von Grundwasserneubildung zu Niederschlagsmenge bestätigte, dass die jährliche Grundwasserneubildungsrate hoch ist, wenn der Großteil des jährlichen Niederschlages in den Monaten November, Dezember, Januar und Februar erfolgt. Daher wurde eine empirische Gleichung entwickelt, welche die jährliche Grundwasserneubildung aus den monatlichen Niederschlagsmenge für das Neubildungsgebiet errechnet. Die jährlichen Neubildungsmengen wurden dann dem Neubildungsgebiet räumlich und zeitlich (monatlich) verteilt zugewiesen. Die Zuweisung basierte auf der Verteilung der Faktoren: Niederschlag, Landnutzung, Geometrie der Grundwasserleiter und Ausstrichbereiche.

Das Westliche Aquifer Becken wurde mit einem 3-Schicht-Model mit dem Programm MODFLOW-2000 simuliert. Zur Modellkalibrierung diente der Zeitraum 1951-2000. Das Modell wurde mit Daten aus dem Zeitraum 2000-2007 in monatlichem Schritt validiert. Das Modell liefert nützliche Informationen über die physikalischen Eigenschaften des Aquifers, die Fließdynamik und die Wasserbilanz. Die Wasserbilanzierung zeigt, dass im Mittel 62 % der natürlichen Grundwasserneubildung im oberen Sub-Aquifer erfolgt und 11 % des gesamten Aquiferabflusses vom unteren zum oberen Sub-Aquifer fließen.

Das transiente Strömungsmodell für das Westliche Aquifer Becken wurde zeitlich bis zum Jahr 2035 ausgedehnt. Ziel war die Evaluierung des Zusammenspiels verschiedener Niederschlags- und Pumpszenarien. Als Ergebnis werden zwei Pumpszenarien vorgeschlagen, welche zu keiner weiteren Wasserspiegelabsenkung führen und einen Quellausfluss sicherstellen: (i) Abpumpen von 85 % des Grundwasserdargebots bei gleichbleibender Niederschlagsmenge (Grundwasserneubildung im Mittel ca. $310 \text{ Mm}^3/\text{Jahr}$) und (ii) Abpumpen von 85 % der erwarteten Grundwasserneubildung (ca. $254 \text{ Mm}^3/\text{Jahr}$) bei Rückgang der Niederschlagsmenge gemäß der Vorhersagen der regionalen Klimamodelle.

الخلاصة

تعتبر المياه الجوفية من أهم مصادر المياه العذبة في الطبيعة. لذلك إدارة هذه المصادر تعتبر ضرورية من أجل الحفاظ على ديمومتها للأجيال المتعاقبة. وللتحديد فإن الإدارة المستدامة للاحواض المائية الجوفية المشتركة بين دولين أو أكثر تعتبر أكثر تعقيداً. وذلك يعود إلى الطبيعة الهيدروجيولوجية التي غالباً ما تكون معقدة بالإضافة إلى الممارسات التي يقوم بها الأطراف المشتركة بهذه الاحواض من حيث الاستخدام أو التسبب في التلوث. لهذا، فإن الإدارة المستدامة لمثل هذه الاحواض تصبح يوماً بعد يوم أكثر إلحاحاً وضروره. تتناول هذه الدراسة الحوض المائي الجوفي الغربي الذي يشترك باستخدامه كل من السلطة الفلسطينية وإسرائيل. يتغذى هذا الحوض بشكل رئيسي من مياه الأمطار التي تسقط على السفوح الغربية لجبال الضفة الغربية. حيث يقدر معدل هذه التغذية بـ 373 مليون م³/سنوياً حسب التقديرات من عام 1951 وحتى 2007. كما وأكدت هذه الدراسة أن معدل التغذية يعتمد بشكل أساسي على كميات المطر السنوية وتوزيعها الشهري، حيث يزداد معدل التغذية للحوض عندما تسقط معظم الأمطار خلال الشهور المطرية: تشرين الثاني، كانون الأول، كانون الثاني وشباط. كما تزداد التغذية كلما أخذ التوزيع الشهري للأمطار السنوية شكل منحني التوزيع الطبيعي. بناءً على ذلك فقد تم تطوير معادله رياضية للتقدير كمية التغذية السنوية للحوض بأعطامها الكميات الشهرية للأمطار خلال الشهور المذكوره سابقاً. كما وتم تطوير الليات للتوزيع الشهري والجغرافي للتغذية السنوية بأعطام كل من التوزيع الجغرافي للأمطار السنوية، استخدام الأراضي، الميلان السطحي والتكشفات الجيولوجية.

تم خلال هذه الدراسة أيضاً تم تطوير نموذج رياضي يمثل الحوض الذي يمتد على مساحة تقارب 6250 م². يتكون هذا النموذج من ثلاث طبقات هيدرولوجية وباستخدام برنامج متخصص MODFLOW-2000. تم بناء هذا النموذج الرياضي للحوض ليحاكي الوضع الشهري للحوض خلال الفترة الواقعة بين 1951-2000. ومن ثم، تم فحص وتأكيده صحة هذا النموذج الرياضي خلال الفترة 2000-2007. قدم هذا النموذج الرياضي معلومات وفيرة ومهمة عن الحوض المائي الغربي من حيث الخواص الفيزيائية للحوض، النظام المائي وحركة المياه الجوفية بالإضافة إلى الموازنه المائية للحوض خلال فتره دراسته. بينت الموازنه المائيه ان 62% من التغذية السنويه تصل إلى الطبقة المائيه العليا وان الطبقة السفلي تقوم بتغذية نفس الطبقة بـ 11% من كميته المياه المستخرجه من الطبقة العلويه للحوض.

ولدراسة مدى تأثير الحوض لعدة احتمالات ضخ تحت ظروف مناخية مختلفة، فقد تم تمديد الفترة الزمنية للنموذج الرياضي لغاية العام 2034/35 لدراسة كل الاحتمالات الممكنة. وكنتيجه لذلك، فقد قدمت هذه الدراسة عدة مقارنات لمدى تأثير هذه الاحتمالات على ديمومة الحوض من حيث وضع مستوى الماء في طبقات الهيدرولوجيه بالإضافة إلى معدل تدفق في التبعات. وبناءً على ذلك، فقد تم اقتراح مستوى ضخ محدد بحيث يحافظ على ديمومة هذا الحوض، الاقتراح الاول والذي يقع ضمن فرضية عدم حدوث تغيير في المناخ وهو ان يتم ضخ ما يعادل 85% من المعدل السنوي للتغذية، اي ما يعادل 310 مليون م³/سنوياً. اما الاقتراح الثاني والذي يفترض حدوث تغيير مناخي ونقصان في معدلات

التغذية فينص على ضخ 85% من معدل التغذية لسبع سنوات سابقة، بذلك فأن الضخ من الحوض سيقفلص الى 254 مليون م³/ سنويا.

LIST OF FIGURES

Figure 1.1: Location map of the three trans-boundary basins.....	27
Figure 1.2: Geological map of the WAB.....	29
Figure 1.3: Digital Elevation Model (DEM) for the WAB.....	30
Figure 1.4: Long- term Average Annual Rainfall (mm).....	31
Figure 2.1: The hydrogeological setting of the WAB aquifer, (after Weinberger et al., 1994).....	44
Figure 2.2: Geological map of the WAB.....	45
Figure 2.3: Stratigraphic column (modified after Weinberger 1994 and SUSMAQ 2004).....	46
Figure 2.4: Hydro-geological map for the northern part of WAB.....	48
Figure 2.5: Cross sections-Part 1 (Obtained from the aquifer geometry of the WAB).....	49
Figure 2.6: Cross sections-Part 2 (Obtained from the aquifer geometry of the WAB).....	50
Figure 2.7: The Afig Clay Channel- Near the coast (SUSMAQ, 2004).....	50
Figure 2.8: Intra-aquifer connection.....	52
Figure 2.9: Annual discharge for Ras Al Ain and Al Timsah springs.....	53
Figure 2.10: Annual pumping rates.....	54
Figure 2.11: Well locations and annual pumping rates.....	55
Figure 2.12: Annual Injection rates.....	56
Figure 2.13: Flow direction map.....	58
Figure 2.14: Chloride concentration in the northern part of the WAB.....	60
Figure 2.15: Sketch of interface location in the northern part of the WAB (Paster et al., 2005).....	61
Figure 2.16: Chloride concentration in the central part of the WAB.....	63
Figure 2.17: Chloride concentration in the southern part of the WAB.....	64
Figure 2.18: Cross section A-A' in the southern part of the WAB (after Weinberger et. al., 1993).....	65
Figure 3.1: Recharge - rainfall relation according to Guttman's Equation.....	71
Figure 3.2: Location of rainfall stations over recharge areas of WAB.....	73
Figure 3.3: Monthly rainfall records over the recharge areas of the WAB.....	74
Figure 3.4: Mean of monthly rainfall over the recharge areas of the WAB.....	75
Figure 3.5: Water level for different observed well within the confined part of the WAB.....	77
Figure 3.6: Average water level in the confined part (generated from monitoring wells and HSI, 2007).....	77
Figure 3.7: Average monthly water level in the confined part during the selected period.....	81

Figure 3.8: Annual recharge estimates with rainfall distribution for the analyzed period.....	84
Figure 3.9: Recharge versus rainfall relations obtained by WLF technique and multi regression	85
Figure 3.10: The shape of rainfall distribution which gives high recharge rates.....	86
Figure 3.11: Typical rainfall distribution with consequently low recharge rates.....	87
Figure 3.12: Characteristics of years with different annual rainfall depths and identical recharge amounts.....	88
Figure 3.13: Years with equal annual rainfall depths and different recharge rates	90
Figure 3.14: Characteristics of years with equal annual rainfall depths and equal recharge rates	90
Figure 3.15: Recharge versus rainfall comparison	92
Figure 3.16: Rainfall in 1976/77 and 2003/04	93
Figure 4.1: Structural maps on Top Judea Group (top of the upper aquifer), Fleischer 2003,	99
Figure 4.2: Location of the used cross sections in the geometry development.....	100
Figure 4.3: The geometry of WAB	101
Figure 4.4: Criteria used for developing the Recharge Distribution Index (RDI)	104
Figure 4.5: Recharge depth for pre-development period	105
Figure 4.6: Location map for observed water level during pre-development period	106
Figure 4.7: Simulated water level	110
Figure 4.8: Horizontal conductivities and k_h/k_v ratios for upper and lower sub-aquifers	112
Figure 4.9: Sensitivity analysis to hydraulic conductivities.....	114
Figure 5.1: Time series of the WAB's outflows	120
Figure 5.2: Annual estimated recharge during the model period	121
Figure 5.3: Location map of the injected wells	122
Figure 5.4: Location of observed wells used for model calibration	123
Figure 5.5: Simulated versus observed water levels in the confined part of the WAB.....	127
Figure 5.6: Simulated versus observed water levels in the unconfined part of the WAB	128
Figure 5.7: Simulated versus observed spring hydrographs.....	129
Figure 5.8: Recharge distribution index for year 2005/2006	131
Figure 5.9: Flow direction in the lower sub-aquifer before and after the wettest year (a) April 1991 and (b) April 1992	133

Figure 5.10: Flow direction in the lower sub-aquifer during (a) April 1953 when the outflow was dominated by springs discharge (b) April 1974 when the outflow was dominated by pumping and also after the Ras Al Ain spring was dried out	134
Figure 5.11: Inflow and outflow from the WAB	137
Figure 6.1: Schematic diagram of WEAP-MODFLOW coupling, (Massmann, 2010).	142
Figure 6.2: Schematic diagram of WEAP-MODFLOW of the WAB	143
Figure 6.3: Normal rainfall scenario.....	145
Figure 6.4: Reduced rainfall scenario.....	146
Figure 6.5: Moving average pumping scenarios.....	147
Figure 6.6: Moving average pumping scenarios.....	148
Figure 6.7: Location map of the main watershed within the WAB	150
Figure 6.8: Potential quantities for artificial recharge.....	150
Figure 6.9: Location map of the observed cells	153
Figure 6.10: Water levels under Sc1.1 and Sc1.2 sub-scenarios	154
Figure 6.11: Al Timsah spring discharge under Sc1.1 and Sc1.2 sub-scenarios	155
Figure 6.12: Water levels under Sc1.3 and Sc7.3 sub-scenarios	155
Figure 6.13: Al Timsah spring discharge under Sc1.3 sub-scenarios	156
Figure 6.14: Water levels under Sc1.1 and Sc7.3 sub-scenarios	156
Figure 6.15: Water levels under Sc7.1 and Sc7.2 sub-scenarios	157
Figure 6.16: Springs discharges under Sc7.1 and Sc7.2 sub-scenarios	157
Figure 6.17: Water levels under Sc2.1, Sc2.2, Sc8.1 and Sc8.2 sub-scenarios.....	159
Figure 6.18: Water levels under Sc4.2 and Sc6.2 sub-scenarios	160

LIST OF TABLES

Table 1.1: Summary of previous numerical models for the WAB	36
Table 1.2: Summary of data sources	38
Table 3.1: Monthly rainfall characteristics over recharge areas of the WAB	74
Table 3.2: Water balance during the period 1989/90 to 2001/02	79
Table 3.3: Recharge estimates by WLF technique compared with other estimation techniques	82
Table 3.4: Correlation test between monthly rainfall and annual recharge (1970/71 – 1996/97)	84
Table 3.5: Characteristics of years with high recharge to rainfall ratios	86
Table 3.6: List of all years within the analyzed period with low recharge to rainfall ratio	88
Table 3.7: Example of years where different annual rainfall amounts generate same recharge rates ..	89
Table 3.8: Characteristics of years with same annual rainfall depths and different recharge rates	89
Table 3.9: Characteristics of years with equal annual rainfall depths and equal recharge rates	91
Table 4.1: Rank for potential to recharge for land use types and geological formations	103
Table 4.2: Recharge distribution to the WAB layers.....	103
Table 4.3: Pre-development water level at specific point locations	108
Table 4.4: Pre-development water budget for the WAB	111
Table 5.1: RMSE for the observed wells.....	130
Table 5.2: Water balance budget for the WAB	135
Table 6.1: Calculation of potential storm water runoff	149
Table 6.2: List of evaluated scenarios	151

LIST OF ABBREVIATIONS

DEM	Digital Elevation Model
EAB	Eastern Aquifer Basin
ECHAM4	European Center Hamburg (Version 4)
GLOWA JR	GLOWA Jordan River Project
GMS	Groundwater Modeling System
HadCM5	5 th Generation of Hadley Climate Model
Km ²	Squared Kilometer
mm/yr	Millimeter per year
mg/l	Milligram per liter
Mm ³ /yr	Million of Cubic Meter per year
MM5	Mesoscale Model (Version 5)
NEAB	North-Eastern Aquifer Basin
NRS	Normal Rainfall Scenario
PHG	Palestinian Hydrology Group
RegCM	Regional Circulation Model
RDI	Recharge Distribution Index
RMSE	Root Mean Squared Error
RRS	Reduced Rainfall Scenario
SUSMAQ	Sustainable Management of the West Bank Aquifers
WAB	Western Aquifer Basin
WEAP	Water Evaluation And Planning system
WLF	Water Level Fluctuation
ZRMSE	Zonal Root Mean Squared Error

Chapter 1

CHAPTER 1: INTRODUCTION TO THE WESTERN AQUIFER BASIN

1.1 INTRODUCTION

Water scarcity may be the most crucial environmental problem facing the Middle-East region in general and more specifically in the Palestinian Authority, Jordan and Israel. Day by day, the natural water resources are deteriorating in both quantity and quality terms. This deterioration is not only limited to the increase of demand as a result of population growth and socio-economic development, but is also anticipated to be a factor of the global warming and its huge impact on the water resources replenishment. In addition to that, quantity of water is a function of its quality; therefore, reduction in the replenishment amounts, over exploitation of the groundwater aquifers to meet the socio-economic development demand will increase the risk for polluting the water resources by sea water intrusion, mixing of fresh water with other salt bodies and many other possible risks that will lead to the contamination of these resources and as a result, reduce the potential fresh water quantity.

In the area where the case study used for the purpose of this research is located, the West Bank and Israel, groundwater could be considered the primary source of water for different purposes. In Israel, around 85% of their demand was supplied from groundwater resources (PHG 2010). In the Palestinian side, the West Bank, there are three main groundwater basins: the Eastern, North-eastern and Western Aquifer Basins, Figure 1.1, comprising the only available source of water for all uses. These aquifer systems are shared between the West Bank and Israel. This makes the sustainable management of these valuable trans-boundary water resources a responsibility of both parties.

Among these trans-boundary aquifer systems, the Western Aquifer Basin (WAB) is the largest basin in terms of area, storage capacity and sustainable yield. The majority of the WAB's yield is fresh and could be used as drinking water. The aquifer is mainly recharged from rainfall over the replenishment areas in the western mountains of the West Bank.

Development activities for the aquifer started in the early 1950s with minor pumping rates which later increased to reach around 300 Mm³ in 1970. After 1970, the pumping was increased depending on the annual rainfall where maximum pumping was recorded to be 570 Mm³ in the dry year 1998/99. The long-term annual recharge was estimated to be 362 Mm³/yr. As the annual pumping rate during dry years is usually more than the replenishment rate. This over exploitation stressed the aquifer system and as a result the water level, springs' discharge and the water quality started to deteriorate.

Currently the aquifer is fully controlled by Israel where around 95% of its pumping is used by Israelis while the remaining is used by the Palestinians in the West Bank. The Palestinian rights in this aquifer are still subject to the results of final status negotiations according to the previous agreements.

1.2 TRANS-BOUNDARY GROUNDWATER RESOURCES

Groundwater, in the Palestinian case, is the only source of fresh water for all uses. Other marginalized sources are water harvesting and treated wastewater. As mentioned the groundwater resources can be divided into three basins, Figure 1.1; the Western Aquifer Basin, the Eastern Aquifer Basin and the North-eastern Aquifer Basin. These three basins were classified as trans-boundary basins between the West Bank and Israel. The water within these basins is good in quality and is largely used for municipal supply.

1.2.1 Western Aquifer Basin, the Case Study

The trans-boundary groundwater aquifer basin, the Western Aquifer Basin (WAB) or “Yarkon Tananim” as referred to in Israeli literature, is one of the most important sources of freshwater for the West Bank and Israel, Figure 1.1. The WAB stretches northward from area south of the Egyptian border all the way up to the foothills of Mountain Carmel and from West Bank mountains in the east heading westward towards the Coastal Plain of the Mediterranean Sea with total area 9000 km².

The WAB is considered as a highly karstic aquifer; with a general thickness ranging between 600 and 1000 meters (Avistar et al, 2002). It consists of three lithological layers; the lower and the upper permeable layers (lower and upper sub-aquifers) are predominantly limestone

and dolomite with thicknesses ranging between 250 and 400 m each. The upper and lower sub-aquifers have high signs for karstifications. The layer in between with a thickness of 80 - 120 m functions as a semi-permeable layer which is dominated by chalky limestone, chalk and marl. This layer permits the flow to exchange between the two permeable upper and lower sub-aquifers. The lower sub-aquifer is underlined by the Kurnub group which consists of limestone, marl, and sand.

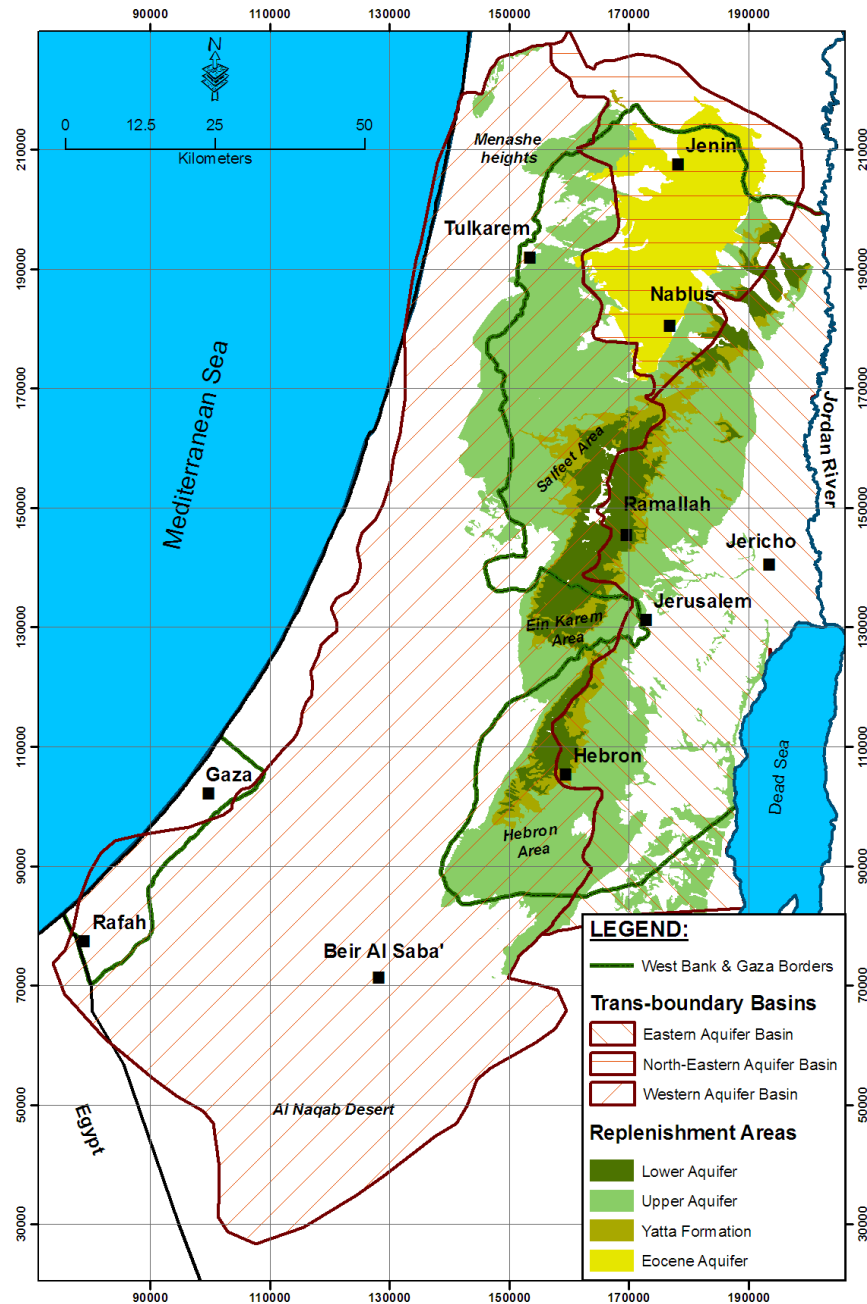


Figure 1.1: Location map of the three trans-boundary basins

On the eastern side of the WAB, the aquifer is unconfined while the western side is confined by the overlying chalky and marl layer (Senonian age) with a thickness that could reach 600 m in some area. WAB is naturally replenished by rainfall on the outcropping formation covering an area of 1932 km² located over the eastern part of the aquifer (i.e. West Bank Mountains). The long-term annual average recharge is estimated at 373 Mm³/yr. During the pre-development period (prior to 1950), the natural outlets of this aquifer were Ras Al Ain (Yarkon) and Timsah (Tananim) springs with a total historical mean annual flow estimated to be 350 Mm³/yr (Weinberger et al., 1994).

Due to the over exploitation of the WAB, the discharge rates of both springs declined. The discharge of Ras Al Ain spring deteriorated with time until it become completely dry in 1973. After the heavy rain in 1991/92, the spring started to discharge once again. The discharge rate reached 36 Mm³ in 1992/93 then decreased to much lower discharge rates (i.e. less than 1 Mm³/yr). The discharge of Al Timsah spring also decreased to 60-40 Mm³/yr during the 1960-1980. After 1980, the spring discharge was fluctuated between 20 and 40 Mm³/yr depending on the rainy season as well as on the pumping rate from the WAB.

The water levels during the early 1950s in the confined part of the WAB gently dropped from 25 - 27m near Beir Al Saba' in the south to 16 m in the Menashe heights in the north (Rosenthal et al., 1992, Dafny et al., 2010). In the unconfined part and for the same period, the water levels stood at 450 - 500 m in Jerusalem area (Ein Karem), in the Hebron mountains water level ranges were found to be 550 - 750 m and 350 - 450 m for the upper and the lower sub-aquifers respectively and 300 - 350 m in Salfet area (Weinberger et al., 1994, Guttman et al., 1988, Dafny et al., 2010). During the last decade, water levels in the same regions stood at 13 - 15 m in Beir Al Saba', 9 - 12 m in the Menashe heights, 440 - 450 m in Ein Karem area, and 520 - 725 m and 275 - 325 m in Hebron mountains for the upper and lower sub-aquifers respectively.

The exploitation of groundwater from the WAB started in the early 1950s (Zeitouni et al., 1996). In 1951, there were 46 wells pumping around 10 Mm³. The pumping rate was increased to around 400 Mm³/yr from 400 productive wells during the 1970s. Currently, there are 493 wells, Figure 1.2; most of which (90%) tap the upper sub-aquifer. The annual

pumping rates depend on the rainy season, as the pumping rate was increased during dry years. For example, the pumping rate was increased to 573 Mm³ during the dry year 1998/99 and decreased to less than 250 Mm³ during the wet year 1991/92.

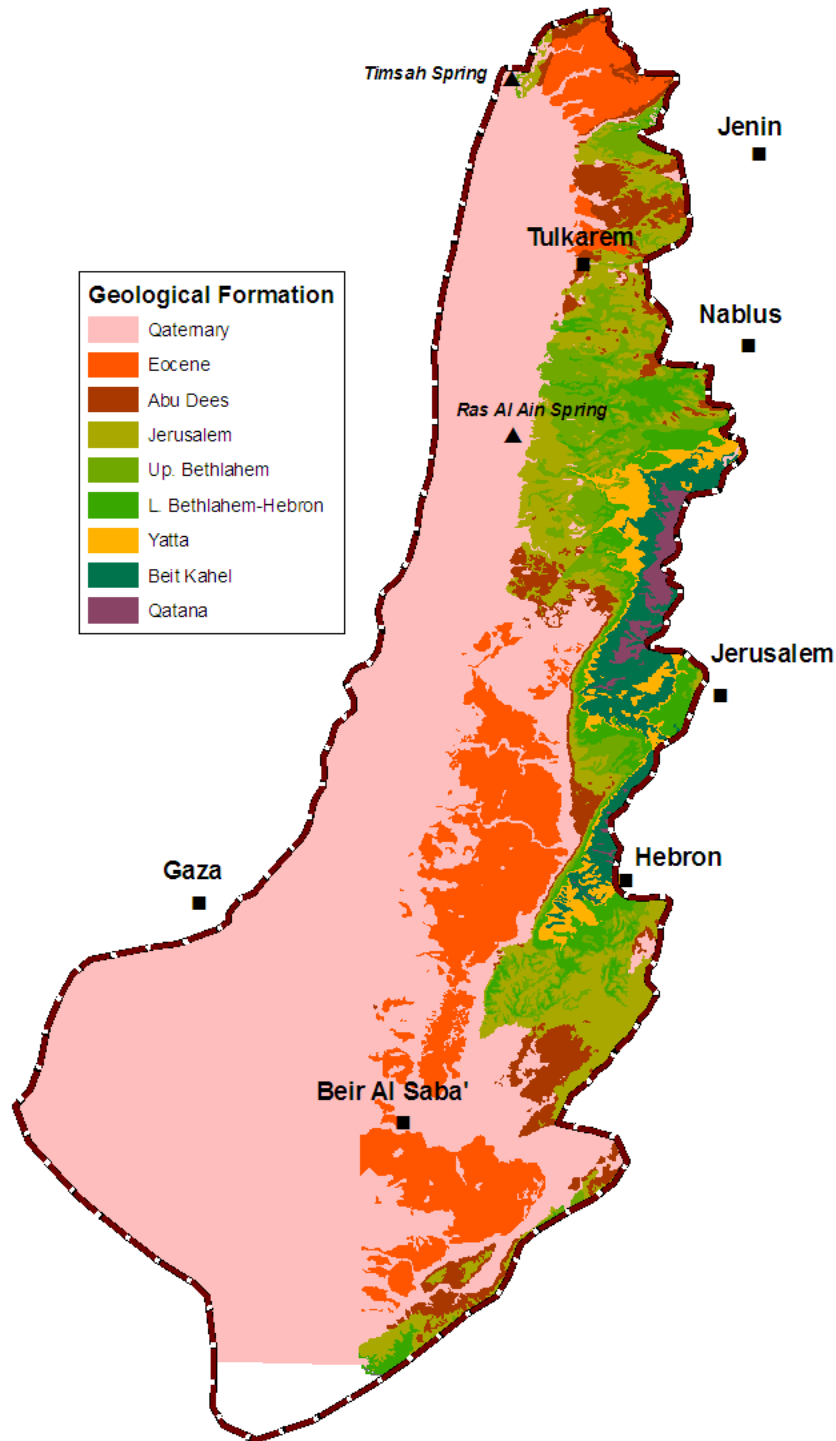


Figure 1.2: Geological map of the WAB

The topographic environment of the WAB varies from sea level on the Mediterranean coast in the western side of the aquifer to an elevation close to 1000 m in the West Bank Mountains on the eastern side of the basin. The WAB domain can be divided from east to west into three longitudinal topographical zones; the coastal plain zone, the foothill and lower slopes zone and the upper slopes and mountain zone, Figure 1.3.

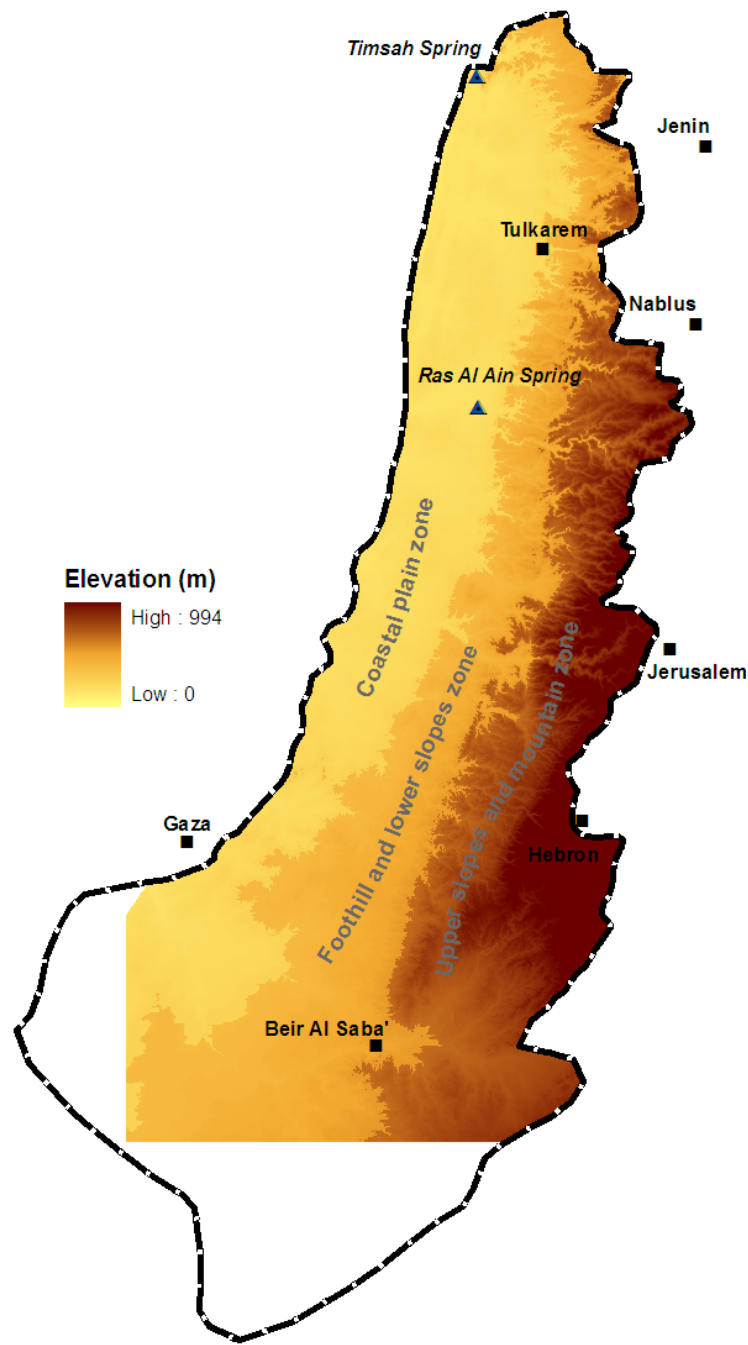


Figure 1.3: Digital Elevation Model (DEM) for the WAB

The Basin is characterised by its Mediterranean climate. Its climate zones range from an arid desert condition in the Al Naqab desert to a sub-humid Mediterranean climate in the centre and north of the Basin. The temperature is moderate with intermediate precipitation that mostly falls during the coldest half of the year (October-April), Figure 1.4. Generally, the mean annual precipitation rate over the replenishment areas of the aquifer is estimated at 560 mm.

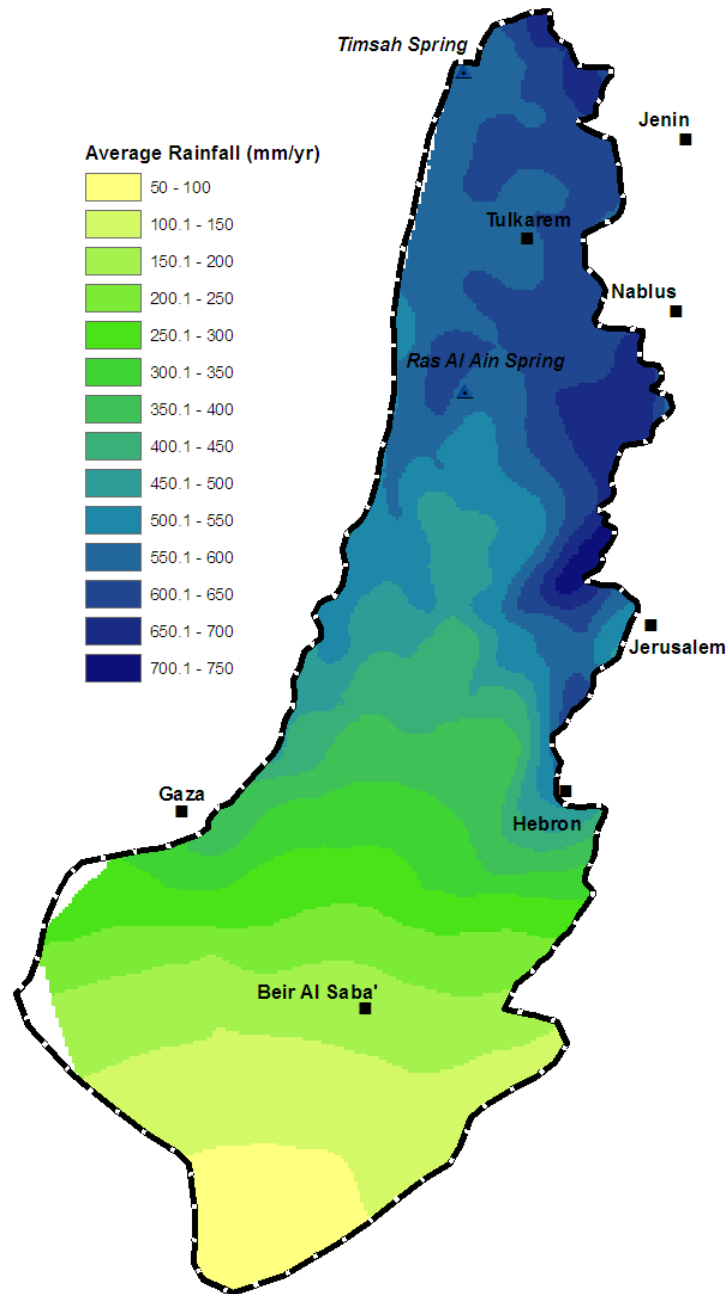


Figure 1.4: Long- term Average Annual Rainfall (mm)

1.2.2 Eastern Aquifer Basin

The Eastern Aquifer Basin (EAB) covers the eastern side of the West Bank. The Basin extends from the north to the south of the West Bank borders and from the Jordan River and the Dead Sea in the east to the water divide on the western side with an area 3100 km², Figure 1.1. Unlike the WAB, the EAB is almost predominantly a Palestinian Aquifer where both recharge and discharge zones are located in the West Bank.

The EAB is a multi-layered system; upper and lower aquifer layers (upper and lower sub-aquifers) separated by a less permeable layer. The upper sub-aquifer, upper Cenomanian to Turonian ages, is mostly unconfined while the lower sub-aquifer, the lower Cenomanian age is mainly confined (CH2MHILL, 2001). These two sub-aquifers are the main fresh water sources available in the eastern side of the West Bank. The separating layer, Yatta formation, composed of yellow marl and bluish bottom clays, and behaves in most of the area as a good to fair permeability layer connecting the two sub-aquifers within the EAB.

The recharge of the EAB is predominantly by the rainfall over outcropping aquifer Albian to Turonian formations in the eastern mountain of the West Bank, Figure 1.1. The long-term annual average recharge is estimated at 125 - 197 Mm³/yr (SUSMAQ 2004). The recharge inflow generated towards the Dead Sea and the Jordan River by gravity where mixes with saline (brackish) water and then emerges through the Dead Sea springs. The water level starts from a round 450 m above sea level on the western side close to the water divide and gradually decreased to the level of the Dead Sea and Jordan River on the eastern side (CH2MHILL, 2001). The outflow of the Basin could be divided into three types: springs, groundwater wells and seepage to the Jordan River and to the Dead Sea.

1.2.3 North-Eastern Aquifer Basin

The Northeastern Aquifer Basin (NEAB) is the smallest trans-boundary aquifer in the West Bank with an area of 1370 km². It starts from the area south of Nablus City as the southern boundary of the aquifer and extends to the north beyond of the West Bank border. The eastern and western sides of the Basin are restricted to two large antinclines in the central mountain of the West Bank.

The NEAB is composed of two superimposed aquifer systems; the Eocene and the upper aquifer. The Eocene is an unconfined aquifer predominately composed of limestone with relatively low hydraulic conductivities. The long-term average recharge is estimated to be around 90 Mm³/yr. Within the West Bank, the well abstraction is approximately sums up to 5 Mm³/yr in addition to 15 Mm³/yr that emerge from the springs. (SUSMAQ 2004).

The deep, upper aquifer, is separated from the Eocene aquifer by the Senonian chalk. Therefore, it is a confined aquifer predominated by highly karstic limestone and dolomite (Cenomanian to Turonian ages). This aquifer has higher conductivity and yield than the Eocene aquifer. It is recharged from the outcropping formations in the central mountain of the West Bank with long-term average of 165 Mm³/yr. (CH2MHILL, 2001).

1.3 OBJECTIVE OF THE STUDY

The WAB is acknowledged as a highly karstified aquifer that significantly contributes to the supply of fresh water for all purposes in both Israel and the West Bank. However, the WAB shows a high level of spatial and temporal variations since:

- a. The aquifer is characterized as a karst aquifer system with high contrast in hydraulic properties with high variations in the recharge pattern in spatial and temporal distributions.
- b. The aquifer is located in a semi arid area with high variation in hydrological conditions. The rainfall which is the main source of recharge has a high level of variation in terms of annual quantity, temporal and spatial distributions and intensity.
- c. There is a high variation in aquifer development in event on monthly and annual scales as well as spatially. The pumping from the Aquifer is not only a function of the demand, but is also inversely related to the annual rainfall which increases the level of the stresses on the WAB.

Consequently, the time, the location and the extent of responses to the different hydraulic stress levels will vary greatly from place to place in this karst aquifer due to the combined permeability provided by matrix, fracture, and conduit-flow components. Accordingly, the

main objective of this research is to investigate the responses of the highly karstified aquifer system (i.e. the WAB) as a result of the intrinsic characteristics (variation of hydrological characteristics and aquifer development schemes) as well as other extrinsic stresses due to global changes (e.g. Climate change).

The approach for achieving the objectives of this study can be summarized in four main points:

- Developing the conceptual model of the WAB which characterizes the flow system of the WAB based on field investigations, measurements, collected data and previous studies (Chapter 2).
- Studying the historical records of the Aquifer's inflow and outflow in order to estimate the aquifer recharge under different rainfall distributions. Then understanding the relation between the amount of generated recharge and type of rainfall (Chapter 3).
- Developing a numerical flow model for the WAB which is considered one of the most important predictive tools needed for better management of the Aquifer. This model can be used to estimate hydraulic parameters, obtain a better understanding of the hydrodynamic processes in karst systems and predict how the Aquifer might respond to changes in pumping and climate (Chapters 4 and 5). The modeling effort will focus on building a continuous numerical model of the WAB starting from the pre-development period (prior to 1950) up to date. This will allow the model to simulate all major events within the aquifer history where the aquifer response for these events will be understood. The model will provide a wide range of information with high confidence level such as:
 - The hydraulic conductivities (values and spatial distribution) that represent the combined permeability provided by matrix, fracture, and conduit-flow components.
 - The aquifer geometry and boundaries.
 - Validate the estimated recharge and its temporal and spatial distributions.

- Distribution of water levels, depth to water level and flow direction.
- Sustainable yield of the aquifer under different climate conditions.

- Studying the response of the Aquifer under different management options and under different rainfall scenarios in order to obtain the best management option for the sustainability of the WAB, (Chapter 6).

1.4 METHODOLOGY

The methodology of this study is based on the principle of maximizing the benefits from the available knowledge regarding the study area as well as from the similar hydrological case studies in the world in order to reach the target goals. Therefore, this study started by reviewing the available literature including scientific papers, annual and monthly reports in addition to interviews with different stakeholders from both Palestinian and Israeli sides. As a result, different types of data, conceptual models, previous experiences and more were accumulated.

Following to the literature review step, all the collected knowledge and data were then analyzed, manipulated and cross checked. As a result, Chapter 2 of this report was developed. This part of the study was used as a guide during the entire study. Also, as one of the main conclusions of the conceptual model of the WAB, the inflow mechanisms still require further investigation. Accordingly, a thorough analysis was conducted to analyse the relation between the rainfall as the main component of recharge and the annual recharge which is presented in Chapter 3.

The modified conceptual model of the WAB was then converted to a numerical model. This conversion was done in two steps; the first step was described in Chapter 4, where a steady state flow model was developed to represent the pre-development period of the aquifer. The model was calibrated and accordingly the conceptual model were revised and modified. The calibrated steady state model were used to study the flow dynamics of the aquifer and also used to provide valuable knowledge which was used for developing the long-term transient flow of model of WAB as described in Chapter 5 which is the second step. The transient

flow model started from the pre-development period up to year 2000, and then was validated during the remaining period of seven years (i.e. 2007). The transient model was calibrated and validated based on the water levels in some monitoring wells, springs discharges and some major observations during the modelling period.

The final step in this study was to reach the goals of the second task, which concentrates on studying the aquifer responses under different management options. Therefore, the WAB response was tested by using the developed transient model with a wide range of climate, pumping and management scenarios as described in Chapter 6. The methodology used in this part of the study aimed to use different levels of stresses on the aquifer in order to reach to the best management scenarios under different possible driving forces.

1.5 PREVIOUS STUDIES

The earliest available study regarding the WAB was published during late 1960s. This paper studied the possibility of operating the aquifer as a reservoir, (Harpaz and Schwarz). After 1970 and up to now, tens of papers have been published by Israeli scientists. On the Palestinian side, the aquifer was kept as a black box until 1999 when a joint project between the Palestinian Water Authority (PWA) and Newcastle University studied the aquifer and a numerical model was developed. The project was completed by 2004; the model and studies were not followed up or updated. Table 1.1, after which summarizes the most of the developed numerical models of the WAB and provides some of the models characteristics.

Table 1.1: Summary of previous numerical models for the WAB, (modified after Dafny et al., 2010)

Reference	Model Domain	Number of Layers	Time step	Model Period	Calibrated Parameters
Y. Harpaz and J. Schwarz	Entire	1	Monthly	1952-1963	Transmissivity and Storativity
Baida et al., 1978	South and Hebron areas	1	6 Months	1956-1976	Transmissivity and Storativity
Shachnai and Goldschtoff, 1980	Confined area	1	6 Months	1952-1976	Transmissivity and Storativity
Meiri and	Jerusalem	1	-	Steady state,	Transmissivity

Guttman, 1984	area			1982	
Guttman, 1991	South	1	6 Months	1976-1990	Transmissivity and Storativity
Baida and Zukerman, 1992	Jerusalem area	1	6 Months	1967-1989	Transmissivity and Storativity
Guttman and Zukerman, 1995	Confined area	1	6 Months	1952-1993	Transmissivity and Storativity
Guttman and Zeitoun, 1996	North	2	6 Months	1971-1994	Transmissivity and Storativity
Berger, 1999	Entire	1	1 Month	1988-1994	Transmissivity and Storativity
SUSMAQ, 2004	Entire	3	12 Months	1989-1998	Vertical and Horizontal hydraulic conductivities and Storativity
Dafny et al., 2010	Entire	3	1 Month	1987-2003	Vertical and Horizontal hydraulic conductivities and Storativity
This Study	Entire	3	1 Month	1951-2007	Vertical and Horizontal hydraulic conductivities and Storativity

1.6 GAPS IN PREVIOUS STUDIES AND UNIQUENESS OF THIS STUDY

While the WAB was well studied by the Israeli authorities and scientists, the Palestinian governmental and non-governmental organizations still need more researches and investigations in order to reach a full understanding of the flow system of the WAB and its potential yields.

Most of the previous studies and models estimate the recharge based on empirical equations that almost linearly relate the annual rainfall with the annual recharge. This study used the water level fluctuation technique as a base for estimating the annual recharge, then, a thorough statistical analysis was conducted to study the relation between the annual recharge and the monthly rainfall distribution. As a result, annual recharge rates were found not only to be related to the annual amounts of rainfall but even more related to the rainfall monthly distributions. Accordingly, a new empirical equation was developed that relates the annual recharge to monthly rainfall.

In terms of numerical modelling, Table 1.1 shows the characteristics of the previous models and the model developed in this study. All previous models were simulated for specific time

horizons or zones and mostly in six months time steps and one layer system. The challenge here was to build a multi-layer model that covers the entire development period of the aquifer in a more refine time step and grid size that enables the simulation of the historical responses of the aquifer with time and also could predict the future responses under different climate and management options.

1.7 DATA ACQUISITION

Although, a significant part of the data used was collected from different published literature (scientific journals, annual reports, deliverables from different related projects, etc), there was good cooperation in between different Palestinian and Israeli institutions coordinated by the GLOWA Jordan River (III) project (GLOWA JR). Table 1.2 summarizes the sources of data used in this study.

Table 1.2: Summary of data sources

Source	Data Type/Format	Details
Palestinian Hydrology Group (PHG)	GIS shape files, maps, meteorological data	Geology, land use, boundaries, wells and springs locations, temperature and rainfall records for some stations.
Palestinian Water Authority (PWA)	Tables	<ol style="list-style-type: none"> 1. Wells locations and monthly abstractions within the West Bank. 2. Springs locations and monthly discharge within the West Bank. 3. Meteorological data for some weather stations (rainfall)
Palestinian Meteorological Department (PMD)	Tables	Complete, monthly meteorological data for all stations in the West Bank

Israeli Water Authority (IWA) through Tahal Company	Tables	<ol style="list-style-type: none"> 1. Wells locations and monthly abstractions within Israel. 2. Springs locations and monthly discharge within Israel.
---	--------	---

1.8 BENEFICIARIES OF THE STUDY

This study was conducted within the framework of the GLOWA project. The model and the results obtained will provide the needed support to the scientific team of the project in order to develop and improve the water management strategies in the region of the case study, or as stated in the BMBF guidelines, to provide “simulation tools and instruments to develop and realize strategies for sustainable water management” under global change. Accordingly, the achieved outputs of this study will be available to all partners within the GLOWA project for further study or analysis.

The main beneficiary of this study will be the PWA. The produced and collected data, models, scenarios as well as reports will be transferred to the PWA data base. Accordingly, the PWA will review and upgrade their technical materials and data bases.

Chapter 2

CHAPTER 2: CONCEPTUAL REVIEW OF THE WAB

2.1 INTRODUCTION

Forecasting the possible effects of climate change and intensive exploitation on available water resources requires knowledge in both regional and local groundwater flow systems. Therefore, building a reliable numerical flow model that enables the simulation of the flow dynamics in space and time under different conditions is very essential. The WAB is known as a karstic, heterogeneous and non-isotropic groundwater system; consequently, the flow dynamics of this aquifer is very complex (Frumkin et al., 2005). Fractured and karstified aquifers usually differ from other porous groundwater systems since they are characterized by dual porosity resulting in two types of groundwater flow systems (Gunn et al., 1985).

1. Diffuse flow system: flow in this type is diffused through joints, fractures, fissures, bedding planes and other small inter connected openings. The water table in this flow system is usually well defined by Darcy Law where hydraulic conductivity is almost uniform.
2. Conduit flow system: the flow is turbulent, carried through solutional passages or underground conduit systems with a wide range of widths from few centimeters to a few meters. These conduits play a significant role in transporting water quickly towards the springs.

The conceptual model of the WAB is based on the assumption that the aquifer is a single continuous, interconnected and structurally undisturbed entity (Mandel 1961). Accordingly, natural recharge generated in the mountains in the eastern side of the basin generally flows to the northwest or southwest then diverts to the north toward the two main natural outlets (i.e. Al Timsah and Ras Al Ain springs). The schematic diagram in Figure 2.1 shows the hydrogeological setting in the central part of the WAB. Accordingly, the geological layers, boundary conditions, salinity distribution, salinization mechanisms, recharge mechanisms, water levels, flow patterns and other important conceptual items were reviewed in this Chapter.

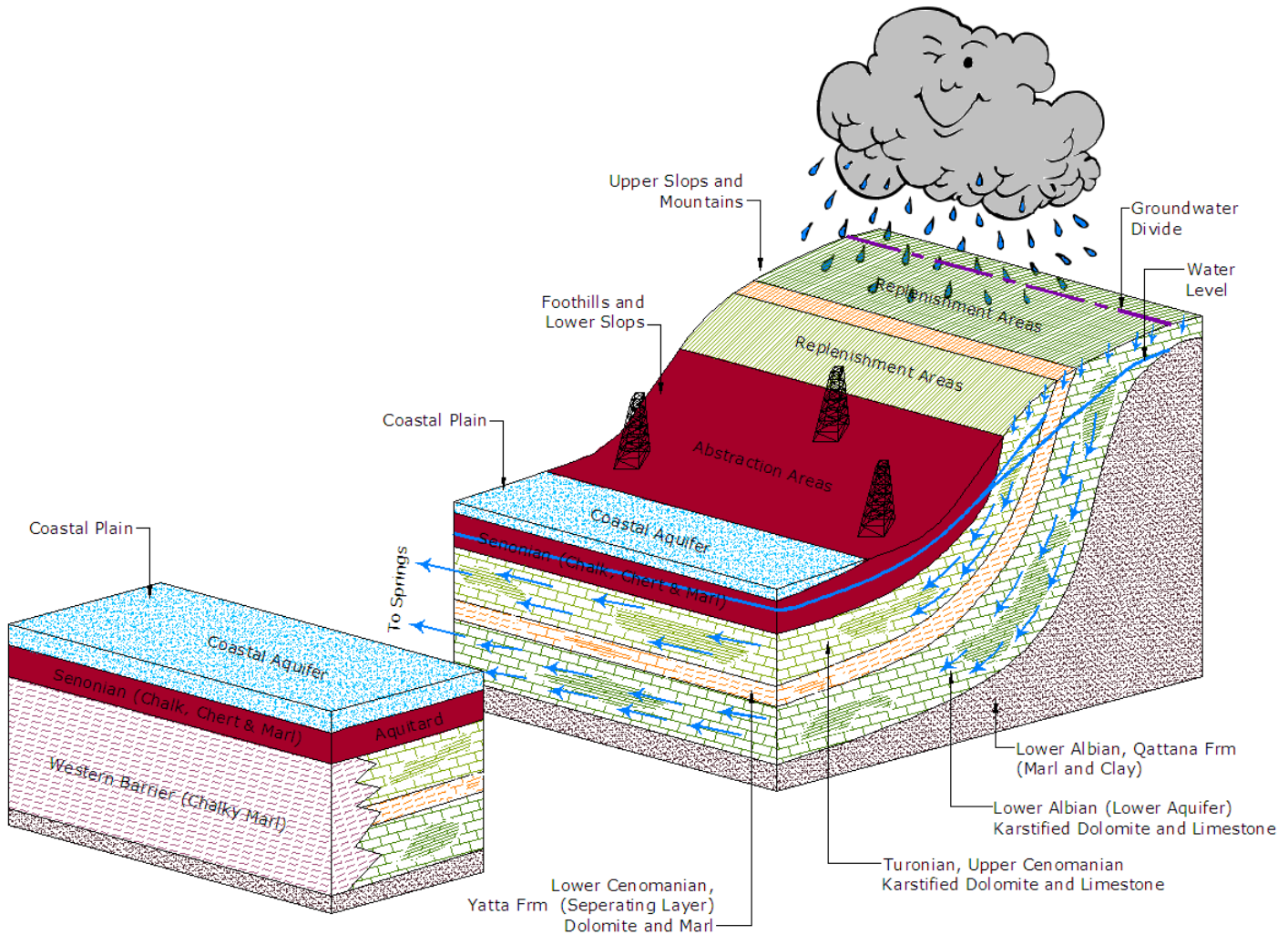


Figure 2.1: The hydrogeological setting of the WAB aquifer, (after Weinberger et al., 1994)

2.2 GEOLOGY AND HYDROGEOLOGY OF THE WAB

The WAB falls in the middle-to-late-Cretaceous Judea Group (Weiss et al., 2007). It is divided into two main sub-aquifers (i.e. upper and lower) separated by a lower permeability layer (i.e. Yatta formation). The upper and lower sub-aquifer rocks are mainly composed of a sequence of hard, karstic and permeable limestone and dolomite with a thickness of 600–1000 m (Avisar et al., 2002). The geological map illustrating the main geological formations is shown in Figure 2.2.

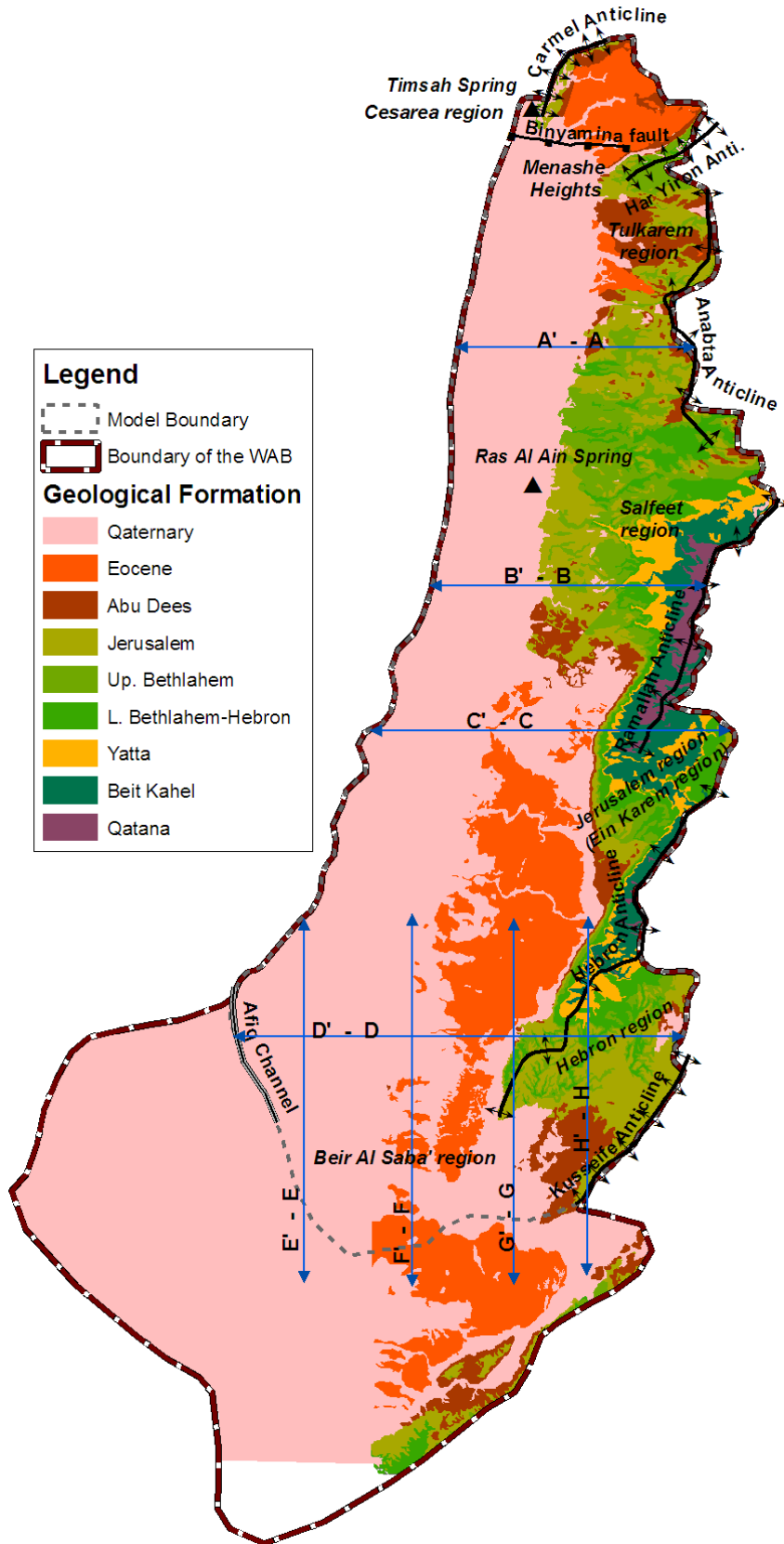


Figure 2.2: Geological map of the WAB

The main stratigraphic units as well as the description of the WAB layers are listed below, Figure 2.3:

Period	Age	Formation	Lithology	Hydrostratigraphy	
Cretaceous	Senonian	AbuDees	Chalk, Chert, Marl	Aquitard	
	Turonian	Daliya	Jerusalem	Upper Aquifer	
	Cenomanian	Undifferentiated Talme Yafe	Bethlehem		Chalky Marl
			Hebron	Dolomite, Limestone, Marl, Chalk	
			Yatta	Chalk, Marl, Limestone	
	Albian		Beit Kahel	Dolomite, Limestone, Marl	Lower Aquifer
			Qatana	Marl, Clay	Aquitard

Figure 2.3: Stratigraphic column (modified after Weinberger 1994 and SUSMAQ 2004)

Aquifer base: The aquicludal Qattana formation, Albian age, underlies the lower sub-aquifer of the WAB. The lithology of this layer alters from marls and clays in the northern portion of the Basin to sandstones, clays and carbonates in its southern area (Weinberger et al., 1993).

Lower aquifer: The Albian-age, Beit Kahel formation is mainly composed of massive dolomite and limestone layers (Lewy et al., 1991). It is described as a high conductivity layer due to strong karstification. Its thickness ranges between 300 and 450 m.

Separating layer: The Cenomanian-age, Yatta formation consists primarily of interbedded dolomite and marl, mainly at the base (Lewy et al., 1991). This impervious layer forms the hydrological barrier separating the upper and lower sub-aquifers (Guttman et al., 1988 and Baida et al., 1989).

Upper aquifer: The Jerusalem formation, Turonian-age, and the Bethlehem and Hebron formations, Cenomanian age, form the upper sub-aquifer. The dominant components of this layer are karstic limestone and dolomite rocks (SUSMAQ, 2004).

Overlaying layer: Abu Dees formation, Senonian age, comprises the overlaying layer of the upper sub-aquifer. The dominant components of this layer are chalk and marl (SUSMAQ, 2004). In some areas, the base of the Abu Dees formation consists of hard, highly fractured chalk (Flexer et al., 1968). These beds are considered as permeable and form in many cases, one hydrogeological entity with the underlying upper sub-aquifer, (Avisar et al., 2002).

Western Barrier: The impervious chalky marls of the Daliya formation and Talme Yafe Group act as impervious barriers along the western boundary of the WAB except in Cesarea region (west of Al Timsah spring), Figure 2.2, where direct connection or connection along the buried Binyamina fault with the Mediterranean Sea is anticipated (Guttman et al., 1995).

2.3 BOUNDARIES

The model boundaries were defined based on hydrogeological and structural evidence. Therefore, a detailed literature review was conducted to define the most realistic boundary conditions for the WAB. The boundaries and their considerations are listed below.

2.3.1 Northern Boundary

The northern boundary was defined based on hydrogeological and structural evidence. Figure 2.4 shows the geological map of the northern part of the WAB including the main structures. The northern boundary is drawn by the anticline in the Carmel Mountain where Jerusalem and Bethlehem formations are exposed. To the north of Timsah spring, the boundary is defined based on the flow direction (east-west) where flow in the Carmel coast line seems to be unaffected by the flow in the WAB (Guttman et al., 1995). The figure also shows the major structure fault in the north (the Benyamina fault) which is located at the southern edge of Carmel Mountain. It has a large throw (~ 700 m) in the west and dies out to the east which brings the upper and lower sub aquifers close to the surface on the northern side of the fault (SUSMAQ, 2004).

On the northeast edge of WAB, close to Menashe syncline, the boundary was defined based on the elevation of the base of the upper sub-aquifer. This boundary is considered as a possible flow boundary where flow could enter or leave the WAB depending on the pumping rates from the WAB or from the adjacent aquifer (the Northeastern Aquifer Basin).

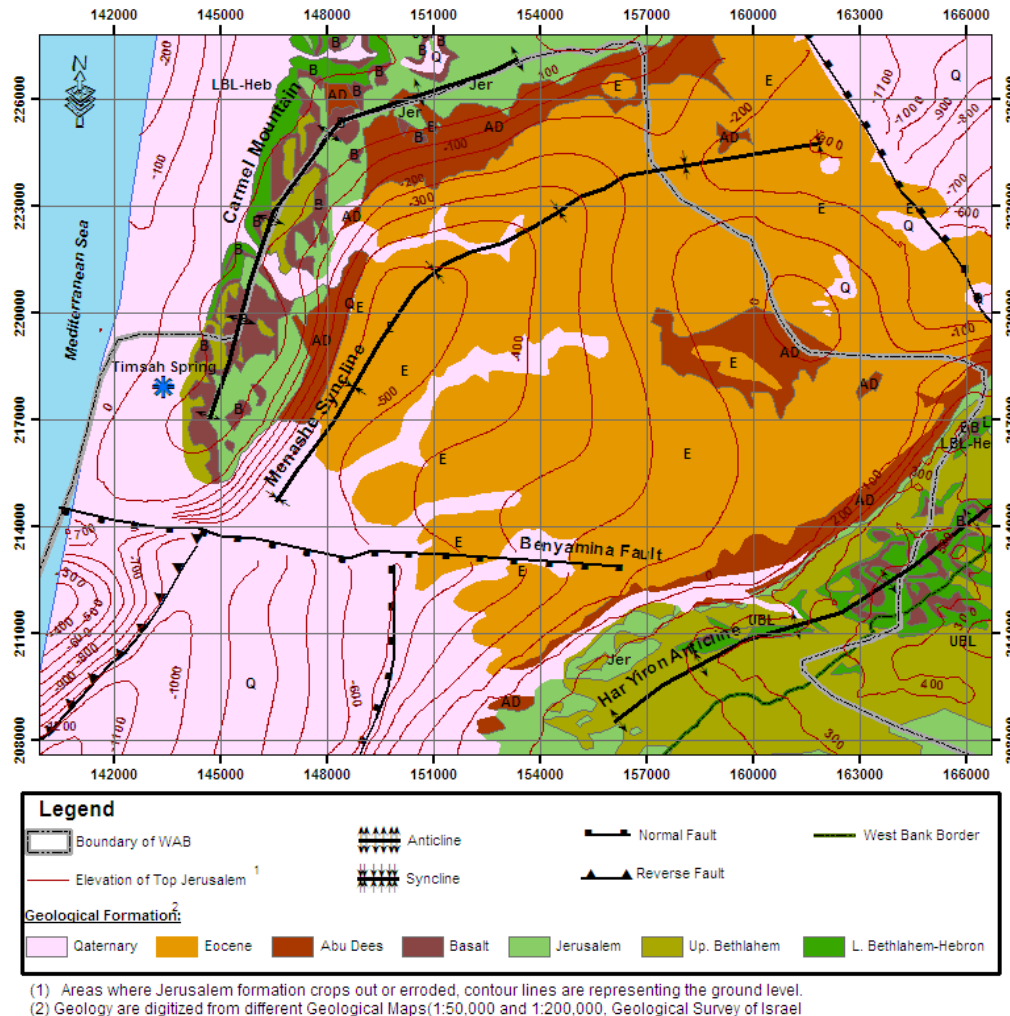


Figure 2.4: Hydro-geological map for the northern part of WAB

2.3.2 Eastern Boundary

The eastern boundary of this aquifer was outlined along the assumed groundwater divide and the hydrological barriers assumed from structural and lithological considerations. This boundary can be traced from the core of the Har Yiron anticline in the north through the Anabta anticline, the Ramallah structural divide, the Hebron structural barrier and the Kusseifa anticlinorium (Goldschtoff et al., 1980; Guttman et al., 1988). These boundaries along anticlinal mountains series act as no-flow boundaries, Figure 2.5. In the Jerusalem and Hebron areas, the boundary was shifted to the east in order to include all areas where the generated flow can move towards the south-west direction. This shift was determined based on the geometry of the WAB.

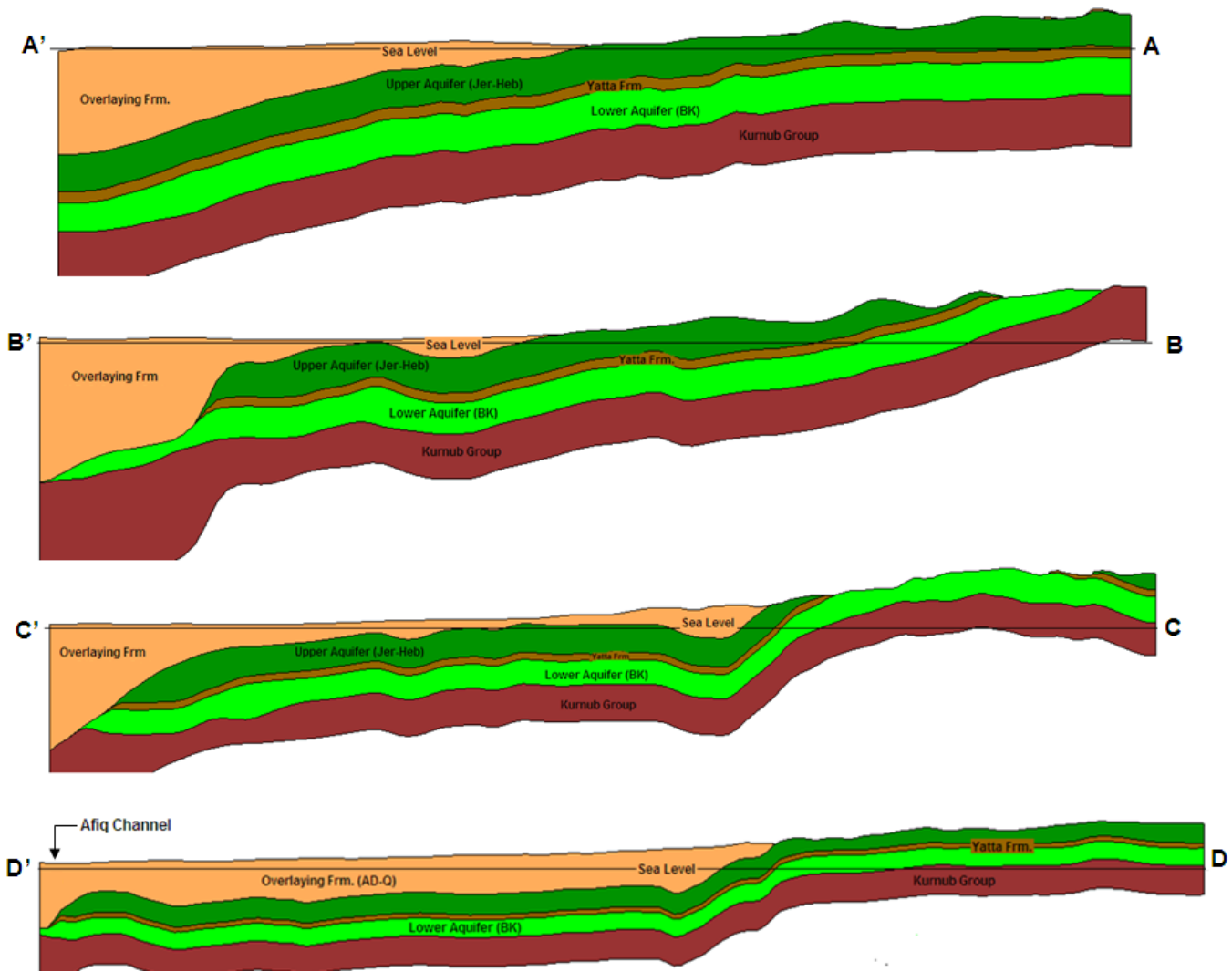


Figure 2.5: Cross sections-Part 1 (Obtained from the aquifer geometry of the WAB)

2.3.3 Southern Boundary

According to different researchers (Goldschtoff et al., 1980; Guttman et al., 1988) the southern boundary of the WAB extends to the east of Al Arish, Egypt. The inflow and outflow of the southern part of the Basin is generally very limited due to the limited rainfall. Therefore, the water dynamics of the northern part of the WAB does not seem to be affected by this area (Guttman et al., 1991). In this research, the model is limited to the area south of Beir Al Saba (North of Al Naqab Desert); from Kusseife anticline in the south-eastern side to Neogene Afiq clay channel in the south-western side of the WAB, Figure 2.6. This clay channel cuts the two sub-aquifers and can be considered as an impervious hydrological barrier (Guttman et al., 1988), Figure 2.7.

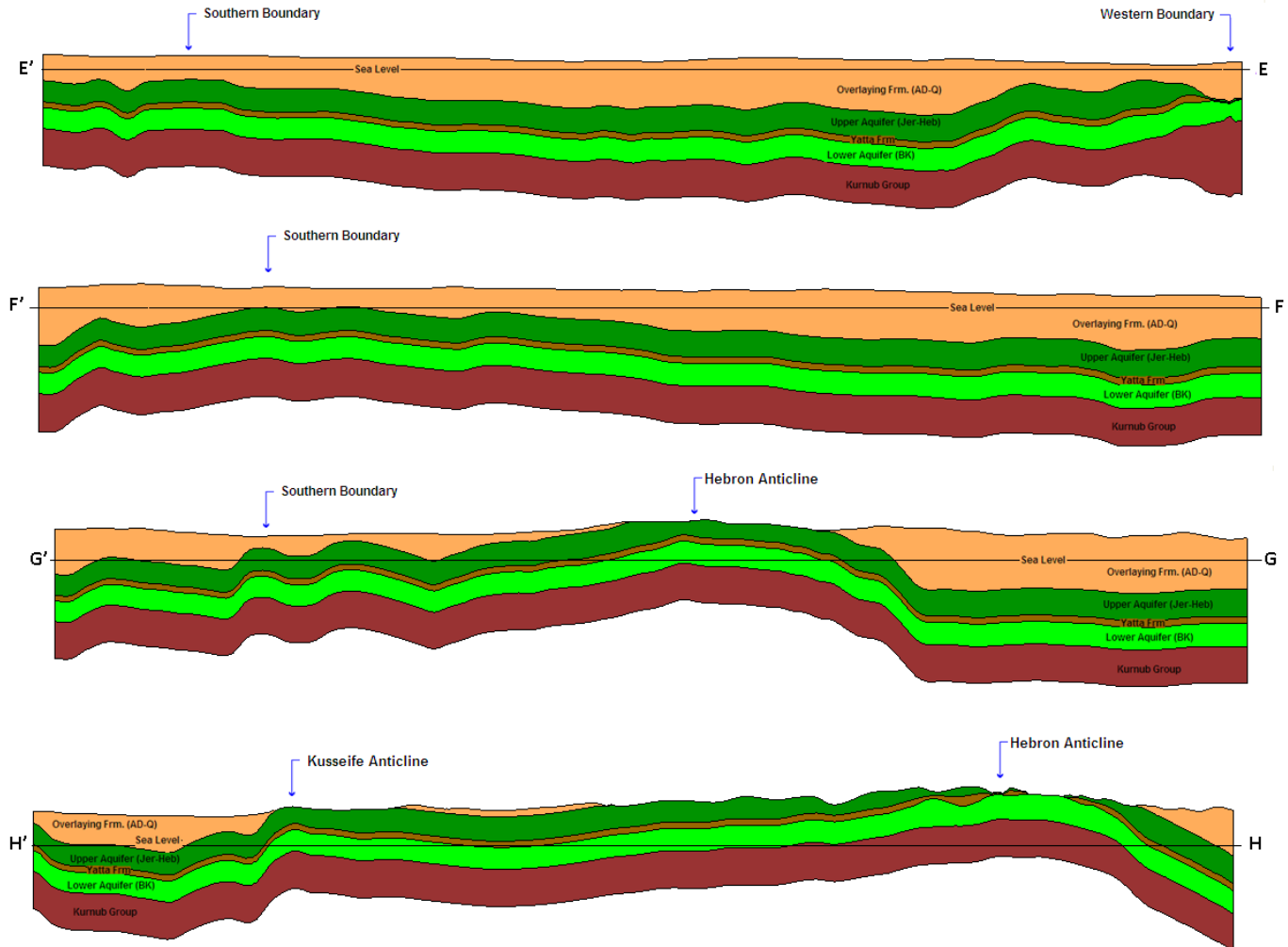


Figure 2.6: Cross sections-Part 2 (Obtained from the aquifer geometry of the WAB)

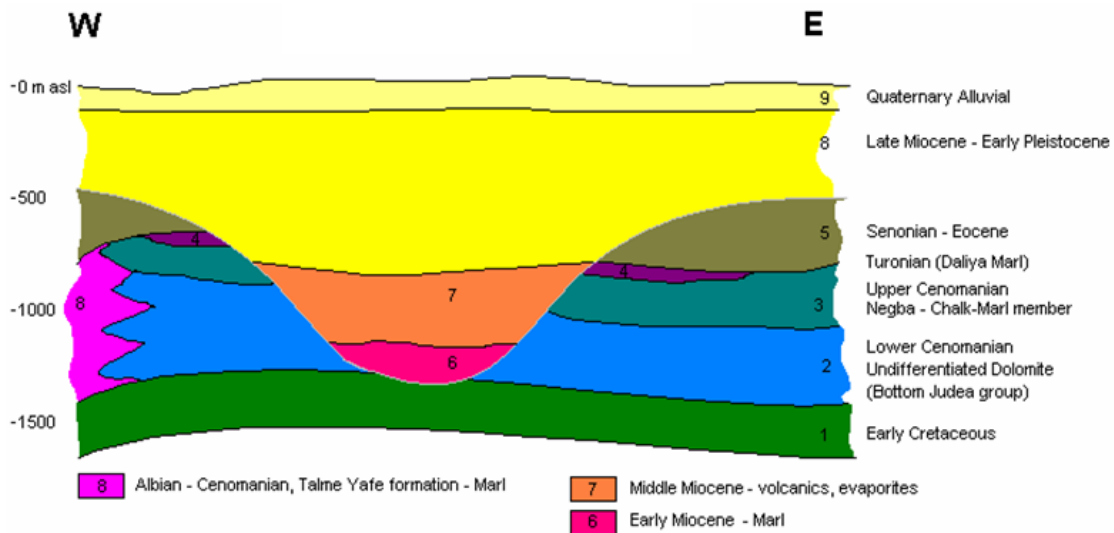


Figure 2.7: The Afig Clay Channel- Near the coast (SUSMAQ, 2004)

2.3.4 Western Boundary

The WAB is separated from the Sea by the Talme –Yafe formation except for a possible connection on the north western edge of the aquifer (Cesarea region). The amount of sea water intrusion was estimated using the chloride mass balance approach (Paster et al., 2005) taking into consideration the historical discharge rate, the water quality of Al Timsah spring which represents the mixture of fresh groundwater and sea water, salinities of both sea water and fresh groundwater (Section 2.11.1). Accordingly, the amount of sea water intrusion during the pre-development period was estimated to be at 3.5 - 3.9 Mm³/yr.

The hydraulic connection between the WAB bedrock and the Mediterranean Sea is modeled as a specified flow boundary type.

2.4 INTRA-AQUIFER HYDROLOGICAL CONNECTIONS

Due to the high marl content of the Yatta formation, many authors, (Mercado, 1980; Guttman et al., 1988; and Baida et al., 1989) suggest that it forms a hydrological barrier separating the upper and lower sub-aquifers. However, this impermeable layer does not totally prevent water from being transferred between the two main sub-aquifers. In some locations, hydrogeological evidence proves that Yatta formation is not uniform and due to severe fracturing it behaves as a permeable layer (Weinberger et al., 1993, Weiss et al., 2007). Accordingly flow may exchange between the two sub-aquifers. Based on different studies (Mercado, 1980; Kroitoru et al., 1987), and considering the groundwater balance, distribution of salinities, and transfer of solutes, (Guttman et al., 1988) have developed a map showing the areas where the two aquifers may be connected, Figure 2.8. The hypothesis hydrological and structural hypothetical considerations were:

1. The Yatta formation in the area of Beteh Tiqva and Lod T/1 wells is composed of dolomite and limestone which is similar to the upper and lower sub-aquifers. Therefore the three aquifer units in this area behave as one aquifer system.
2. The distinction of chloride concentration in Qiryat Gat #1 well (i.e. 7000 mg/l) in the lower sub-aquifer and high quality of water in the upper sub-aquifer indicates the discontinuity of connection between upper and lower sub-aquifers. However, to the

east of this well, the lower and upper sub-aquifers both have high quality fresh water, therefore, a connection between the two sub-aquifers was assumed between the area of this well and the foothills in the east.

3. In Ashalim#1 well in the south, the natural recharge is limited to the upper sub-aquifer while pumping is exclusively extracted from the lower sub-aquifer. Therefore, the upper and the lower sub-aquifers seem to be connected.
4. From the Ras Al Ain Spring in the central part of the aquifer and to the northern part of the WAB, the distinct water qualities in both sub-aquifers prove the discontinuity of the two sub aquifers (Mercado, 1980).

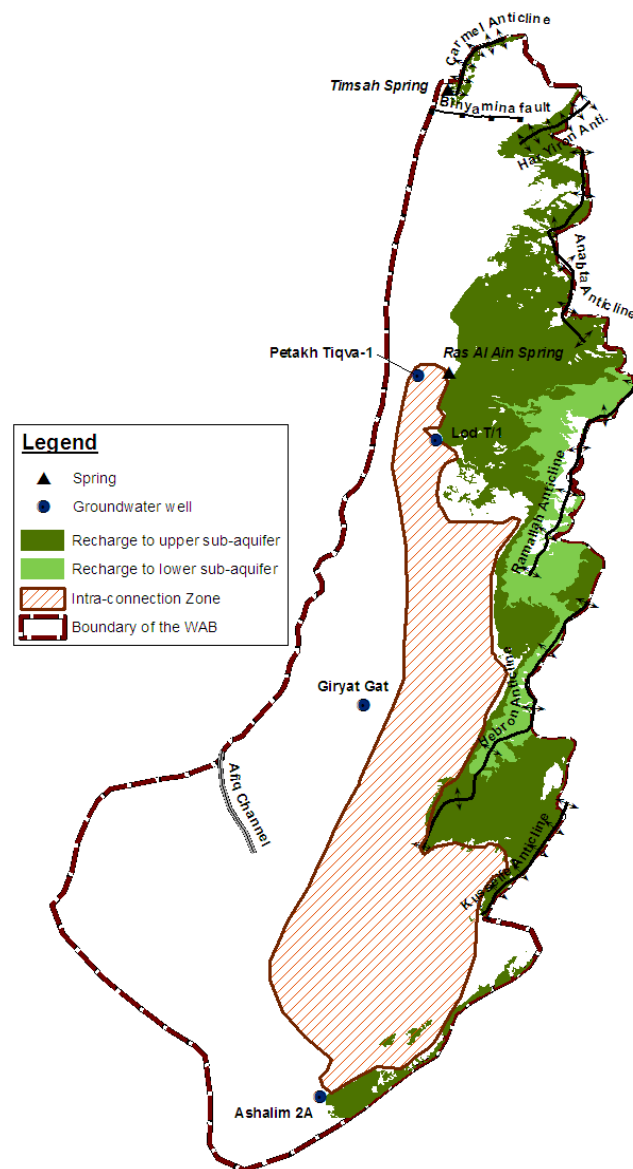


Figure 2.8: Intra-aquifer connection

2.5 NATURAL AQUIFER OUTLETS

Historically, the outflow from the WAB was limited to the two main springs; Al Timsah (Taninim) spring in the northern part of the aquifer and the Ras Al Ain (Yarkon) spring in the central part. Based on different literature, the average pre-development mean annual flow range of Ras Al Ain spring was 220 - 280 Mm³/yr and 90 - 120 Mm³/yr from Al Timsah springs (Mercado, 1980, Zukerman et al., 1999, and Berger et al., 1999).

As a result of intensive exploitation of groundwater since the 1950s, the discharge rates of both springs declined. The discharge of Ras Al Ain spring deteriorated with time until the spring became completely dry in 1973. After the heavy rain in 1991/1992, the spring started to discharge once again with a rate that reached 36 Mm³ in 1992/1993 then again decreased to much lower rates (i.e. less than 1 Mm³/yr). The discharge of Al Timsah spring also decreased from around 90-100 Mm³/yr during the 1950s to 60 - 40 Mm³/yr during the 1960 - 1980 period. After 1980, the spring discharge fluctuated between 20 - 40 Mm³/yr depending on the rainy season as well as on the pumping rate from the WAB, Figure 2.9.

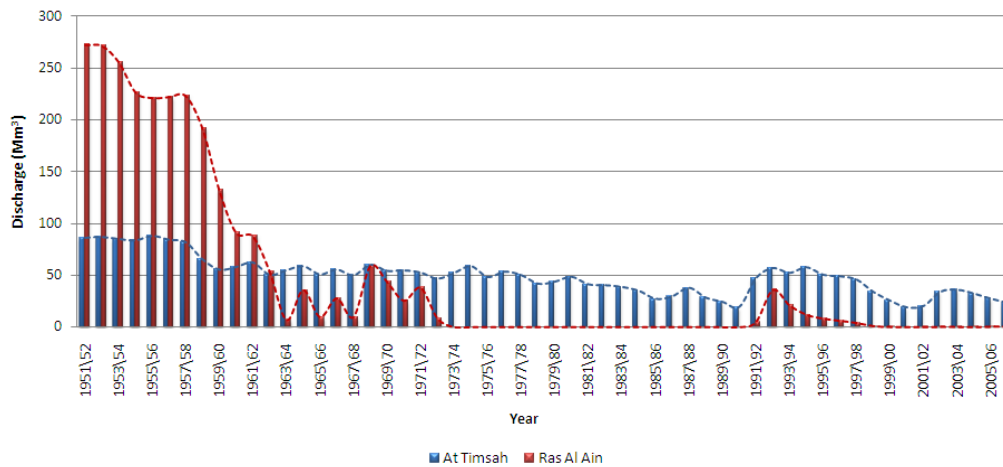


Figure 2.9: Annual discharge for Ras Al Ain and Al Timsah springs

It was assumed that the sum of the spring discharge is within the range of the long-term annual average recharge (i.e. 360-375 Mm³/yr). The two springs were modeled as drain with constant heads with their discharge is a function of the gradient near the springs and the hydraulic conductivity.

The spring discharge levels were set at 4 m and 18 m for Timsah and Ras Al Ain springs respectively then tuned during calibration in order to achieve the spring's discharge rates. For steady state modeling, the pre-development discharge of the two springs were set at $255 \pm 10 \text{ Mm}^3/\text{yr}$ for Timsah spring and $105 \pm 10 \text{ Mm}^3/\text{yr}$ for Ras Al Ain spring while the hydraulic conductivities near the two springs were obtained from model calibration.

2.6 PUMPING AND INJECTION

The exploitation of groundwater from the WAB started in the early 1950s (Zeitouni et al., 1996). In 1951, there were 46 wells pumping around 10 Mm^3 . The pumping rate was increased to around $400 \text{ Mm}^3/\text{yr}$ from 400 productive wells during the 1970s. Currently, there are 493 wells with annual pumping rates that depend on the rainy season, as the pumping rate was increased during dry years, Figure 2.10. For example, the pumping rate reached 573 Mm^3 during the dry year 1998/99; on the other hand, the pumping was decreased to less than 250 Mm^3 during the wet year 1991/92.

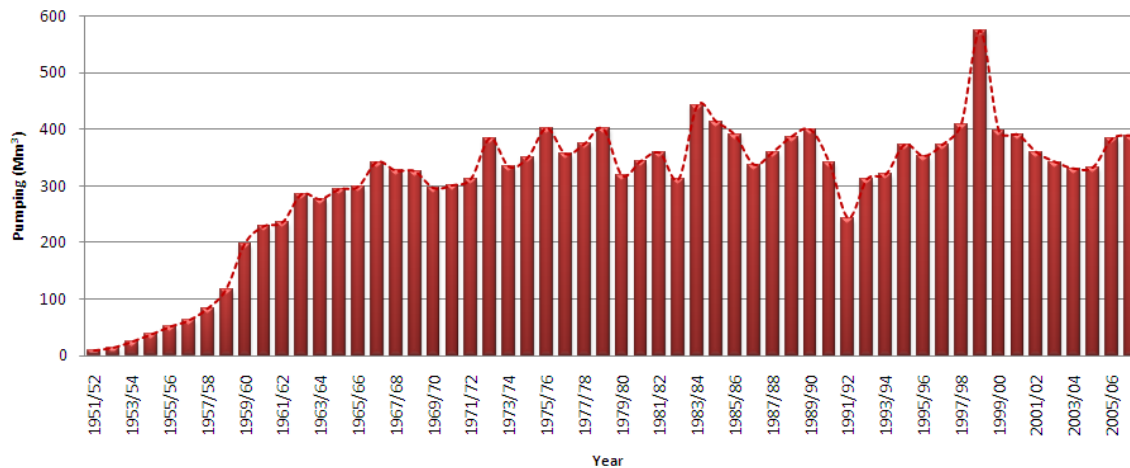


Figure 2.10: Annual pumping rates

In the south, Beir Al Saba' zone, pumping started in 1953 with 0.6 Mm^3 and then gradually increased to 40 Mm^3 in the early 1990s. Consequently, in order to keep the balance between the fresh water in the WAB layers and the deep aquifers, saline water was to pumped in 1970 with rate 0.1 Mm^3 , increasing with time to reach 2.4 Mm^3 in 1990 (Zeitouni et al., 1996). Figure 2.11, shows the locations of all groundwater wells in both layers classified according

to the pumping rates. It is clear that the majority of wells are located on the edge of the foot hills as well as within the flow passage discussed in section 2.7. Therefore, these wells capture replenishment water generated in the Hebron mountain areas of the WAB.

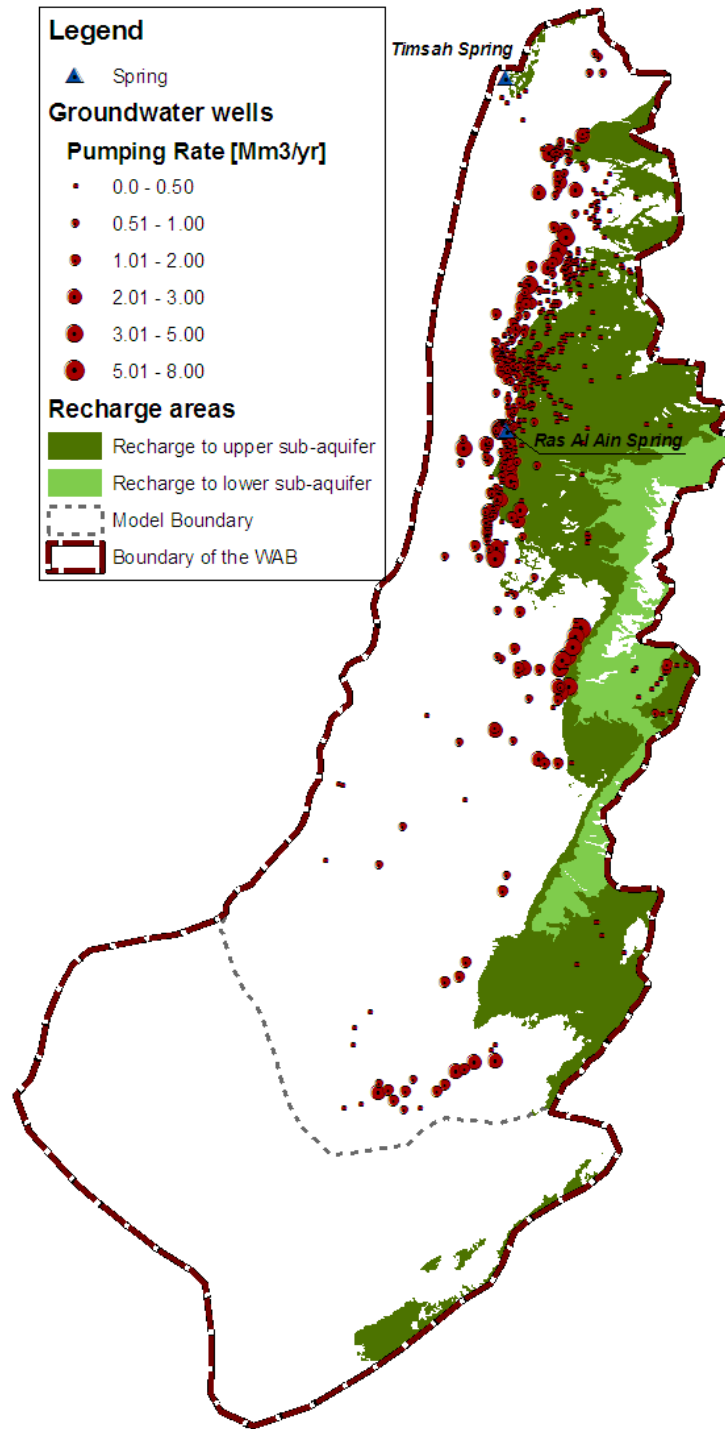


Figure 2.11: Well locations and annual pumping rates

However, a high percentage of annual natural recharge (i.e. up to 50%) flows to the lower sub-aquifer (Section 2.6), currently, around 90% of the well the upper sub-aquifer. This extensive pumping from the upper aquifer as well as the springs discharges imply significant flow from the lower to the upper sub-aquifer at a rate near the total annual replenishment of the lower sub-aquifer (Miro, 1979; Mercado, 1980).

In addition, there are 37 wells located in the northern part of the WAB used for injecting water to the aquifer during the winter season. Injecting water to the WAB was initiated after 1967 with around 10 Mm³ which later reached around 55 Mm³ in 1975. The injection rate was then decreased to lower rates after the wettest year 1991/1992, Figure 2.12.

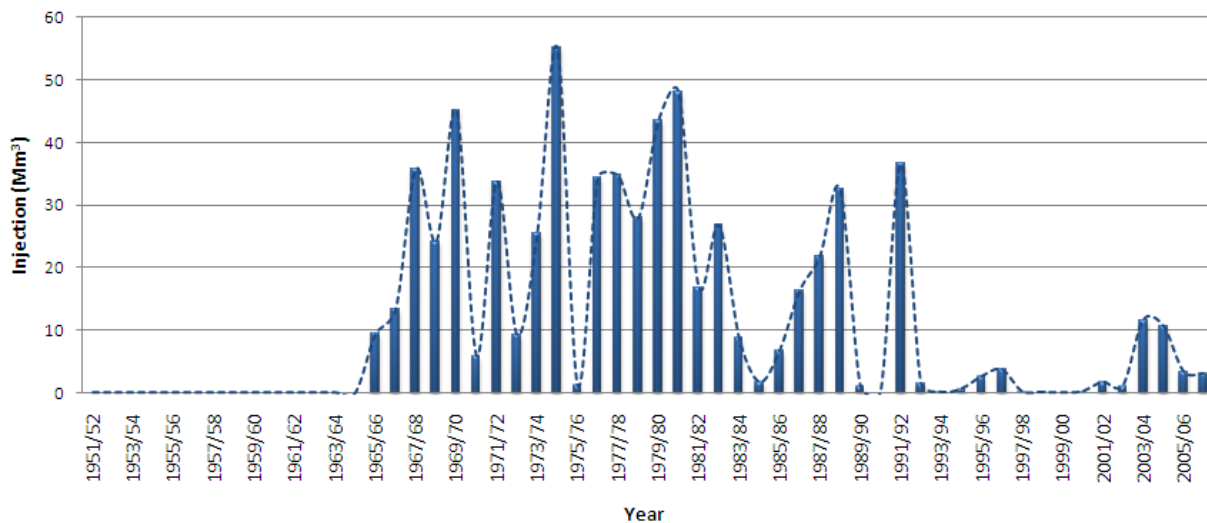


Figure 2.12: Annual Injection rates

2.7 RECHARGE

Geographically, the upper and lower sub-aquifers outcrop in the mountains in the eastern side of the WAB, Figure 2.8. While, there are many sources contributing to the aquifer recharge such as return flow from agriculture, leakage from water networks and wastewater drainage systems, rainfall over the replenishment areas is considered the major component of recharge. The mechanism of generated recharge from rainfall can take the shape of direct infiltration or infiltration through the beds of the storm water drainage systems.

The recharge is also distributed to upper and lower sub-aquifers. In the northern part of the WAB, the natural recharge to the upper sub-aquifer is relatively high while, in the central and

southern part of the WAB, high rates of recharge to the lower sub-aquifer were found (Mercado, 1980). In general, the annual rate of recharge varies according to the rainfall based on the annual amount, temporal and spatial distribution and intensity. Therefore, annual recharge ranges between the lowest value 178 Mm³ which was estimated during the dry year 1998/99 and the highest value 1005 Mm³ estimated in 1991/92. According to the characteristic of the annual rainfall, 25% - 50% flows to the lower sub-aquifer (Mercado, 1980).

2.8 WATER LEVEL

The water level in the WAB could be classified into two types according to confinement conditions. The water level in the confined part is almost flat, during the pre-development period, it is gently drops from 25-27 m near Beir Al Saba' in the south to 16 m in the Menashe heights in the north (Rosenthal et al., 1992 and Dafny et al., 2010). Due to the extensive exploitation, the water level in the confined part currently stands in the range of 14 m in the south to a range of 9 m in the north. However, the water levels in both sub-aquifers are similar in the water level distribution; the water levels in the lower sub-aquifer seem slightly higher than in the upper sub- aquifer (Baida et al., 1989). Also, due to the high continuity of the WAB, the piezometric level responds the same all over the aquifer (Weinberger et al., 1994).

In natural replenishment areas, the water level is significantly influenced by the layer geometry; accordingly, the water levels in the two sub-aquifers are different. During the pre-development period, the water levels were 450 - 500m in Jerusalem area (Ein Karem), in Hebron Mountains water level was 350 - 450 m in the lower sub- aquifer and 550-700m in the upper sub-aquifer and 300 - 350m in Salfit area (Weinberger et al., 1994, Guttman et al., 1988, Dafny et. al., 2010).

2.9 FLOW DIRECTIONS

Groundwater flows from the replenishment areas of the WAB towards the confined part in both upper and lower sub-aquifers. In the northern part of the replenishment areas, Tulkarem and Salfit zones, water flow towards the northwestern direction. In the central and southern

parts, Jerusalem and Hebron zones respectively, water flows towards the southwestern direction due to Ramallah and Hebron anticlines, Figure 2.13. The water reaching Beir Al Saba' in the south from Hebron zones is diverted to the north due to the impervious western barrier impeding flow seaward (Weinberger et al., 1994). This flow accumulates with other flows coming from the replenishment areas in the northern and central parts of the WAB and flows to the north through narrow passages of 8 - 10 km length to the west of foothills (Weinberger et al., 1994).

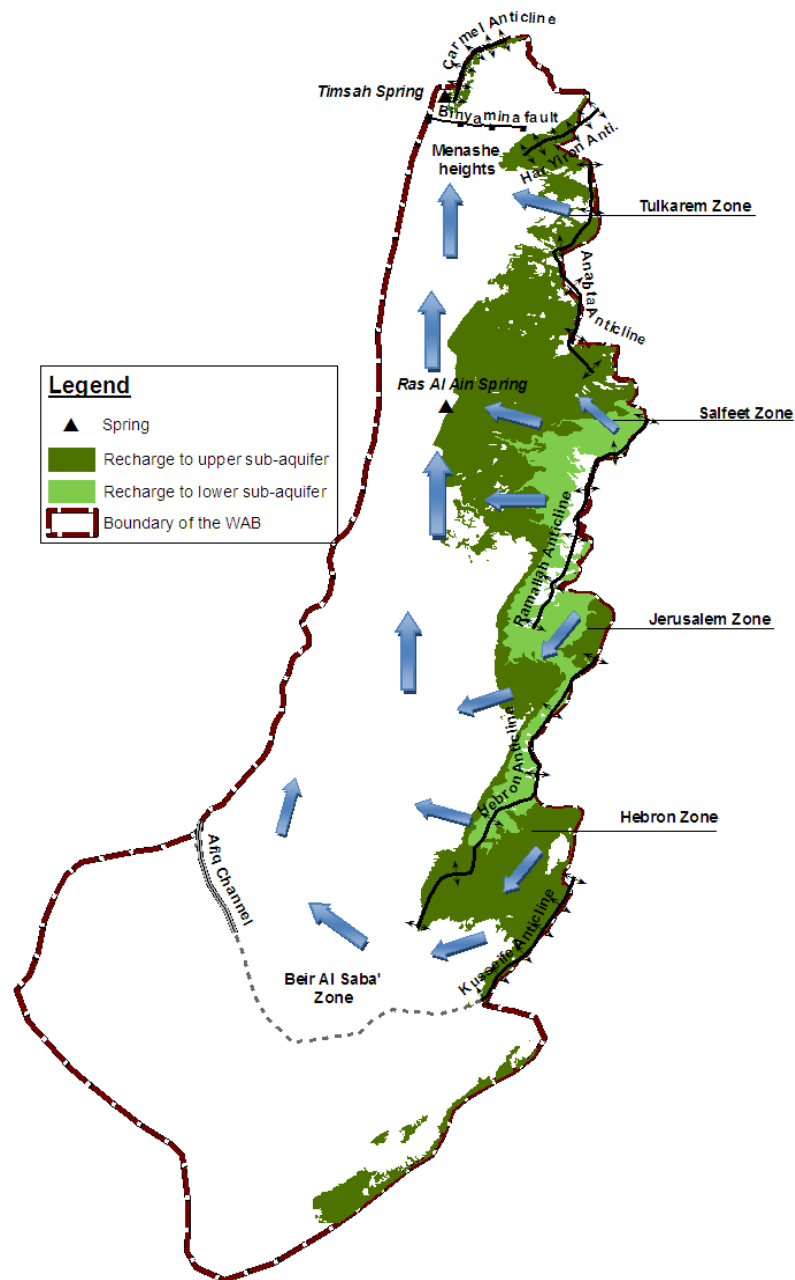


Figure 2.13: Flow direction map

2.10 PHYSICAL PROPERTIES

According to pumping test analysis results, the transmissivities in the unconfined part of the aquifer were estimated at about hundreds of squared meters per day (m^2/d). On the contrary, in the confined areas, the transmissivity in both sub-aquifers were estimated to be very high within the range of tens and even thousands of squared meters per day (Berger et al., 1999; Guttman, et al., 1995). The vertical conductivity was estimated to be within a very low range from 1.3×10^{-6} to 2.2×10^{-4} m/d (Weiss et al., 2007).

Previous studies, in addition to field observations show high conductivity in the confined sections of the central part of the WAB as a result of high karstification. Some of these observations have been used later to verify the numerical model developed for the aquifer:

- In Ayalon and Kefar Urriya wells, Figure 2.15, no measurable drawdown was observed during pumping tests (Frumkin et. al., 2005).
- In the same area, water level rises faster during wet years (Ecker et. al., 1995 and Shachnai et. al., 1999).
- During the wet year 1991/92, the water level in the central part rises to higher levels than the southern area (i.e. Beir Al Saba'). This reverses the normal flow direction where water flows from the center to the south area (Ecker, et. al., 1995 and Shachnai et. al., 1999).

The storativity values also vary from confined to unconfined areas of the WAB. The storativity values in confined areas were found to be between 10^{-4} of 10^{-5} (Guttman et. al., 1995) while in the unconfined areas, the specific yield ranges between 1.8% - 8% (Tsukerman et al., 1999). These values were found to be similar to other karstic aquifers (Dafny et. al., 2010, and Peleg et. al., 2010).

2.11 SALINITY AND SALINIZATION PROCESS

The salinity within the WAB is different from place to place. For this reason, the aquifer is divided into three zones where the salinity, the source of saline water and the salinization process are clarified.

2.11.1 Northern Area

The chloride concentrations vary from 30-100 mg/l in the eastern part of the Basin close to the replenishment areas of the aquifer in both upper and lower sub-aquifers, Figure 2.14, and then sharply increase to the west to salinity values exceeding 10000 mg/l as encountered in the Gaash 1, Netanya Oil and Tananim Deep oil (Weinberger et. al., 1994, Mandell et, al., 2002, and Paster et, al., 2005).

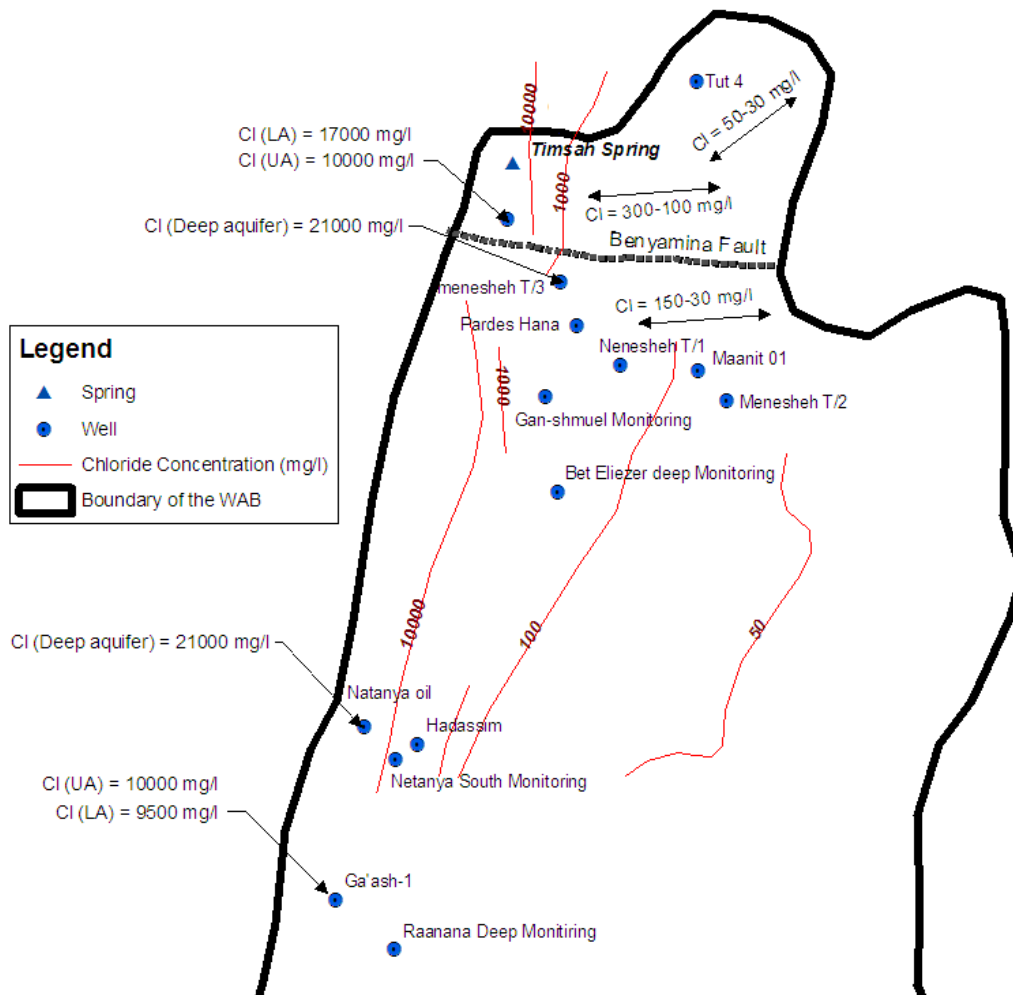


Figure 2.14: Chloride concentration in the northern part of the WAB

In the deep aquifer (Al Kumb), very high chloride concentrations (i.e. 16,000–21,000 mg/l) were found close to that of sea water. This was found near the western boundary of the aquifer, at depths of 700–1000 m and more (Paster et, al., 2005).

In the northern part of the WAB, different researchers described the salinization processes and mechanism. (Bar-Yossef et al., 1978) assumed that salinity occurred along the Binyamina fault when seawater encroached into the lower sub-aquifer and dispersed into the overlying, upper sub-aquifer. (Mercado, 1980) added to the assumption that the source of salinity could be due to upflowing brines originating from deep-seated and confined Lower Cretaceous-Lower Cenomanian layers. Additionally, researchers mentioned that the WAB is overlain by Senonian group and underlain by the Lower Cretaceous Kurnub group. In both groups, saline groundwater exists which may percolate either along faults or along leaking and badly maintained well-casings to the WAB sub-aquifers. (Mandell et al., 2002) concluded that the salinity in the northern part of the aquifer comes as a result of mixing of sea water and saline water from the deep aquifer.

(Paster et al., 2005) used the data obtained from the new monitoring wells drilled in the northern part of the WAB to study the salinization process and mechanisms. The main finding was that saline water body in the deep aquifer is not geologically separated from the fresh water, where the fresh and saline is separated with relatively thin transmission zone, Figure 2.15. Additionally, the fact that head of saline water (h_s) is lower than sea level confirms that the deep aquifer and the Sea are not connected.

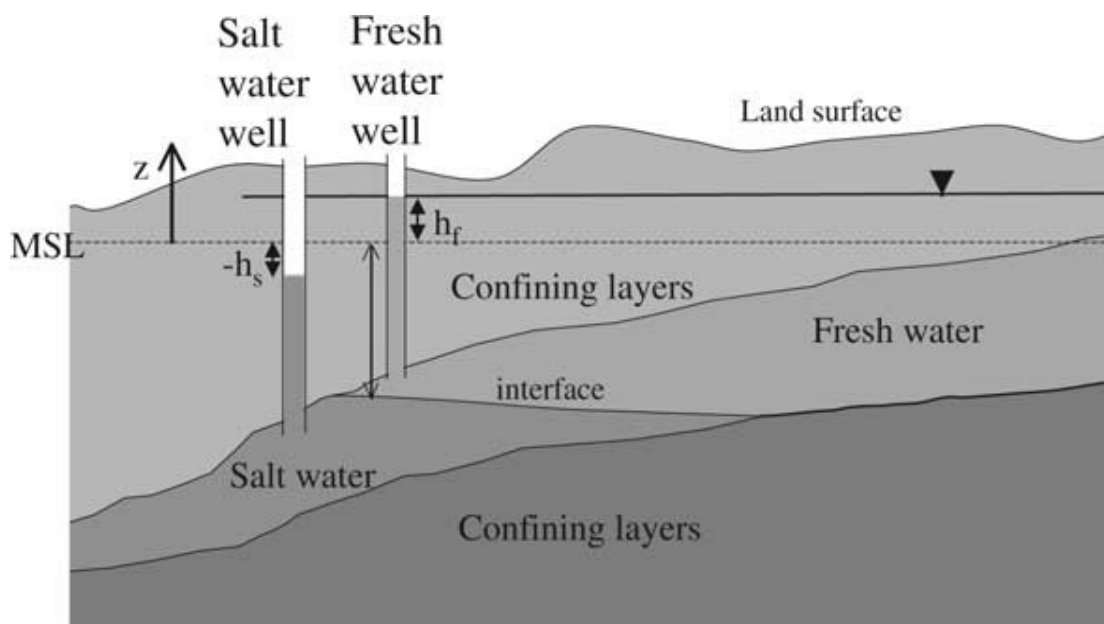


Figure 2.15: Sketch of interface location in the northern part of the WAB (Paster et al., 2005)

(Paster et al., 2005) supported the hypothesis that connection of the WAB with the Sea through a low permeability zone that operates under the difference between sea level and the (hs). This connection may convey the sea water to the lower sub-aquifer.

According to recent results, (Paster et al., 2005), assumed that equilibrium between the deep saline water and the fresh water had been reached during the pre-development period. Accordingly, a permanent sea water intrude to the WAB was flushed out by fresh water through the Timsah spring. Using the available data in the early 1950s, sea water intrusion was estimated use the following equation:

$$Q_{ST} C_S + (Q_T - Q_{ST}) C_F = Q_T C_T \quad \text{Eq.2.2}$$

Where:

Q_{ST} : Sea water intrude to the WAB (Mm^3/yr)

C_S : Chloride concentration in the sea water (22,000 mg/l)

Q_T : Pre-development discharge of Al Timsah spring (95–100 Mm^3/yr)

C_F : Chloride concentration in the fresh aquifer water (100 mg/l)

C_T : Chloride concentration of the pre-development spring discharge (900–950 mg/l)

By solving Eq.2.2, the amount of sea water intrusion ranged between 3.5 and 3.9 Mm^3/yr .

2.11.2 Central Area

In the central part of the Basin close to Kefar Urriya wells, an abnormal brackish groundwater spread over an area of about 200 km^2 having an ellipsoid form was found (Frumkin et al., 2005). The highest concentration at the center reaches around 500 mg/l and then decreases in all directions to reach high quality water on the edges, Figure 2.16. Consequently, the lateral flow of saline water to this area was excluded as a source of saline water. Most of the studies referred the salinity in the central part of the WAB to two possible sources; the first mechanism assumed that the salinity comes from the top since the salinity decreases with depth in the upper 150 m of the aquifer (e.g. Gimzu 1 and Kefar Uriya 4

wells) (Frumkin et al., 2005). Many authors (Avisar et al., 2002, Ecker et al., 1995, Mandell et al., 2002) suggested that salts are:

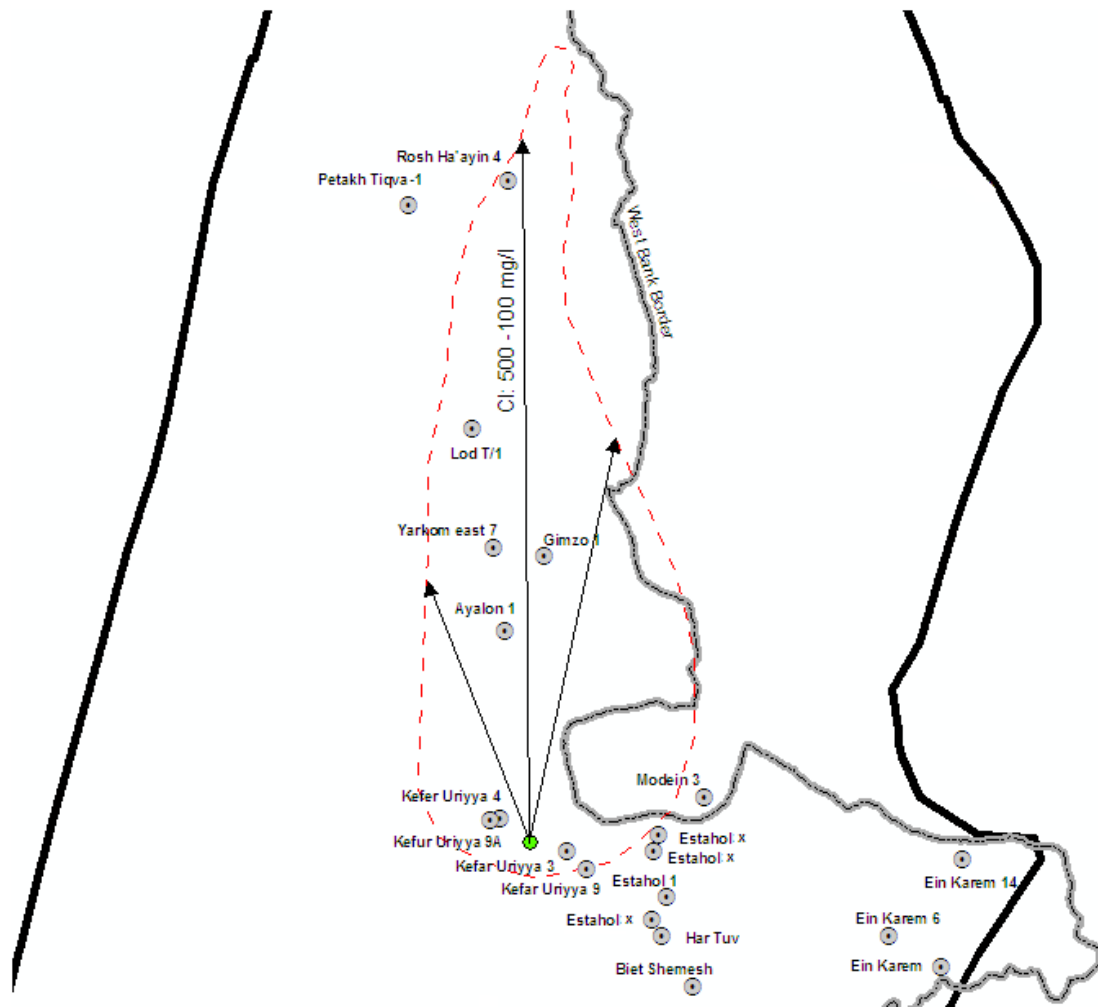


Figure 2.16: Chloride concentration in the central part of the WAB

1. Flushed from the chalks in the overlaying layer (i.e. Abu Dees)
2. Leached of sewage effluent (Ronen and Kanfi, 1978)
3. Percolated by natural recharge through soils and rock debris characterized by high concentration of salts (Frumkin et al., 2005).

The second mechanism suggests deep source of the salinity. Based on geochemical analysis, (Frumkin et al., 1999 and Katz et al., 2001), proposed vertical upward flow of the saline water.

2.11.3 Southern Area

The chloride concentration in the replenishment area in the east is low within the range of 60 mg/l and then increases to the south and west to higher concentrations, Figure 2.17. In Beir Sheva' and Hazerim #1 wells, the chloride concentrations reached around 250 mg/l and then exceeded 1000 mg/l in the western and southern areas.



Figure 2.17: Chloride concentration in the southern part of the WAB

The salinity in this region originated from either the underlining deep salty aquifer (Al Kurnb) or the overlaying chalky layer (Weinberger et al., 1994). There are two mechanisms identified for the salinization of the southern part of the WAB:

1. Saline water from the top percolates downwards along poorly cemented well casings.

2. Along fault cuttings, the WAB layers are vertically displaced against both underlying Al Kurnub group and overlying Senonian group, Figure 2.18. Thus, saline water from both groups can flow to the WAB layers which then mixed with fresh water (Weinberger et. al., 1993).

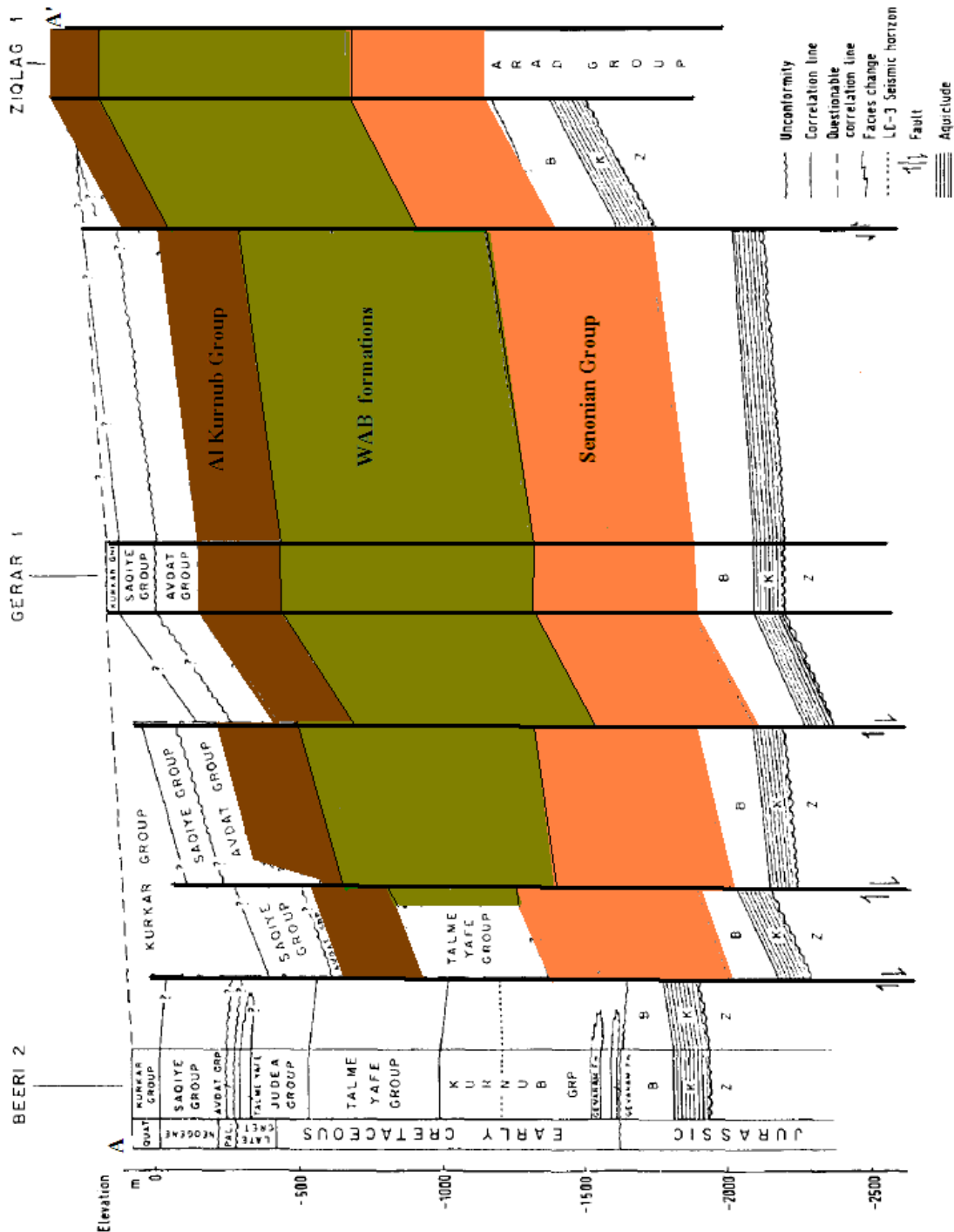


Figure 2.18: Cross section A-A' in the southern part of the WAB (after Weinberger et. al., 1993)

Chapter 3

CHAPTER 3: RAINFALL ANALYSIS AND ESTIMATION OF GROUNDWATER RECHARGE

3.1 INTRODUCTION

In general, rainfall over a certain area can undergo evaporation, runoff and infiltration into the soil and later reach groundwater. Directing precipitation to any of these paths will chiefly be based on different spatial and temporal distributions of both meteorological and physical factors. The land use, soil type, topography and other physical characteristics as well as rainfall characteristics, temperature, wind speed and direction, solar radiation, and many other meteorological parameters will also contribute in determining the percentages and distribution of each of the water cycle components.

In arid and semi-arid regions, as the case in the WAB, rainfall is limited to a short period of time within the year with high variation in seasonal quantity, distribution and intensity. Accordingly, this variation in rainfall plays a major role in determining the rates of annual generated recharge. The rainfall over the replenishment area of the WAB most often starts in October and ends in April with an average annual precipitation of around 560 mm. The larger portion of rainfall occurs during four months: November, December, January and February representing 60-90% of the annual precipitation amounts.

The environmental and physical characteristics in the study area increase the complexity in quantifying the water cycle components. To estimate these components, the availability of extensive data and formulation of detailed modeling were required. In the context of this study, quantifying groundwater recharge for the WAB is highly sensitive for better aquifer management and for building the numerical model that takes the recharge variation into account.

The recharge of the WAB was previously estimated based on empirical equations that relate the annual rainfall to annual recharge. These equations ignore the high variation of annual rainfall and its distribution. Therefore, an alternative technique that takes the rainfall variation and its impact on the recharge component is needed. In this chapter, the annual

recharge was determined based on the water level fluctuation approach and then detailed analysis of the impact of temporal rainfall variation on the estimated recharge was carried out. For this reason, the historical records of the water levels, inflows and outflows of the aquifer were used. In light of the obtained results, a new empirical equation taking the rainfall variations into account was developed.

3.2 THE PREVIOUS RECHARGE ESTIMATION TECHNIQUE

It was found that the annual precipitation over the replenishment areas is the dominant natural source of recharge for the WAB (Blake et al., 1947; Mercado et al., 1980; Guttman et al., 1988; Rosenthal et al., 1992). Generally, the up to date accepted approach for estimating the annual recharge for the WAB is the empirical equation (Guttman's equation) which correlates the annual recharge with annual rainfall, Eq. 3.1. This equation was developed by using an inverse calibration technique, whereby recharge is estimated by following the calibration of heads and groundwater flow rates (Weiss et al., 2007).

$$Rc(T) = \begin{cases} 0.45 \times [Rf(T) - 180] & Rf(T) < 600mm \\ 0.88 \times [Rf(T) - 410] & 600 < Rf(T) < 1000mm \\ 0.97 \times [Rf(T) - 463] & Rf(T) > 1000mm \end{cases} \quad Eq\ 3.1$$

Where:

$Rc(T)$: Annual recharge (mm)

$Rf(T)$: Annual rainfall (mm)

T : year

Accordingly, since the annual precipitation ranges between 250 and 1350 mm, groundwater recharge in the WAB will range between 6% and approximately 65% of the rainfall (Weiss et al., 2007). The average recharge to rainfall coefficient was estimated within the range of 30 - 33%. The recharge to rainfall ratio was considered high for the WAB compared to the other aquifers due to the high karstification (Guttman et al., 1995). However, Eq. 3.1, related the annual recharge to the annual rainfall, it neglected the temporal variation in rainfall distribution, Figure 3.1. This approach requires review and further rainfall and recharge analysis are still needed.

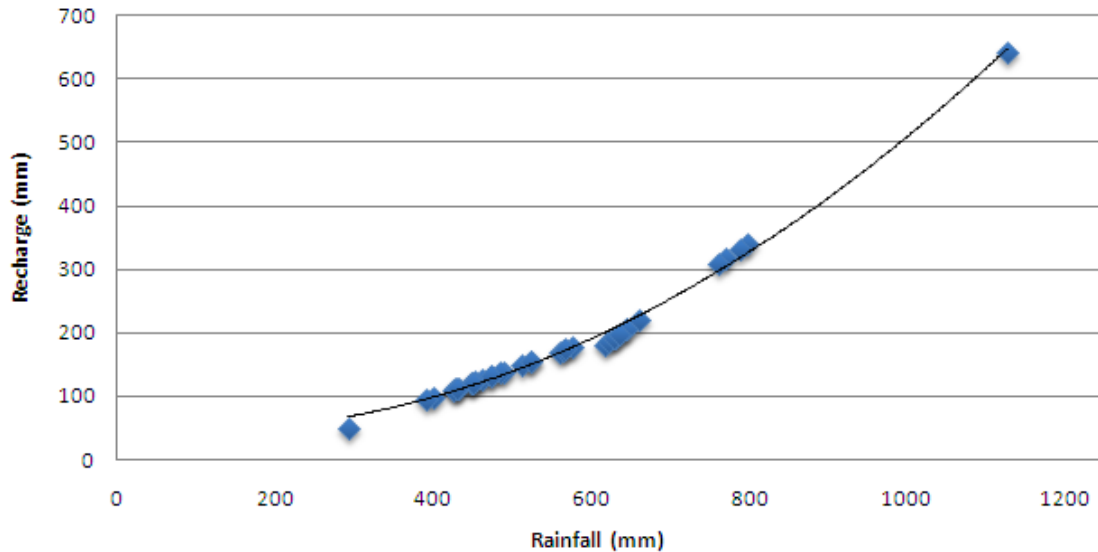
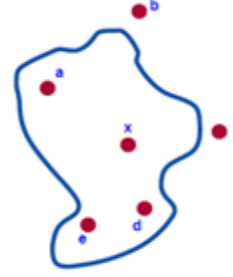


Figure 3.1: Recharge - rainfall relation according to Guttman's Equation

3.3 RAINFALL OVER THE WAB

The WAB is characterized by its Mediterranean climate with climate zones ranging from arid desert conditions in the Al Naqab desert to sub-humid Mediterranean climate conditions in the centre and north of the basin. Within the boundary of the West Bank, there are 48 rainfall stations distributed over the replenishment areas of the WAB with monthly records. These stations were used to estimate the monthly average of rainfall over the replenishment areas of the WAB for the period from September 1970 to August 2006. The procedure for developing the average monthly rainfall time series is clarified in the following steps:

1. Defining the replenishment areas of WAB which include all impermeable outcropping formations.
2. Building a Thiessen polygon network for all rainfall stations.
3. Remove all polygons that do not intersect with the replenishment area and then select all relevant stations.
4. Filling all the data missing for these stations, using the normal ratio method. For example, estimating the missing rainfall value in a station (x) is based on the nearby stations (a, b, c, ..., etc.) as in Eq. 3.2:



$$R_x(t) = \frac{\bar{R}_x}{n} \left(\frac{R_a(t)}{R_a} + \frac{R_b(t)}{R_b} + \dots + \frac{R_n(t)}{R_n} \right)$$

Eq 3.2

Where:

$R_x(t)$: Estimated rainfall for the time interval t at location x

$R_{x,a,b,\dots,n}(t)$: Measured rainfall for the time interval t at locations a, b, \dots, n

$\bar{R}_{x,a,b,\dots,n}$: Long-term average rainfall at used station

n : Number of the stations used excluding station x

5. Using ArcGIS, the recharge areas within the Thiessen polygons were overlapped and intersected with the replenishment areas. Then all areas not overlapping with the replenishment areas were removed. Relevant rainfall station was also assigned to each recharge polygon, Figure 3.2.
6. Finally, using the areas of the final replenishment polygons and the monthly rainfall time series, the monthly average rainfall for the recharge areas of the WAB were calculated using Eq. 3.3.

$$R_{avg}^i = \frac{\sum_{j=1}^N (R_j^i \times A_j)}{\sum_{j=1}^N A_j} \quad \text{Eq 3.3}$$

Where:

R_{avg}^i : Average rainfall over replenishment area in month i

R_j^i : Rainfall in month i , Thiessen polygon j

A_j : The sum of areas of all replenishment polygons located in Thiessen polygon j

N : Number of Thiessen polygon j

Accordingly, the average monthly rainfall time series during the period September 1970 to August 2007 were achieved for all replenishment areas of the WAB. This long-term average

rainfall were analyzed and used later for estimating the accumulated annual recharge of the basin, Figure 3.2.

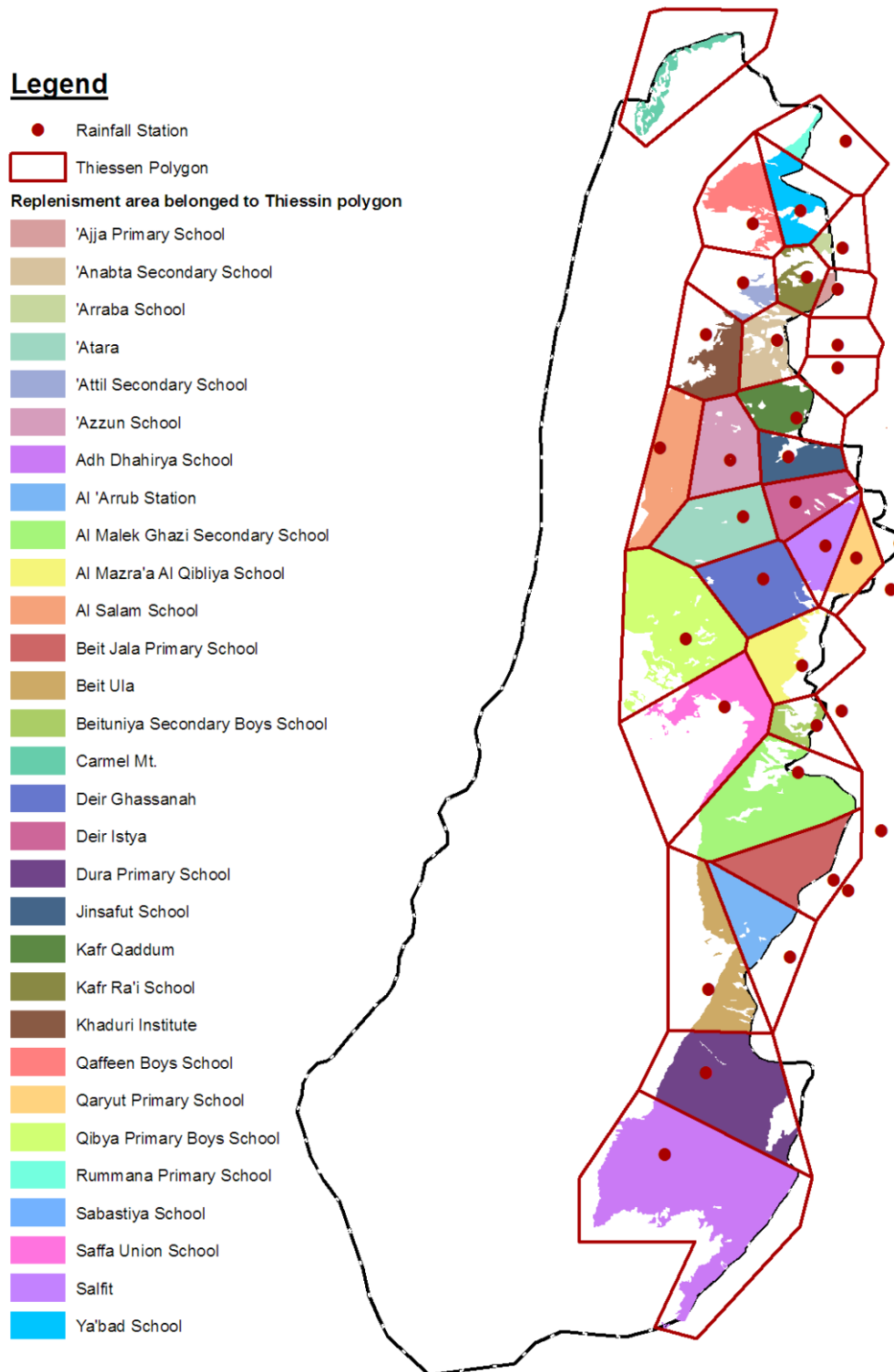


Figure 3.2: Location of rainfall stations over recharge areas of WAB

The mean monthly rainfall in the recharge area of the WAB and its characteristics are shown in Table 1.1.

Table 3.1: Monthly rainfall characteristics over recharge areas of the WAB

Parameter	Unit	Monthly Rainfall Characteristics									
		Sep	Oct	Nov	Dec	Jan	Feb	Mar	Apr	May	Total
% Annual Average	%	0.0	3.1	11.1	21.3	24.7	20.8	13.9	4.4	0.6	100
Mean	mm	0.2	17.5	62	119.1	138.2	116.2	77.7	24.5	3.6	559
Standard Deviation		0.6	17.4	56	77.2	69.2	69	41.6	32.9	6.8	155.2
Maximum		3	66	235	350	387	325	168	180	33	1126
Minimum		0	0	3	12	36	28	7	0	0	293

The mean annual rainfall was calculated to 559 mm/yr. The distribution, Figure 3.3, shows a high variability of annual rainfall with a high standard deviation of 155.2 mm. This is best elaborated by a comparison between the maximum and minimum annual rainfall values as well as its monthly distribution; the years of 1991/92 recorded the maximum rainfall amounts of 1123 mm, while the minimum recorded rainfall was 293 mm in the year 1998/99.

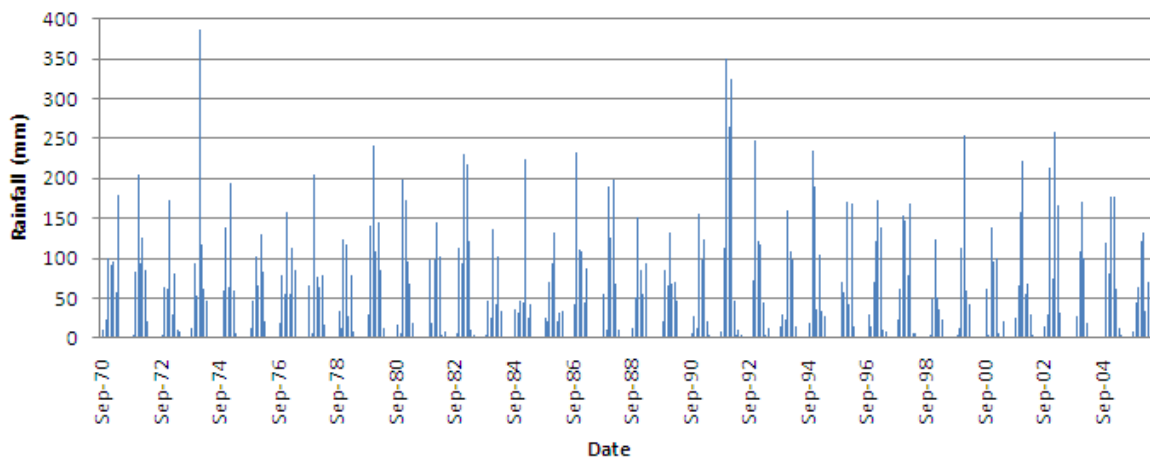


Figure 3.3: Monthly rainfall records over the recharge areas of the WAB

In addition to the high variation of monthly rainfall over the replenishment areas of the WAB, the rainfall has the following characteristics:

- The shape of the annual distribution of rain is normal to a log-normal distribution skewing to the right (towards March and April), Figure 3.4.



Figure 3.4: Mean of monthly rainfall over the recharge areas of the WAB

- January shows the highest average amount of rainfall of 138.2 mm representing 24.7% of the annual average. Additionally, in January, the highest monthly rainfall rates were found for January 1974 reaching a total of 387 mm.
- Most of the annual rainfall occurs during December, January and February with an average of 65% of the mean annual rainfall.
- The rainfall during September and May present the lowest values during the year standing for less than 1% of the annual average.
- Rainfall in April is generally very low (4.4% of the annual average), with a few exceptions of high intensity storms such as that in 1971, which generated approximately 180 mm.
- November and March have moderate average rainfall depths (11.1% and 13.9% respectively).
- Records show that rainfall during summer months is almost nonexistent (June, July and August).

3.4 RECHARGE ESTIMATION TECHNIQUE

The water level fluctuation (WLF) technique is considered as one of the traditional approaches for estimating groundwater recharge (Gieske, 1992). Accordingly, recharge can be determined by examining water level fluctuations shown in well hydrographs, where it is assumed that if no recharge occurred, then the hydrograph recession would continue until a base level is reached. By extending the hydrograph recessions, the difference between the

extrapolated recession curve and the actual groundwater level, multiplied by the specific yield, corresponds to the amount of recharge for that time period, taking into account any abstractions or infiltrations/injections and the net balance of inflows and outflows (Kruseman, 1997).

While, the WLF technique is commonly used in unconfined aquifers, it can also be used for the WAB as a special case due to many reasons; first, it is composed of two layers which both have confined and unconfined conditions. Second, the two sub-aquifers are connected in many places due to severe fracturing affects as well as due to the composition of Yatta formation which is not uniform, therefore, in many places; it behaves as a one permeable layer (Weinberger et al., 1993 and Weiss, et al, 2007). Accordingly, flow could exchange between the two sub-aquifers and also water levels in both layers in the confined part are almost the same (Baida et al., 1989).

Third, the water levels in the confined part of the two sub-aquifers were distributed systematically from north to south. Figure 3.5, shows a sample of water levels at some observed wells which proves that water levels within these wells are highly correlated, meaning that water levels in the entire aquifer will be systematically affected as a result of any abstraction, injection or natural recharge. Accordingly, the WLF technique could be applied where the average drop/rise of the water level in the confined part of the aquifer could be used as an indicator for the amount of inflow or outflow and could be mathematically described based on the Kruseman approach, 1997, using the following equation, Eq. 3.4:

$$R(T) = \alpha \times \Delta h(T) + Q_o(T) - Q(T)_{\text{other inflows}} \quad \text{Eq. 3.4}$$

Where:

R: Recharge (m^3) during period *T*

Δh: Average change in water table elevation (*m*) during period *T*.

α: Storage coefficient (m^3/m)

Q_o: Sum of outflow (m^3)

Q_{other inflows}: Sea water intrusion, artificial recharge, lateral flow (m^3) during period *T*

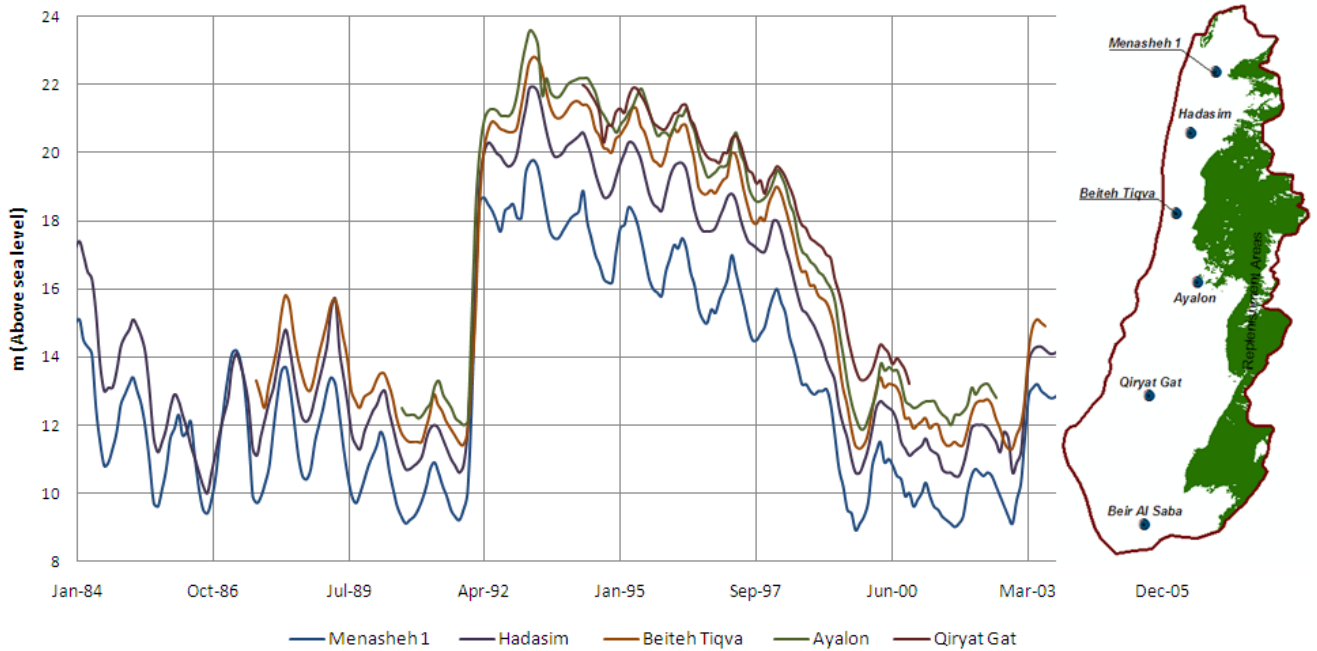


Figure 3.5: Water level for different observed well within the confined part of the WAB

Since α is not yet defined, Eq. 3.4 has two unknowns. As a result, quantifying recharge for any time interval is still not possible. This problem can be solved by looking for a period within the historical records of the average water level where the start and the end of the selected period have the same level (one complete cycle), Figure 3.6. During this period, the net storage of the aquifer should be equal to zero. Accordingly, the term $(\alpha \times \Delta h)$ becomes zero, R over this period will then equal the net outflow during the same period.

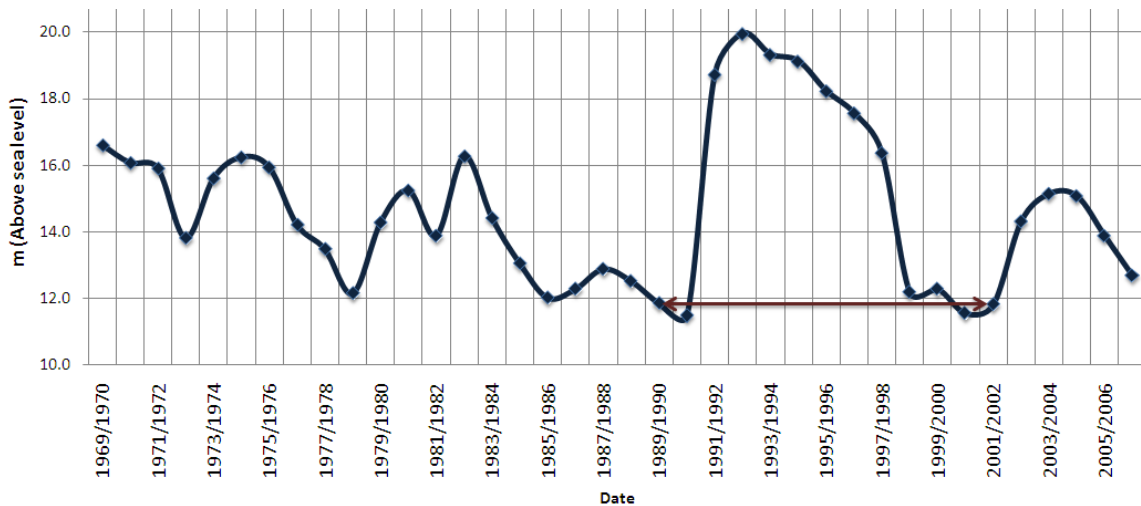


Figure 3.6: Average water level in the confined part (generated from monitoring wells and HSI, 2007)

The average water level in the confined part of the WAB was generated from the water level time series of the observed wells within the confined part of the aquifer, Figures 3.5 and 5.6, and validated by the mean annual water level which was calculated by the Hydrological Service of Israel (HSI, 2007) using the same monitoring wells. The figure shows different water level cycles. The cycle restricted between 1989/90 and 2001/02 was selected and water balance analyses have been conducted.

3.5 INFLOW AND OUTFLOW

The sum of outflow from the WAB is equal to the wells' abstraction and springs' discharge rates. While, the sum of inflow to the WAB is equal to the natural recharge, sea water intrusion and injected water. Consequently, subtracting the total amounts of water flowing into the aquifer through both artificial recharge and sea water intrusion from the sum of annual outflow, for the past 13 years, yields a value equal to the sum of recharge over that same period, Eq. 3.5. This means that for any specific year, the recharge is equal to outflow plus the change in aquifer storage. Table 3.2 shows the total amounts of annual inflow and outflow with all its items during the analyzed period as well as the net annual outflow (Q_{net}) from the WAB.

$$\sum_{1989/90}^{2001/02} R_i = \sum_{1989/90}^{2001/02} (Q_i^w + Q_i^s) - \sum_{1989/90}^{2001/02} (Q_i^{ar} + Q_i^{se}) \quad Eq\ 3.5$$

Where:

i : Year

R : Recharge (Mm^3)

Q^w : Pumping (Mm^3)

Q^s : Springs discharge (Mm^3)

Q^{ar} : Artificial recharge (Mm^3)

Q^{se} : Sea water intrusion (Mm^3)

Table 3.2: Water balance during the period 1989/90 to 2001/02¹

Year	Pumping from the WAB	Total spring discharge	Sea water intrusion ¹	Total injection	Net outflow
	Mm ³				
1989/90	400.8	26.2	3.9	1.1	422
1990/91	342.3	18.8	3.9	0	357.2
1991/92	245.1	59.5	3.9	36.6	264.1
1992/93	313.6	97.2	3.9	1.5	405.4
1993/94	321.5	75	3.9	0.1	392.5
1994/95	374.4	70.7	3.9	0.6	440.6
1995/96	354.7	59	3.9	2.6	407.2
1996/97	375.2	57.8	3.9	3.7	425.4
1997/98	412.7	51.6	3.9	0.2	460.2
1998/99	576.1	35	3.9	0.1	607.1
1999/00	400.8	27.1	3.9	0	424
2000/01	395.3	19.2	3.9	0.2	410.4
2001/02	364.7	20.3	3.9	1.7	379.4
Sum	4877.2	617.4	50.7	48.4	5395.5

As a result, the sum of recharge over the past 13 years is equal to the sum of the net outflow (i.e. 5395.5 Mm³ = 415 Mm³/yr). For the same period, the average estimated recharge using Guttman's equation was equal to 341 Mm³/yr, which is 74 Mm³ less than the recharge estimated by the water level fluctuation (WLF) technique meaning that the recharge was underestimated.

3.6 STORAGE COEFFICIENT

The storage coefficient of the WAB (α) is defined as the total water that could be abstracted from or injected into the WAB per one meter drop/rise in the confined part of the WAB. Based on this definition and taking the water level during year 1989/90 as a reference, the

¹ See Chapter 1, the upper limit is used for the water balance.

amount of water stored in the aquifer at time (t) is calculated through the following equation Eq. 3.6:

$$S(t) = \alpha \times h(t) \quad \text{Eq 3.6}$$

Where:

$S(t)$: Storage at time t after the water level exceed the reference water level (m^3)

$h(t)$: Average water level in the confined part (m) at time t

α : Storage coefficient of the WAB (m^3/m)

Reference year: 1989/90

During the period 1989/90 and 2001/02, the net sum of inflow was equal to the outflow (i.e. the net storage is equal to zero). Therefore, the integral of $S(t)$ over the same period is equal to the net outflow or net inflow. Then Eq. 3.6 is reduced to the following, Eq. 3.7:

$$\int_{\text{Oct 1989}}^{\text{Sep 2002}} S(t) dt = \alpha \int_{\text{Oct 1989}}^{\text{Sep 2002}} h(t) dt = \sum_{\text{Oct 1989}}^{\text{Sep 2002}} \text{inflow} = \sum_{\text{Oct 1989}}^{\text{Sep 2002}} \text{outflow} \quad \text{Eq 3.7}$$

The integral of water level (h) over the same period is equal to the area under the water level curve. For an accurate calculation of storage coefficient; monthly records of water level were used, Figure 3.7. As a result, the storage coefficient of the WAB could be calculated using the following equation, Eq. 3.8:

$$\alpha = \frac{Q}{\int_{\text{Oct 1989}}^{\text{Sep 2002}} h(t) dt} = \frac{5395.5}{52.9} = 102 \frac{Mm^3}{m} \quad \text{Eq 3.8}$$

Where:

Q : Sum of outflow over the considered period (m^3)

$h(t)$: Average water level (m)

α : Storage coefficient of the WAB (m^3/m)

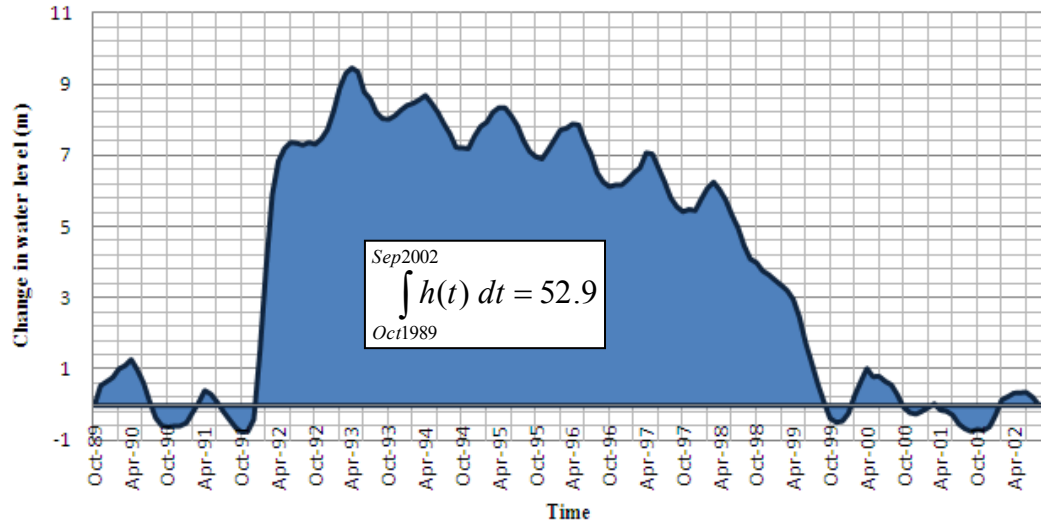


Figure 3.7: Average monthly water level in the confined part during the selected period

Once this equation was applied, it was concluded that for every meter drop or rise in the confined area within the WAB, the aquifer storage will lose or gain 102 Mm^3 . This quantity appears to almost match the result obtained from (Guttman et al., 1988) where they concludes that between 1977 and 1987 the cumulative groundwater deficit was in the order of 300 Mm^3 , a volume equivalent to a three meters drop in water level for the confined part of the WAB.

This step was followed by the calculation of the annual recharge by incorporating the storage capacity coefficient, the annual change in water level in the confined part and the net outflow from the WAB as shown in the following equation, Eq. 3.9.

$$R_i = Q_o^i + \alpha \times \Delta h_i \quad \text{Eq 3.9}$$

Where:

R_i : Recharge in year i (Mm^3)

Q_o^i : Net outflow in year i (Mm^3)

α : Storage coefficient of the WAB = $102 \text{ Mm}^3/\text{m}$

Table 3.3 displays the results obtained for the annual recharge of the WAB over the period from 1970/71 to 2005/06 through the application of Eq. 3.9 as well as a comparison with the values attained by the Guttman's empirical equation. The average recharge during this period

yielded 385.2 Mm³/yr which is a value higher than the values obtained by Guttman's equation (i.e. 329.6 Mm³/yr)

Table 3.3: Recharge estimates by WLF technique compared with other estimation techniques

Year	Avg. water level	Change in water level	Change in storage	Net outflow	Estimated recharge (WLF)		Estimated recharge (Guttman's Eq.)	
	m		Mm ³		Mm ³	Rc/Rf (%)	Mm ³	Rc/Rf (%)
1970/71	16.1	-0.5	-51.0	347.8	296.8	27.5%	329.6	30.5%
1971/72	15.9	-0.2	-17.0	334.3	317.3	26.6%	351.5	29.5%
1972/73	13.8	-2.1	-214.2	418.8	204.7	24.5%	218.9	26.2%
1973/74	15.6	1.8	183.6	362.5	546.0	36.7%	612.5	41.2%
1974/75	16.2	0.6	64.6	351.8	416.4	41.1%	299.5	29.6%
1975/76	15.9	-0.3	-30.6	445.9	415.3	46.5%	245.4	27.5%
1976/77	14.2	-1.7	-176.8	373.0	196.2	18.0%	334.2	30.6%
1977/78	13.5	-0.7	-74.8	387.1	312.3	31.6%	288.3	29.2%
1978/79	12.1	-1.3	-136.0	412.9	276.9	35.8%	191.7	24.8%
1979/80	14.3	2.1	217.6	319.7	537.2	36.5%	596.9	40.6%
1980/81	15.2	1.0	98.6	344.3	442.9	39.8%	343.8	30.9%
1981/82	13.9	-1.4	-139.4	381.1	241.7	26.5%	254.0	27.8%
1982/83	16.3	2.4	244.8	326.2	571.0	37.1%	656.9	42.7%
1983/84	14.4	-1.9	-190.4	471.1	280.7	37.2%	183.4	24.3%
1984/85	13.0	-1.4	-139.4	444.7	305.3	34.9%	236.9	27.1%
1985/86	12.0	-1.0	-105.4	408.1	302.7	36.6%	215.8	26.1%
1986/87	12.3	0.3	27.2	350.8	378.0	31.1%	373.2	30.7%
1987/88	12.9	0.6	61.2	376.5	437.7	34.3%	425.9	33.4%
1988/89	12.5	-0.4	-37.4	382.3	344.9	39.8%	233.8	27.0%
1989/90	11.7	-0.8	-78.2	422.0	343.8	36.4%	268.6	28.4%
1990/91	11.5	-0.3	-27.2	357.2	330.0	38.2%	232.3	26.9%
1991/92	18.7	7.3	741.1	264.1	1005.2	46.3%	1243.2	57.3%
1992/93	20.0	1.2	125.8	405.4	531.2	44.3%	357.9	29.9%
1993/94	19.3	-0.6	-64.6	392.5	327.9	37.7%	234.8	27.0%
1994/95	19.1	-0.2	-20.4	440.6	420.2	33.7%	399.4	32.1%

1995/96	18.2	-0.9	-91.8	407.2	315.4	31.2%	298.4	29.5%
1996/97	17.6	-0.7	-68.0	425.4	357.4	32.6%	336.9	30.7%
1997/98	16.4	-1.2	-122.4	460.2	337.8	27.2%	396.5	31.9%
1998/99	12.2	-4.2	-428.4	607.1	178.7	31.6%	97.9	17.3%
1999/00	12.3	0.1	10.2	424.0	434.2	46.4%	264.2	28.3%
2000/01	11.5	-0.7	-74.8	410.4	335.6	40.8%	214.1	26.0%
2001/02	11.8	0.3	27.2	379.4	406.6	33.5%	370.5	30.5%
2002/03	14.3	2.5	255.0	378.8	633.8	41.6%	643.0	42.2%
2003/04	15.1	0.8	85.0	357.8	442.8	53.2%	218.1	26.2%
2004/05	15.1	-0.1	-6.8	358.4	351.6	28.7%	383.0	31.2%
2005/06	13.9	-1.2	-122.4	411.9	289.5	31.7%	254.5	27.9%
Avg/Total	14.7	-0.1	-7.6	392.8	385.2	35.5%	329.6	30.6%

Figure 3.8 illustrates recharge values estimated by the two different methods (Water level fluctuation and Guttman's equation) drawn out on the same graph with the annual rainfall over the period 1970-2006. The estimates obtained from the WLF technique generally have trends similar to those of the Guttman method, due to the fact that the generated recharge is directly proportional to rainfall amounts. However, it was obvious that in many years the generated recharge was influenced more by the intensity and temporal distribution of rainfall. For example, the year 2003/04 had a much higher recharge rate than was estimated by Guttman equation. Similarly, the year 1976/77 had a much lower rate than other estimate owing to the factors mentioned above.

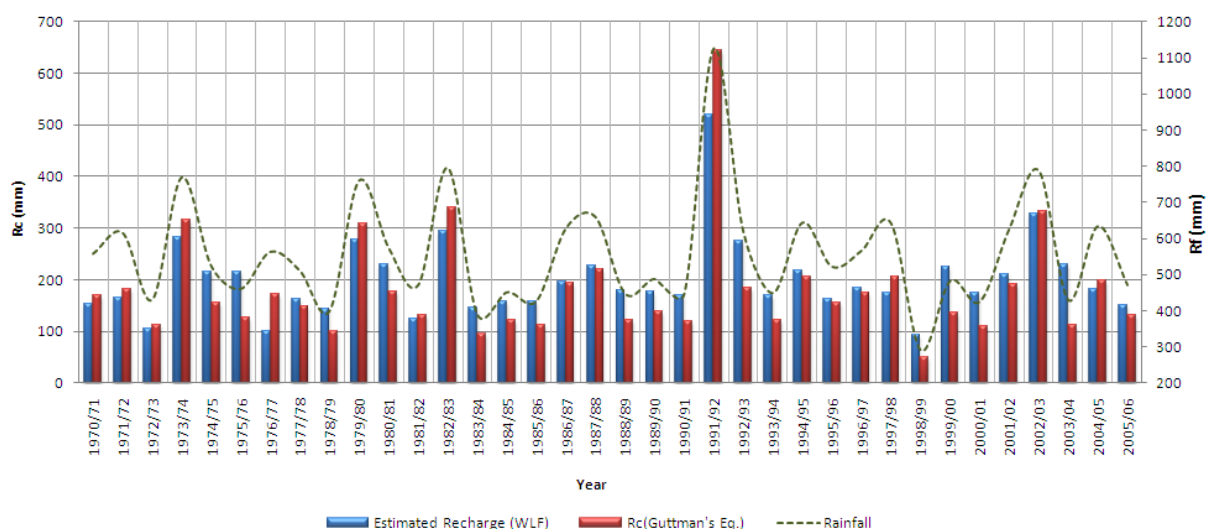


Figure 3.8: Annual recharge estimates with rainfall distribution for the analyzed period

The ratio between recharge and rainfall (R_c/R_f) were obtained by dividing the annual recharge estimates by the annual rainfall. The table shows large differences in the ratios between the coefficients R_c to R_f in the two methods used. This variation is a direct consequence of the dissimilarity between the two methods in the level of consideration of the temporal distribution of the monthly rainfall and quantity for each year. The average R_c/R_f ratios estimated by applying the two techniques WLF and Guttman's equation during the analyzed period are 35.7% and 30.5% respectively.

3.7 RECHARGE EQUATION

As discussed before, to consider the temporal distribution of rainfall, the monthly rainfall amounts from 1970/71 to 2005/06 were used to simulate the annual recharge quantities. The data set was divided into two parts; the first (1970/71 – 1996/97) was used to develop an empirical equation which relates the annual recharge with monthly rainfall. The second was used to validate the developed equation. A correlation test between monthly rainfall and the annual estimated recharge (i.e. WLF estimates) has been carried out. The rainy year 1991/92 was removed from the correlation test since it is an exceptional year where rainfall is twice the mean annual rainfall. Table 3.4 shows the correlation values as well as the significance levels of the correlated parameters. The result proved that the rainfall during December, January and February highly correlated with a high significance to annual recharge; November is also correlated but with less significance. All other rainy months were totally not correlated. Accordingly, the annual recharge is considered as a function of four rainy months within the year; November to February.

Table 3.4: Correlation test between monthly rainfall and annual recharge (1970/71 – 1996/97)

		Monthly Rainfall								
		Sep	Oct	Nov	Dec	Jan	Feb	Mar	Apr	May
Recharge	Pearson Correlation	0.072	0.002	0.25	0.7	0.38	0.68	-0.164	-0.243	-0.089
	Sig. (2-tailed)	0.363	0.495	0.082	0.006	0.046	0.007	0.211	0.115	0.332

Based on the correlation results, the empirical equation of annual recharge and monthly rainfall was developed using a multi-regression technique. The result of multi-regression provided the equation coefficients within a high significant level (less than 5%). The recharge equation has been noted below (Eq. 3.10), through which 39.6 Mm³/yr has been assumed the value representing all recharge from rainfall reaching the WAB during the months of March to October as well as from other minor sources of recharge (i.e. leakage from agricultural and domestic networks and return flow from irrigation). This value represents around 19.8% of the average recharge reaching the WAB.

$$Rc = 0.197 \times R_{Nov} + 0.382 \times R_{Dec} + 0.381 \times R_{Jan} + 0.413 \times R_{Feb} + 39.7 \quad Eq\ 3.10$$

Where:

Rc: Annual Recharge (mm)

R: Monthly Rainfall (mm)

The equation above was used to generate annual recharge estimates for the complete data set (1970/71 - 2005/06). The result, Figure 3.9, shows an excellent match for both simulation and validation periods. As a result, this equation is proved to be applicable for estimating the annual recharge for any synthetic rainfall scenario taking into consideration the monthly rainfall variations.

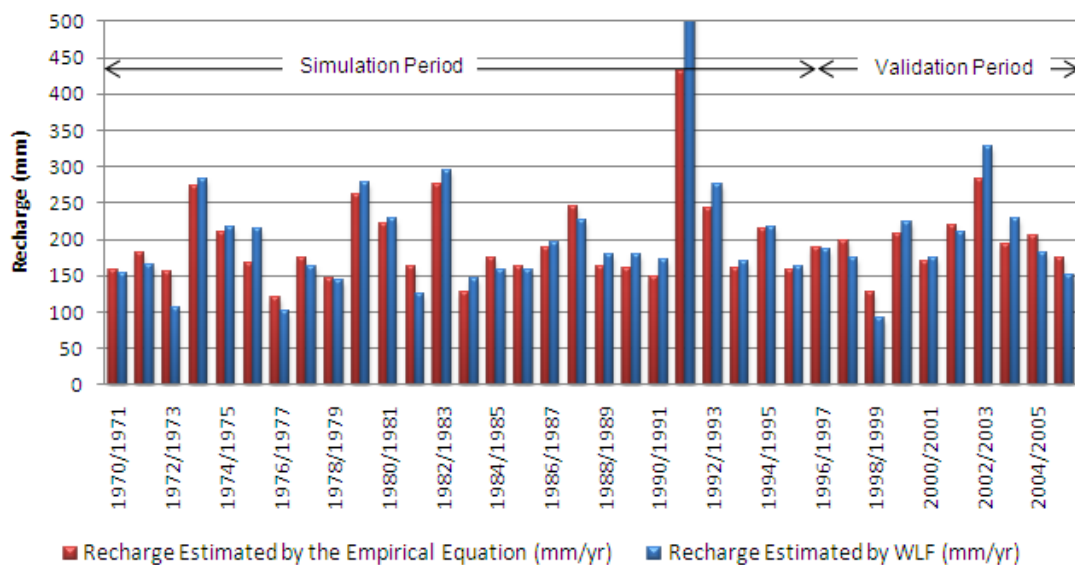


Figure 3.9: Recharge versus rainfall relations obtained by WLF technique and multi regression

3.8 ANNUAL RECHARGE VERSUS MONTHLY RAINFALL

The estimated annual recharge was compared with monthly and annual rainfall over the replenishment areas of the WAB. The rainy season is divided into two parts; the first part includes the three main rainy months within the year (December to February). The second part represents the remaining rainy months (September to November and March to May). The reason for this division is to facilitate the analysis and to check the impact of monthly distribution of rainfall. The analysis proved that annual recharge is predominantly governed by the monthly rainfall distribution rather than the total annual amount. The major findings are summarized as follows:

Years with high recharge to rainfall ratios (> 40%): with a rainfall distribution similar to that of a normal distribution, Figure 3.10, whereby more than 75% of the annual rainfall occurred during December to February. Table 3.5 shows all the years with high recharge to rainfall ratios. Moreover, it appears that all these years produce a graph skewing to the right.

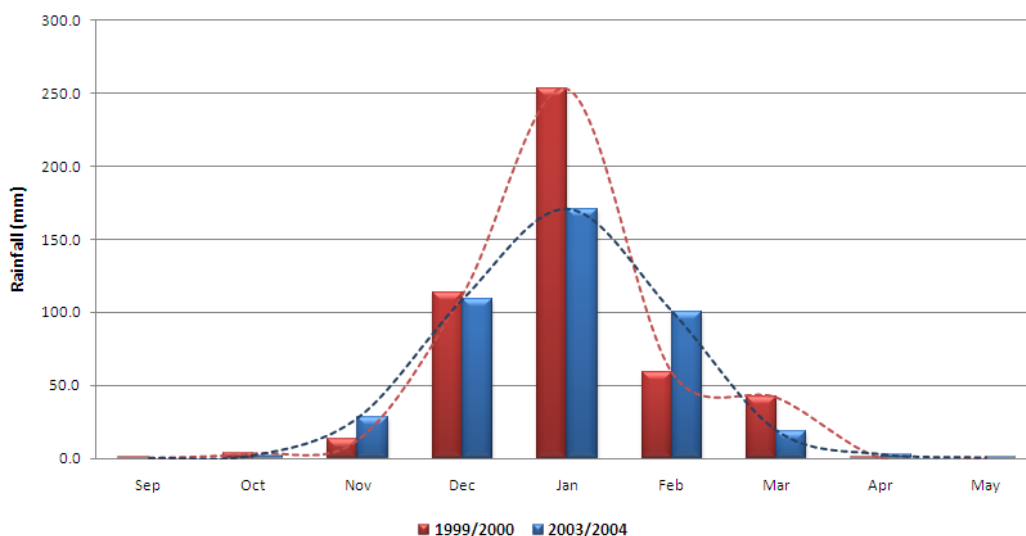


Figure 3.10: The shape of rainfall distribution which gives high recharge rates

Table 3.5: Characteristics of years with high recharge to rainfall ratios

Year	Rainfall (Rf)	Recharge (Rc)	Rf/Rc (%)	Rainfall during (Dec, Jan & Feb)		Rainfall during (Sep, Oct, Nov, March, Apr and May)	
	mm	mm		Sub-total	%	Sub-total	%
1974/75	524	216	41.1%	396.9	75.7%	127.5	24.3%
1991/92	1123	520	46.3%	939.0	83.6%	184.1	16.4%

1992/93	621	275	44.3%	486.6	78.4%	133.9	21.6%
1999/00	484	225	46.4%	424.9	87.8%	59.0	12.2%
2003/04	431	229	53.2%	379.8	88.2%	51.0	11.8%

Low recharge to rainfall ratios (< 30%): were obtained when rainfall shows a high variation in its monthly distribution. For example, Figure 3.11 shows two years with low recharge to rainfall ratios, as explained by the following factors:

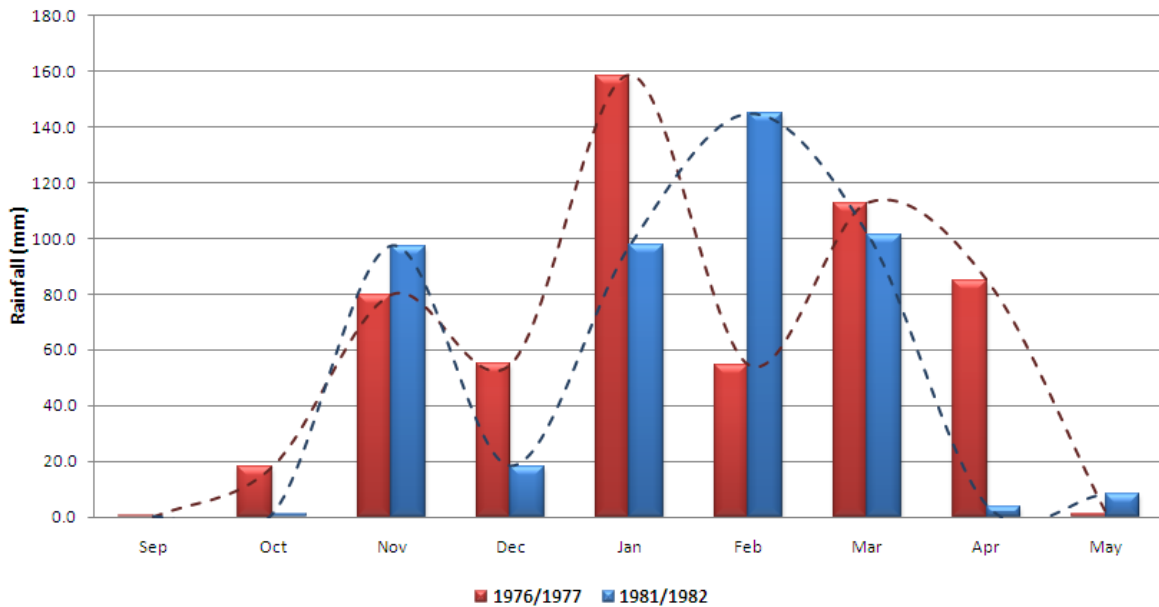


Figure 3.11: Typical rainfall distribution with consequently low recharge rates

- Both years had at least one dry month during the main recharge months (i.e. December 1981, December 1976, and February 1977). For instance, December 1981 experienced very low levels of rainfall with the soil drying out, eventually resulting in reduced levels of recharge. This period was followed by high rainfall depths in January 1982 mainly used up to re-wet the soil resulting in reduced recharge depths.
- Rainfall during both years shifted towards March and April when potential evapotranspiration is considerably higher than in the main rainy months (Tal et al., 2007).
- Rainfall during November followed by a very dry period (summer season) where, as noted above, a high percentage of precipitation was taken up by the soil. Together with high potential evapotranspiration, recharge consequentially decreased considerably.

Table 3.6 lists all the years with low recharge/rainfall ratios including all relevant statistical characteristics. The main rainy months showed low rainfall depths where annual rainfall is distributed over all rainy months (i.e. September to May).

Table 3.6: List of all years within the analyzed period with low recharge to rainfall ratio

Year	Rainfall (Rf)	Recharge (Rc)	Rf/Rc (%)	Rainfall during (Dec, Jan & Feb)		Rainfall during (Sep, Oct, Nov, March, Apr and May)	
	mm	mm		Sub-total	%	Sub-total	%
1970/71	559.1	153.6	27.5%	286.8	51.3%	272.3	48.7%
1972/73	431.8	105.9	24.5%	265.7	61.5%	166.1	38.5%
1976/77	564.4	101.6	18.0%	267.8	47.5%	296.6	52.5%
1981/82	472.2	125.1	26.5%	260.5	55.2%	211.7	44.8%
1997/98	643.2	174.9	27.2%	378.5	58.8%	264.7	41.2%

Different annual rainfall depths resulting in identical recharge amounts: In this case, some years had the same generated recharge despite the rainfall amounts being completely different in terms of quantity and distribution. For example, the years of 1987/88 and 1999/00 both displayed high recharge to rainfall ratios and a nearly identical recharge amount, notwithstanding the fact that 1999/00 experienced high intensity rain during the main rainy months (i.e. 88%) as well as that the rainfall has a normal distribution shape which is not the case in year 1987/88, Table 3.7 and Figure 3.12.

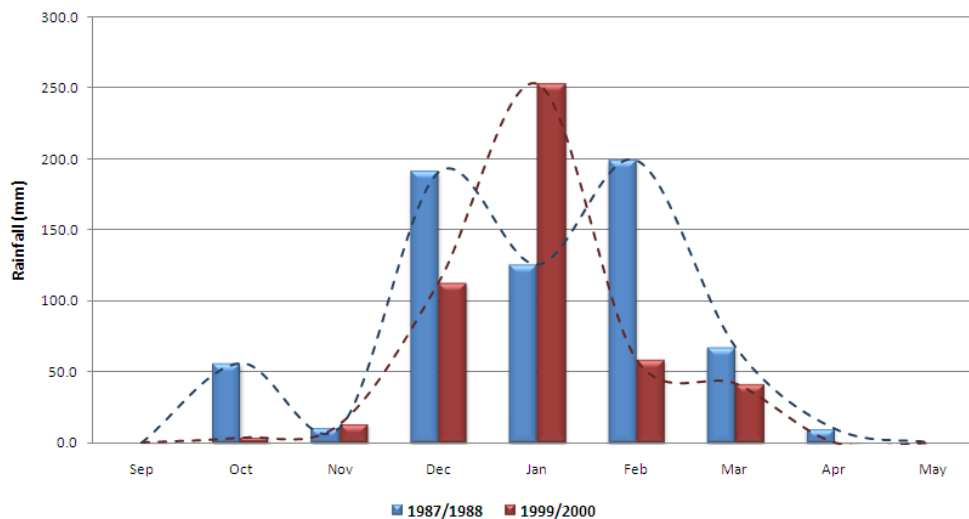


Figure 3.12: Characteristics of years with different annual rainfall depths and identical recharge amounts

Table 3.7: Example of years where different annual rainfall amounts generate same recharge rates

Year	Rainfall (Rf)	Recharge (Rc)	Rc/Rf (%)	Rainfall during (Dec, Jan & Feb)		Rainfall during (Sep, Oct, Nov, March, Apr and May)	
	mm	mm		Sub-total	%	Sub-total	%
1987/88	660.5	226.5	34.3%	516.2	78.2%	144.3	21.8%
1999/00	483.9	224.7	46.4%	424.9	87.8%	59.0	12.2%
1988/89	448.9	178.5	39.8%	291.3	64.9%	157.6	35.1%
1997/98	643.2	174.9	27.2%	378.5	58.8%	264.7	41.2%

Identical rainfall depths with different recharge rates: to the opposite of the previous point, Table 3.8 and Figure 3.13 display examples of years that experienced the same rainfall depths but generated different recharge amounts. The year 2003/04 had a rainfall of 432 mm, but its distribution showed a specific concentration of the rainfall around the month of January (88.2% of the rainfall at the three main rainy months) which resulted in a high rainfall/recharge ratio. On the other hand, the rainfall distribution during 1972/73 takes a low recharge shape (Figure 3.12) where rain during February was very low and relatively high during November 1972 and March 1973. The two months that had experienced the highest rainfall amounts of 1972/73 (November and March) were characterized by high evapotranspiration rates and dry soils taking up a lot of moisture with low recharge rates as a consequence.

Table 3.8: Characteristics of years with same annual rainfall depths and different recharge rates

Year	Rainfall (Rf)	Recharge (Rc)	Rf/Rc (%)	Rainfall during (Dec, Jan & Feb)		Rainfall during (Sep, Oct, Nov, March, Apr and May)	
	mm	mm		Sub Total	%	Sub Total	%
1972/73	431.8	105.9	24.5%	265.7	61.5%	166.1	38.5%
2003/04	430.9	229.2	53.2%	379.8	88.2%	51.0	11.8%
1974/75	524.5	215.5	41.1%	396.9	75.7%	127.5	24.3%
1995/96	523.2	163.3	31.2%	270.3	51.7%	252.9	48.3%

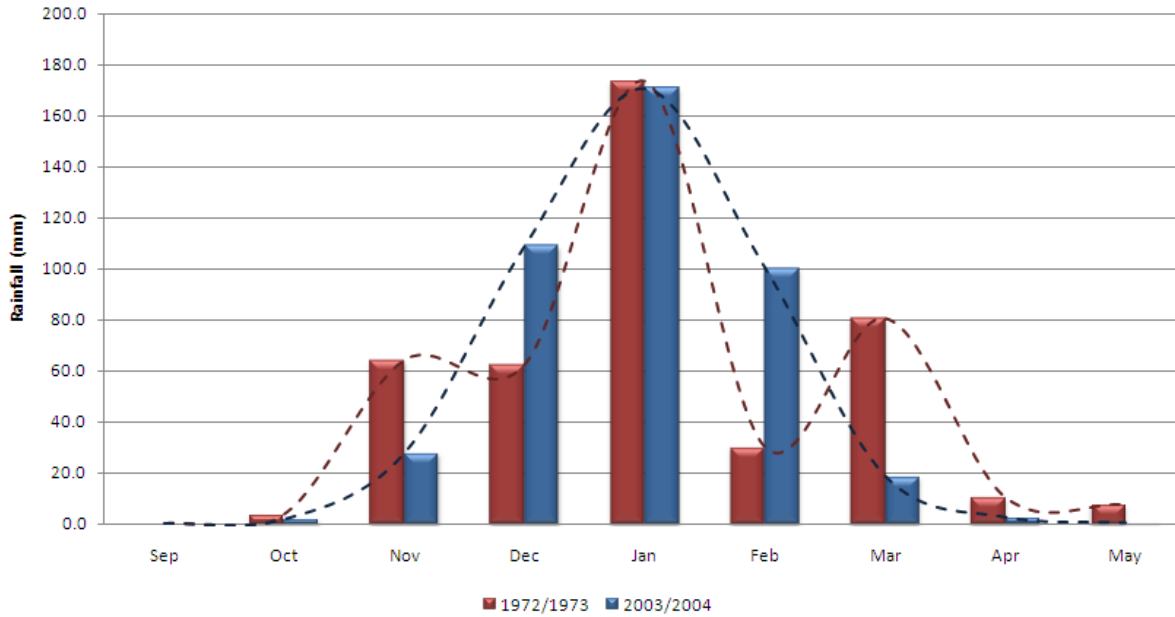


Figure 3.13: Years with equal annual rainfall depths and different recharge rates

The effect of similarities: This example is used to validate the hypothesis that if rainfall in two years displays similar quantities and similar distributions, then the generated recharge will be the same. Figure 3.14 and Table 3.9 show two years with the same amount of rainfall and almost the same monthly distribution. Both years showed equal recharge depths during March with a decreased recharge to rainfall ratio as a consequence.

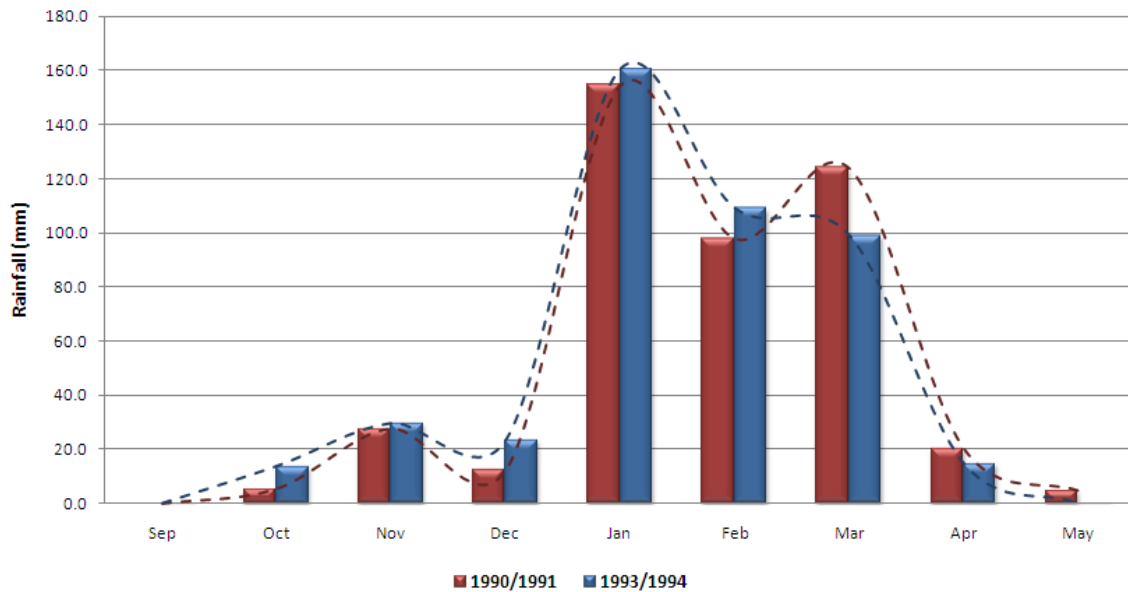


Figure 3.14: Characteristics of years with equal annual rainfall depths and equal recharge rates

Table 3.9: Characteristics of years with equal annual rainfall depths and equal recharge rates

Year	Rainfall (Rf)	Recharge (Rc)	Rf/Rc (%)	Rainfall during (Dec, Jan & Feb)		Rainfall during (Sep, Oct, Nov, March, Apr and May)	
	mm	mm		Sub Total	%	Sub Total	%
1990/91	447.2	170.8	38.2%	265.1	59.3%	182.2	40.7%
1993/94	450.1	169.7	37.7%	292.9	65.1%	157.2	34.9%

3.9 CONCLUSION OF THE RECHARGE ESTIMATION

It was displayed that annual recharge of the WAB could be estimated based on a more realistic technique. The WLF technique as an alternative approach was successfully applied using the historical records of inflows, outflows and water levels. As a prerequisite condition for applying this technique, finding a water level cycle within the records is required. Within this water level cycle, the net aquifer storage equal to zero. This period also formed the basis for the estimation of the storage coefficient of the WAB (α), i.e. the amount of water that could be abstracted from or recharged into the aquifer per one meter drop/rise. This factor provides a good tool to estimate the annual recharge by using the annual change in water level and the net outflow from the aquifer.

The estimated annual recharge of the WAB proved that the amount of annual recharge is affected by the monthly rainfall distribution more than by the annual amount of rainfall. Therefore, simply estimating annual recharge from total annual rainfall amounts is an inaccurate approach and will probably lead to either over or under estimating the annual recharge amounts. The annual recharge was estimated by the WLF technique for the last 37 years (1971-2007) and then the time series of annual recharge and monthly rainfall were used to develop an empirical equation relating annual recharge to the monthly rainfall. This newly developed recharge equation will improve the future estimate of annual recharge by taking into account the monthly distribution of rainfall. The equation shows that recharge is highly dependent on rainfall amounts during four main rainy months: November, December, January and February. The equation also concludes that the monthly rainfall in the months March to October is not effective for generating recharge; where the generated recharge from

rainfall in these months and other minor recharge components was estimated by the a value of $39.6 \text{ Mm}^3/\text{yr}$ during the analyzed period (1970/71-2005/06).

The developed recharge to rainfall relation using two approaches was shown in Figure 3.15. The estimated recharge by the WLF technique shows higher rates compared with recharge estimated by Guttman's equations for low rainfall rates and the opposite for high rainfall rates. The comparison of the rainfall/recharge relation in the two WAB recharge estimation techniques is summarized as follows:

- Recharge estimates using Guttman's equation: recharge estimates are strictly proportional to the annual amount of rainfall, yet estimates intensify with higher rainfall amounts due to the polynomial nature of the graph that was generated via a second-order polynomial equation. Furthermore, this technique does not take into account the rainfall intensity nor its temporal monthly distribution.
- Recharge estimation using WLF: In this technique, the estimated annual recharge values show less correlation with the annual amount of rainfall. The examination of historical records proved that the relation between annual recharge and rainfall is not that well developed, thus the monthly distribution was considered as a supporting factor. This factor constitutes the underpinning elements of the WLF technique and was thus deployed in the development of the consequent computational equation.

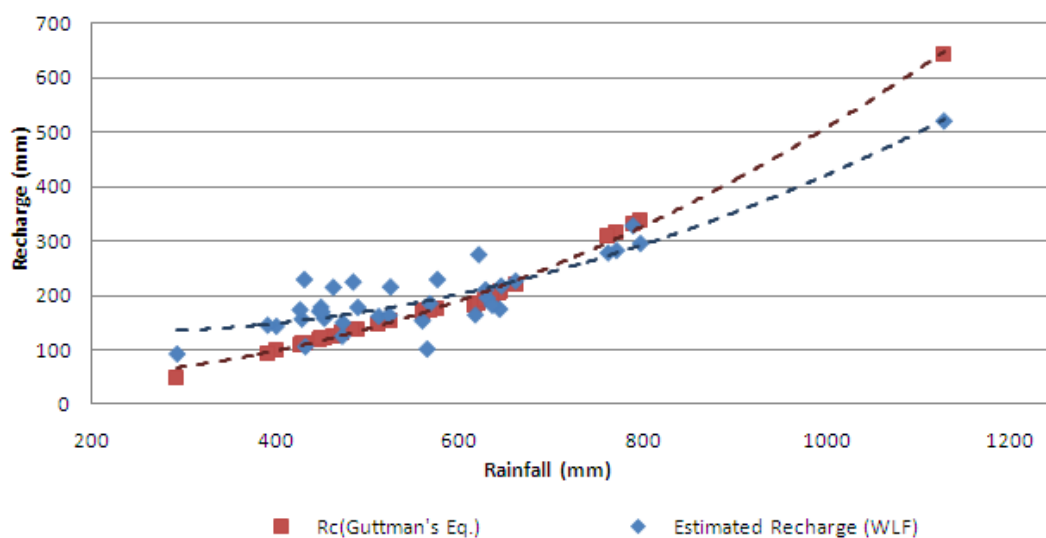


Figure 3.15: Recharge versus rainfall comparison

To define the characteristics of rainfall that maximize the annual generated recharge, Figure 3.16 illustrates two years when the generated recharge has been fundamentally influenced by the temporal monthly distribution of rainfall rather than the total annual amounts. These two years have the highest and lowest Rc/Rf ratios (52.4% in year 2003/04 and 19.3% in year 1976/77). The figure reflects the characteristics of the seasonal rainfall for the two years that led to high and low recharge to rainfall ratios. The characteristics of seasonal rainfall that have high Rc/Rc ratios (e.g. year 2003/04) and that have low Rc/Rc ratios (Year 1976/77) were:

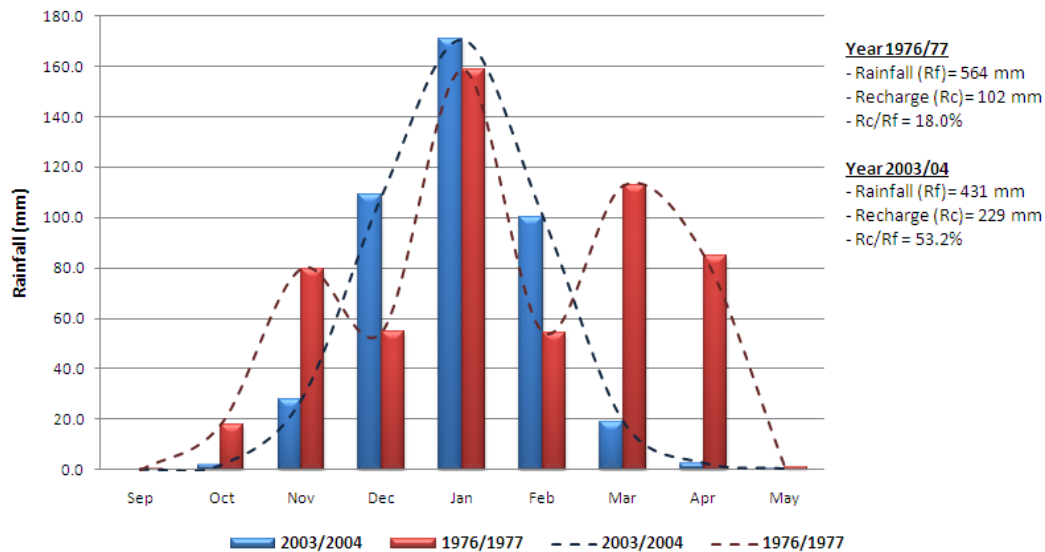


Figure 3.16: Rainfall in 1976/77 and 2003/04

High Rc/Rf ratio (e.g. year 2003/04):

- The graph representing the monthly temporal distribution throughout the year takes the shape of a normal distribution.
- More than 70% of the annual rainfall accumulates during four consecutive months (November, December, January and February). It is worth mentioning that these four months have the lowest potential evapotranspiration rates (Tal et al., 2007).

Low Rc/Rf ratio (e.g. year 1976/77):

- The graph representing the monthly temporal distribution throughout the year takes a shape far from a normal distribution.

- Generally, this case pointed out relatively low rainfall amounts during the main rainy months (November, December, January and February).
- High percentages of rainfall occurred during October, March and April, a period characterized for having elevated potential evapotranspiration rates especially compared to November, December, January and February (Tal et al., 2007).

Chapter 4

CHAPTER 4: GROUNDWATER FLOW DYNAMICS UNDER PRE-DEVELOPMENT CONDITIONS

4.1 INTRODUCTION

A groundwater model can be defined as a simplified version of the real groundwater system. It describes the flow characteristics and gives relevant assumptions and constraints. In general, groundwater models are based on two well-known equations: Darcy's equation and the equation of conservation of mass. The combination of these two equations results in a partial differential equation that can be solved by numeric approximation. The two best-known approximation methods are the finite difference and the finite element methods. Both require space to be divided into small intervals. The sub-areas thus formed are called cells and presented by nodes; each node is connected mathematically to its neighbors. The nodes (cells) make it possible to replace the partial differential equation with a set of algebraic equations. The conceptual model of the WAB was described in Chapter 2. This conceptual model could be converted to a numerical groundwater model.

This chapter aims to develop a numerical flow model for the WAB during the pre-development period. Whenever the model is calibrated, it will validate the conceptual model of the real groundwater system, then the hydrogeology and the flow dynamics of the WAB will be understood. The results will include water level heads, flow pattern, aquifer geometry, water budget, hydraulic properties and more during the pre-development period when the aquifer has not yet been utilized. In addition, this is considered as a further step for developing the transient flow model in the following chapter.

The numerical flow model of the WAB representing the hydraulic state of the early forties (1940s), when the aquifer was only insignificantly disturbed, was developed. For the initial model, the pumping rate from groundwater wells was neglected and outflow from the aquifer was assumed to be strictly through natural discharge at the location of the two main springs of the WAB (Al Timsah and Ras Al Ain springs). The model will be calibrated based on the

pre-development discharge of these springs as well as different locations within the Basin where water levels were known.

4.2 NUMERICAL MODEL SOFTWARE

The main objective of the pre-development numerical model of the WAB is to evaluate and test the validity of various interpretations about its flow dynamic systems. Generally, the application of a numerical model in karstic aquifers such as the case of the WAB is limited; due to the high contrast in hydraulic properties of the conduits and matrix blocks as well as heterogeneity of the aquifer system (Rani et al., 2010). However, for long-term flow modeling where the short-term response of the aquifer following recharge events is not important, an equivalent porous medium model is intensified (Sauter, M. 1992). The steady state flow model of the WAB was developed using MODFLOW 2000 which solves the governing equation for groundwater flow through anisotropic and heterogeneous porous media in three dimensions under saturated conditions (Weiss et al., 2007). In the karstic aquifer, the groundwater flow; both matrix flow and karst conduits flow, were averaged into a bulk conductivity of the model cells. This approach was found to be appropriate for well-connected fracture systems at a fairly large scale (Ford and Williams, 2007).

MODFLOW is a 3D, cell-centered, finite difference, saturated flow model developed by the United States Geological Survey (McDonald & Harbaugh, 1988). It simulates steady and non-steady flow in an irregularly shaped flow system in which aquifer layers can be confined, unconfined, or a combination of both. It also allows for a wide variety of boundary conditions and input options.

MODFLOW is integrated with the Groundwater Modeling System interface (GMS) developed by Aquaveo, LLC in Provo, Utah. GMS supports MODFLOW as a pre- and post-processor. These processors are used to prepare all input files to MODFLOW and then read and present the output files in a proper way.

4.3 MODEL GEOMETRY

The model's geometry was constructed to comprise four layers representing four hydrogeological units of the WAB. The top layer (i.e. the cover layer) includes the Abu Dees

formation and all other overlying formations. This layer is modeled as an aquitard layer with very low vertical and horizontal conductivities. Layers 2 and 4 are the upper (Hebron, Bethlehem and Jerusalem formations) and the lower (Beit Kahel formation) aquifers respectively known as the upper and lower sub-aquifers. The upper and lower sub-aquifers are separated by Layer 3; the Yatta formation.

The Digital Elevation Model (DEM), Figure 1.3, was used to generate the elevation of the first layer (i.e. ground elevation). The top elevation of the upper sub-aquifers was digitized from the Structural Maps on Top of the Judea Group (top of the upper aquifer formations) (Fleischer 2003), and using ARCGIS 9.3 software. In addition, different cross sections, outcropping geology and wells lithology were also used to estimate the bottom elevations for the remaining layers, as a result, the geometry of the WAB was developed. Figures 4.1 and 4.2 show samples of the structural maps and locations of cross sections used in developing the geometry of the Basin, Figure 4.3.

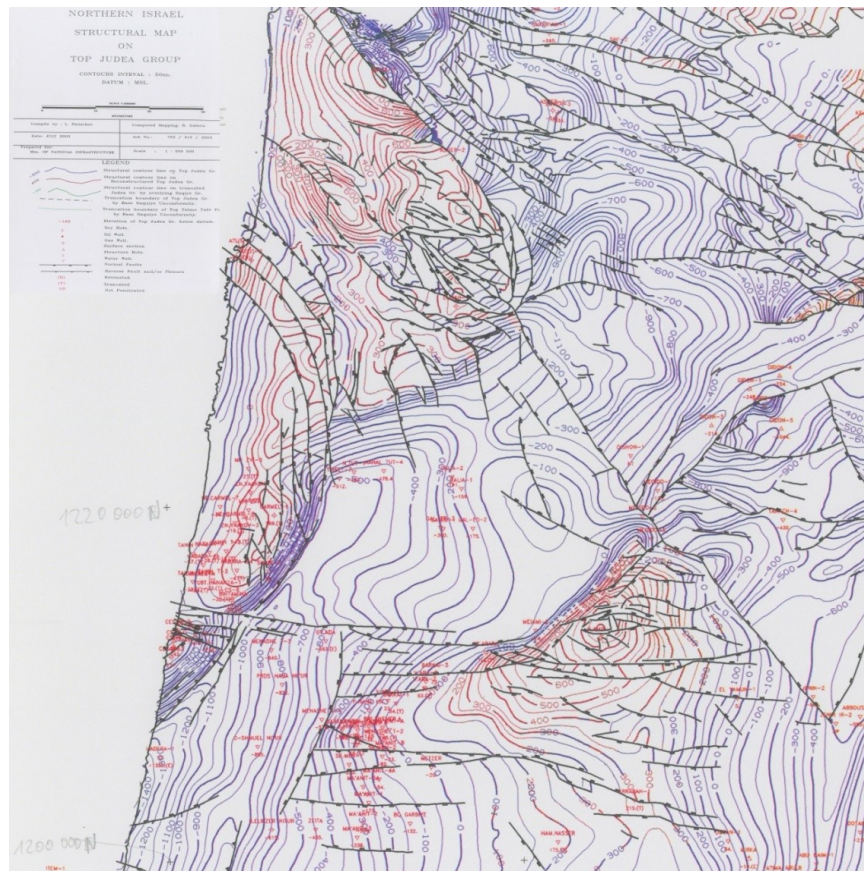


Figure 4.1: Structural maps on Top Judea Group (top of the upper aquifer), Fleischer 2003,

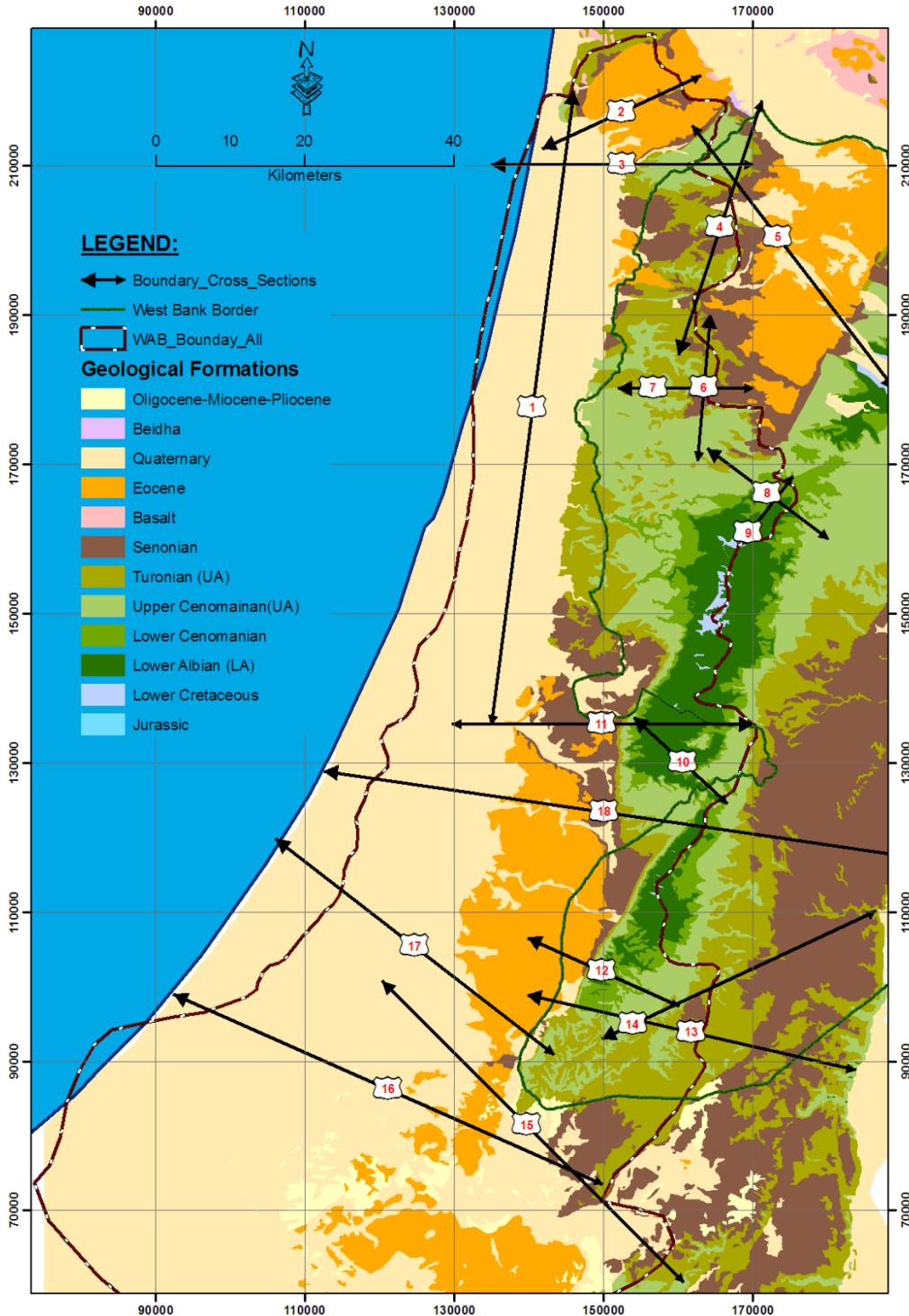


Figure 4.2: Location of the used cross sections in the geometry development

The cell dimensions vary from 200 to 750 meter. The smaller grid sizes were used in the unconfined part of the WAB as well as around the two main springs. The cell sizes increase further away from these areas.

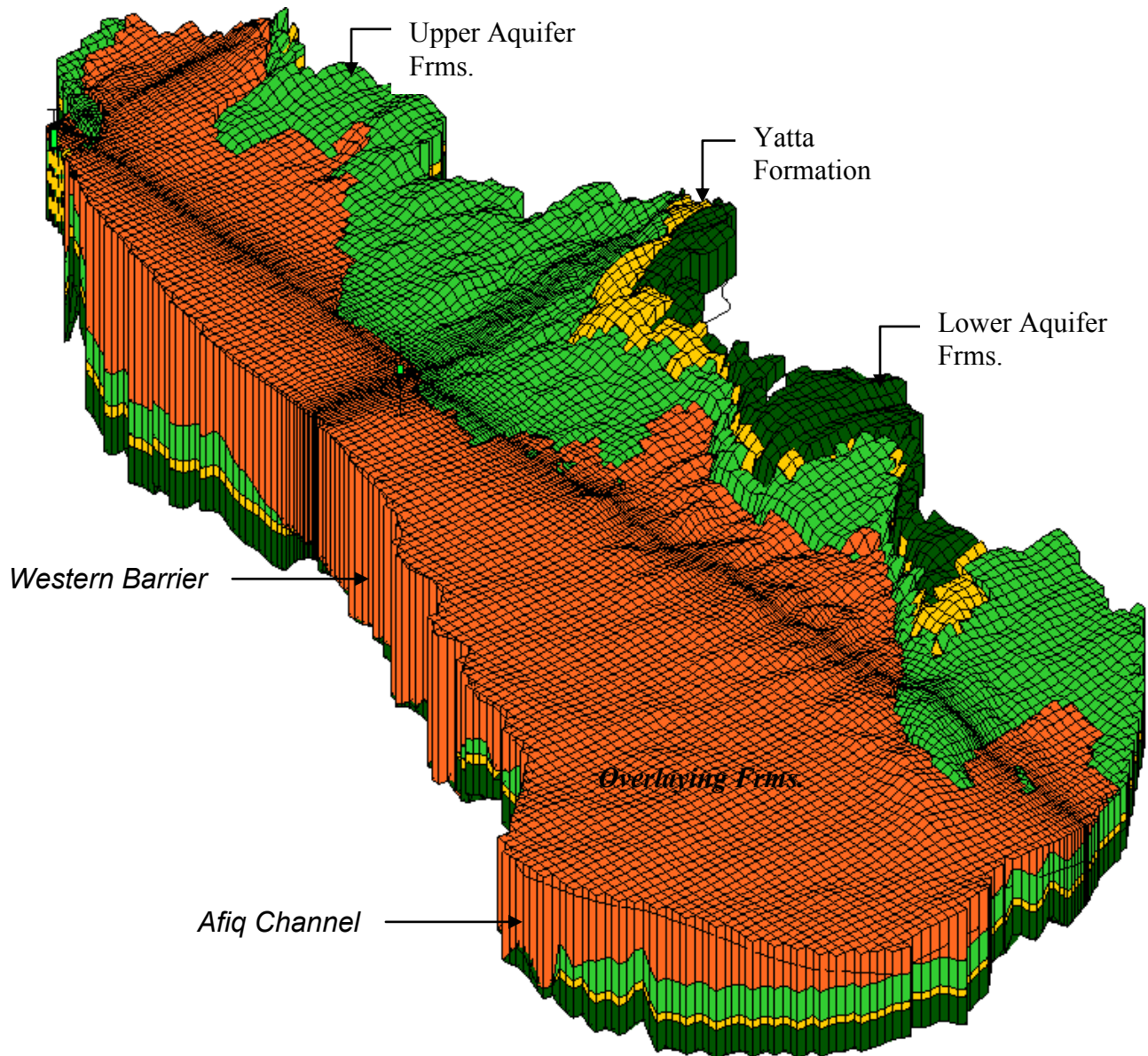


Figure 4.3: The geometry of WAB

For simplification, the 50-90 m thick Yatta formation, Layer 3, was later aggregated within the two sub-aquifers. This simplification aims at decreasing running time of the steady state and transient models. The vertical conductivity was used to separate the upper and lower sub-aquifers. In the areas where the two aquifers are separated, very low vertical conductivities (in order of 10^{-6} m/d) were used implying that very limited flow could be exchanged between the two sub-aquifers. In the areas where the sub-aquifers are assumed to be connected, 1/10 to 1/100 of the horizontal conductivities were used.

4.4 RECHARGE

Recharge in the WAB is mainly generated from rainfall over the replenishment areas of the aquifer. As discussed in Chapter 3, the rainfall is limited to winter months (October to April) and characterized by high variation in terms of quantity, temporal and spatial distributions and intensity from month to month as well as from year to year. The annual recharge has been estimated using the water fluctuation technique taking into consideration the variations of rainfall. The long-term average recharge (1951-2007) was found to be about 373 Mm³/yr. This long-term annual average of recharge was used for model simulating the pre-development state of the aquifer.

The recharged amount was spatially distributed over the replenishment areas based on different criteria. The used methodology assumed that recharge is spatially distributed based on the rainfall distribution, geological outcropping formation, slope, land use and surface flow accumulation (i.e. drainage system). The flow accumulation was used to reflect the recharge from runoff accumulated in the drainage system. In addition, it was assumed that the criteria do not have the same level of significance to recharge distribution. Therefore, different weightings based on the different literatures (SUSMAQ 2004) were used as shown in Eq. 4.1.

$$RDI_i = 0.3 \times G_i + 0.25 \times Fa_i + 0.20 \times Rf_i + 0.10 \times LU_i + 0.15 \times S_i \quad Eq\ 4.1$$

Where:

RDI_i: Recharge distribution index for cell *i*

G_i: Normalized geology index for cell *i*

Fa_i: Normalized flow accumulation index for cell *i*

Rf_i: Normalized rainfall index for cell *i*

LU_i: Normalized landuse index for cell *i*

S_i: Normalized slope index for cell *i*

The normalized values of the criteria were calculated based on Eq. 4.2 (AbuSaada et. al., 2006). Furthermore, to differentiate the influences of geological formation and land use types on recharge distribution, different scores were used for each type of the criterion items, Table 4.1.

$$NC_i^j = \frac{C_{worst}^j - C_i^j}{C_{worst}^j - C_{ideal}^j} \quad Eq 4.2$$

Where:

NC_i^j : Normalized index of criterion j for cell i

C_{worst}^j : The worst value of criterion j

C_{ideal}^j : The ideal value of criterion j

C_i^j : The value of criterion j for cell i

Table 4.1: Rank for potential to recharge for land use types and geological formations

Item	Formation	Rank (Potential to Recharge)	Ideal Value	Worst Value	Normalized Rank
Geology	Jerusalem	1	10	0	0.9
	Upper Bethlahem	2			0.8
	Lower Bethlahem-Hebron	3			0.7
	Yatta	5			0.5
	Beit Kahel	2			0.8
Land Use Types	Field Crops	2	10	0	0.8
	Orchards	2			0.8
	Shrublands	1			0.9
	Urban	5			0.5

Applying the described approach led to the Recharge Distribution Index (RDI), Figure 4.4. This index was used to distribute the accumulated annual recharge over the replenishment areas of the WAB and finally the recharge distribution were achieved, Figure 4.5. Table 4.2 shows the recharge to each layer.

Table 4.2: Recharge distribution to the WAB layers

Aquifer	Recharge (Mm ³)	Recharge (%)
Lower Aquifer	48.9	13.1%
Yatta formation	30.6	8.2%
Upper Aquifer	293.6	78.7%
WAB (Total)	373	100%

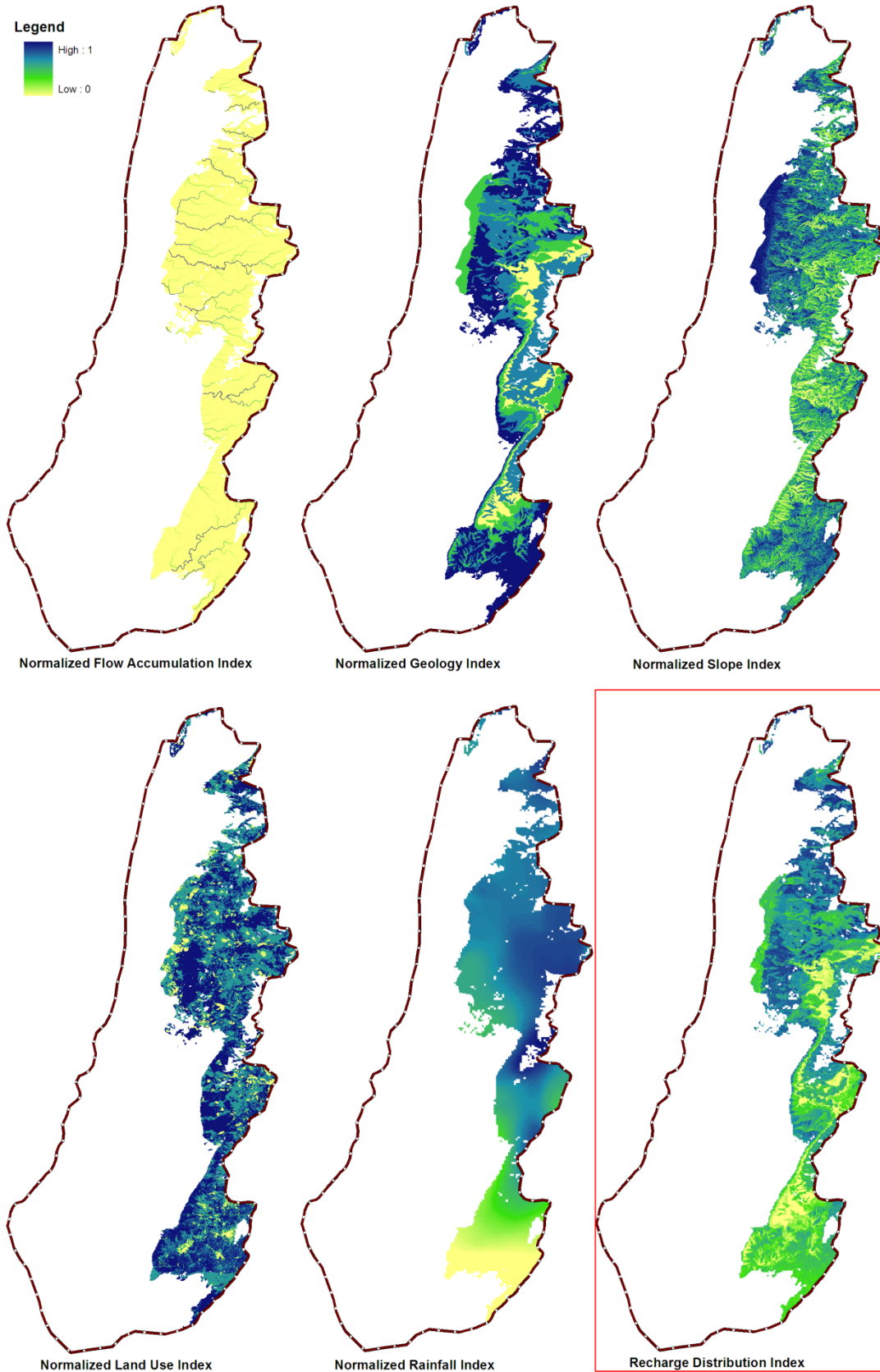


Figure 4.4: Criteria used for developing the Recharge Distribution Index (RDI)

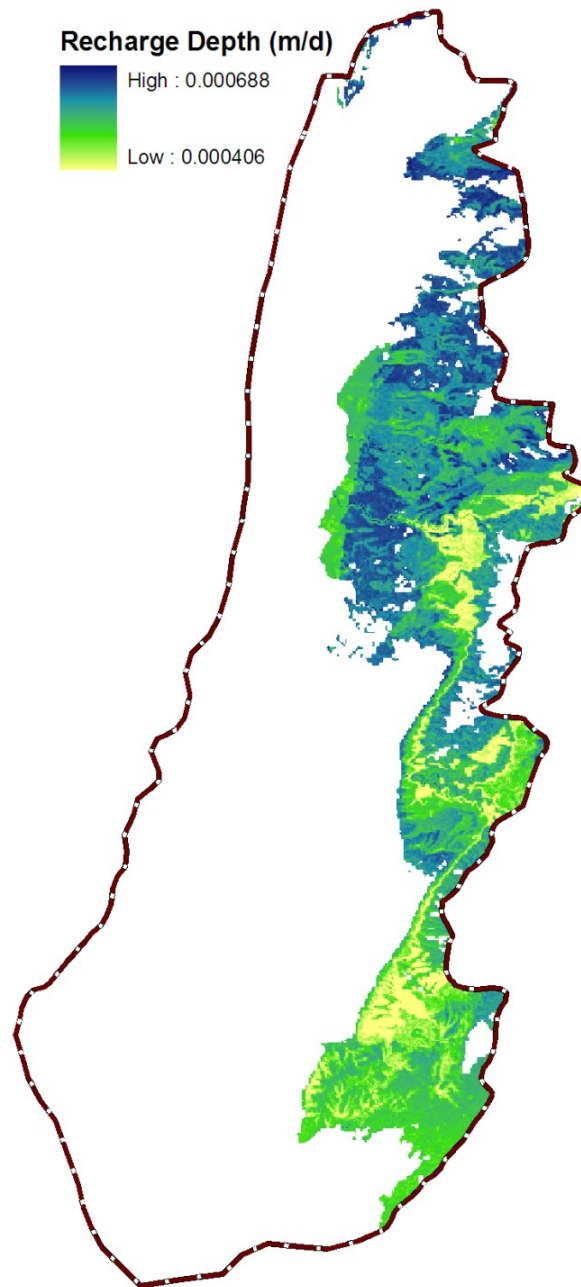


Figure 4.5: Recharge depth for pre-development period

4.5 WATER LEVEL

Measured historic water levels at different locations within the model domain are essential for a sound model calibration. However, water level records during the pre-development period are very rare. The water level records mainly date back to the mid 1960s after the aquifer was already intensively developed are available. The available literature indicates that the pre-development water levels in the confined part of the WAB gently drop from 25 -

27 m near Beir Al Saba' in the south to 16 m in the Menashe heights at the north (Rosenthal et. al., 1992 and Dafny et. al., 2010). In the unconfined part, the relatively pre-development water levels were at 450 - 500 m in Jerusalem area (Ein Karem), in Hebron Mountains the water level was 350 - 450 m in the lower sub-aquifer, 550 - 700 m in the upper sub-aquifer and 300 - 350m in Salfeet area (Weinberger et al., 1994, Guttman et. al., 1988 and Dafny et. al., 2010). The pre-development water level at specific points (33 wells) used in the model calibration are listed in Table 4.3 and Figure 4.6.

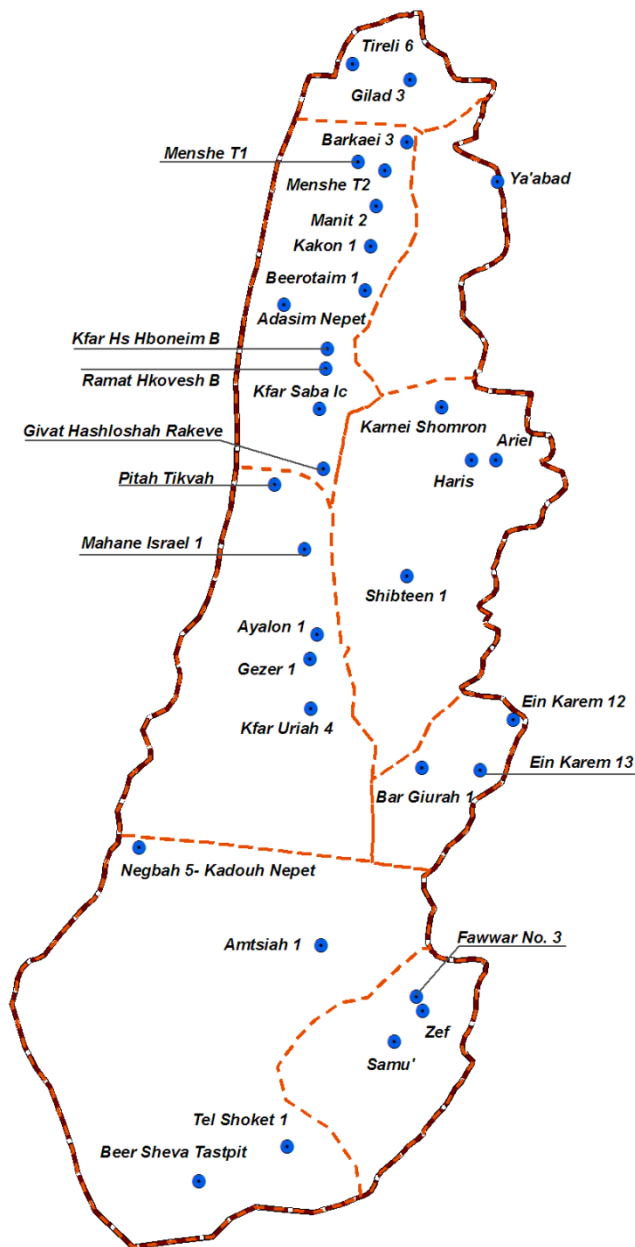


Figure 4.6: Location map for observed water level during pre-development period

4.6 NATURAL OUTFLOW OF THE WAB

During the pre-development period, the outflow from the WAB was limited to two main springs; Al Timsah spring in the northern part and the Ras Al Ain spring in the central part of the Aquifer. Based on different literature sources, the average pre-development mean annual flow range for Ras Al Ain spring was 220 - 280 Mm³ and that of the Timsah spring was 90-120 Mm³ (Mercado et. al., 1980, Zukerman et. al., 1999 and Berger et al., 1999).

It was assumed that the sum of the spring discharge is within the range of the long-term annual average recharge (i.e. 350 - 380 Mm³/yr). The two springs were modeled as drain with constant heads with their discharge is a function of the gradient near the springs and the hydraulic conductivity. For calibration, the spring's discharges were set to 255 ± 10 Mm³/yr for Timsah spring and 105 ± 10 Mm³/yr for Ras Al Ain spring. The rest points and the hydraulic conductivity of the two springs were obtained as a result of the model calibration.

4.7 MODEL CALIBRATION

In order to achieve the water level distributions during the pre-development period and the historical discharge of the two springs, horizontal conductivities as well as the hydraulic conductivities and rest points of the two springs were used. The model domain was divided into different zones based on the geological formations, faults, gradients, synclines and anticlines. Initial values were used for each zone and then modified by calibration to achieve the steady state conditions. The hydraulic conductivities in each zone were considered an average value which represent the conductivities for both conduits and diffuse flow.

During calibration, vertical conductivity was used to represent the connection between upper and lower aquifers. In the areas where the upper and lower sub-aquifers assumed to be connected, vertical anisotropy 1: 10 ($K_h = 10 K_v$) was used. In all other cases, a very low vertical conductivity (i.e. 10^{-6} m/d) was used to define the separation between the two aquifers. During calibration, these ratios were modified in order to reach the steady state conditions. In the unconfined areas, higher ratios between horizontal and vertical conductivities were used (K_h : 500 - 1000 K_v). These ratios reflect high conductivity due to the karstic conditions.

The water level calibration was conducted based on 33 wells distributed throughout the entire Basin, Table 4.3 and Figure 4.6. For each well, the pre-development water level and a range of water level uncertainty figures were carefully set. The calibration was stopped when the simulated water level in all wells and the historical spring discharge rates were achieved. According to their locations within the model domain, these target wells were clustered into 8 groups and a Zonal Root Mean Squared Error (ZRMSE) was calculated based on Eq. 4.3:

$$ZRMSE = \sqrt{\frac{1}{2} \sum_{i=1}^n (O_i - S_i)^2} \quad \text{Eq 4.3}$$

Where:

n =Number of observed wells in each group

O = Observed water level

S =Simulated water level

Table 4.3: Pre-development water level at specific point locations

Well Name	Zone	Layer	Observed heads (m)	Uncertainty (m)	Simulated heads (m)	Error (m)	ZRMS E (m)
Negbah 5-Kadouh Nepet	Beir As Saba	2	25.7	1	26.0	0.35	0.7
Amtsiah 1	Beir As Saba	2	26.2	1	26.3	0.09	
Tel Shoket 1	Beir As Saba	2	26.7	2	27.9	1.19	
Beer Sheva Tastpit	Beir As Saba	2	26.4	1	26.9	0.52	
Ein Karem 12	Jerusalem	3	502.0	5	498.7	-3.32	2.0
Bar Giurah 1	Jerusalem	3	239.0	2	239.9	0.90	
Ein Karem 13	Jerusalem	3	445.0	5	445.8	0.76	
Fawwar No. 3	Hebron	2	657.0	5	655.2	-1.77	2.4
Samu'	Hebron	2	552.0	5	555.7	3.68	
Zef	Hebron	3	360.0	5	360.8	0.83	
Barkaei 3	Khudera	2	16.9	2	18.0	1.08	0.5
Menshe T1	Khudera	2	18.6	1	18.4	-0.25	
Menshe T2	Khudera	2	19.3	1	18.8	-0.47	

Manit 2	Khudera	2	19.7	1	19.7	-0.01		
Kakon 1	Khudera	2	20.0	1	20.4	0.41		
Beerotaim 1	Khudera	2	20.8	1	21.0	0.20		
Adasim Nepet	Khudera	2	21.6	1	21.4	-0.20		
Kfar Hs Hboneim B	Khudera	2	21.6	1	21.5	-0.08		
Ramat Hkovesch B	Khudera	2	21.8	1	21.6	-0.19		
Kfar Saba Ic	Khudera	2	22.3	1	21.6	-0.67		
Givat Hashloshah Rakeve	Khudera	2	22.8	2	21.6	-1.16		
Pitah Tikvah	Ras Al Ein	2	23.0	1	22.1	-0.91		0.5
Mahane Israel 1	Ras Al Ein	2	23.8	1	23.2	-0.58		
Ayalon 1	Ras Al Ein	2	24.0	1	24.3	0.31		
Gezer 1	Ras Al Ein	2	24.5	1	24.5	0.03		
Kfar Uriah 4	Ras Al Ein	2	25.0	1	25.0	-0.02		
Karnei Shomron	Shibteen	3	76.5	1	76.7	0.20	0.9	
Ariel	Shibteen	3	425.0	5	423.3	-1.66		
Haris	Shibteen	3	295.3	5	295.1	-0.19		
Shibteen 1	Shibteen	2	93.0	1	92.5	-0.47		
Tireli 6	Timsah	2	14.3	2	15.9	1.61	1.3	
Gilad 3	Timsah	2	16.0	1	16.9	0.93		
Ya'abad	Tulkarem	2	40.0	2	39.9	-0.06	0.1	

The calibrated water level distributions for both confined and unconfined areas showed a good match with the observed water levels in all measured wells within the defined uncertainty ranges. The uncertainty range for most wells located in the confined part of the Basin varies between -1 and 1 m and from -5 to 5 m in the unconfined areas. The ZRMSE varies between 0.5 - 2.4 m. The water levels and the flow patterns for the upper and lower sub-aquifers are shown in Figure 4.7.

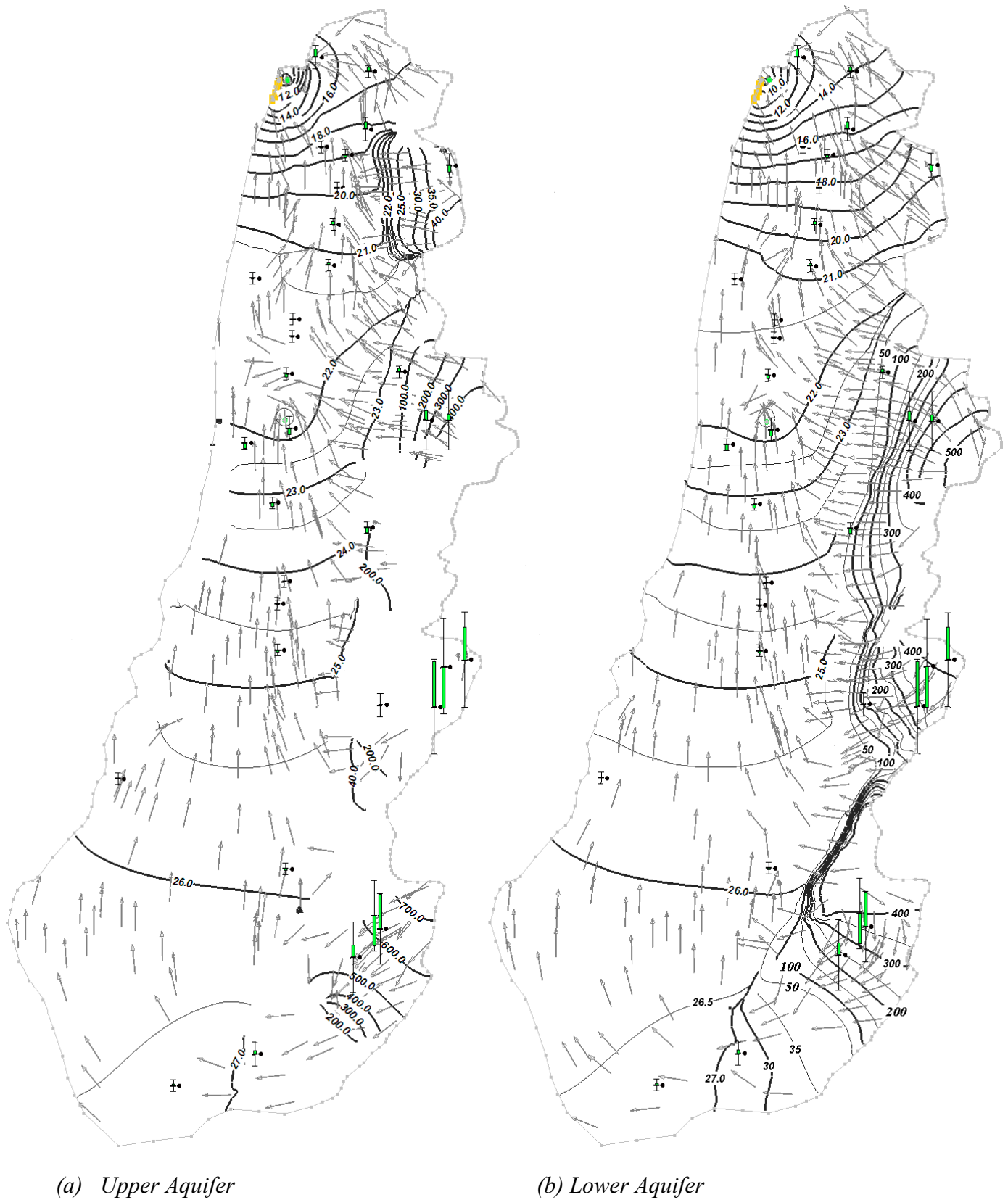


Figure 4.7: Simulated water level

The water balance for the Basin during the pre-development period (observed and simulated) is shown in Table 4.4.

Table 4.4: Pre-development water budget for the WAB

Layer	Recharge	Sea water	Al Timsah Spring		Ras Al Ain spring		Balance (Inflow-Outflow)
			Measured	Simulated	Measured	Simulated	
Mm ³							
Upper Aquifer	308.8	3.9	105 ± 10	56.1	255 ± 10	-133.3	-0.8
Lower Aquifer	64.2			56.2		-128.2	
Total	373			112.3		-261.5	

4.8 HYDRAULIC PROPERTIES OF THE WAB

The calibrated transmissivity values were found double to triple of those measured in specific wells. This result confirmed the double continuity system within the WAB where two flow systems exist; diffuse and conduit flows (Chapter 2). The existence of conduits or channels in the aquifer system as a result of high karstification of the aquifer with high hydraulic conductivities increase the lumped value in each calibrated zone.

In addition, high variation of spatial distribution of hydraulic conductivities was found for both confined and unconfined areas. The calibrated hydraulic conductivity ranges are shown in Figure 4.8. Generally, the upper and lower sub-aquifers have almost similar values except in the mountain areas where hydraulic conductivities are different. The horizontal hydraulic conductivity ranges between less than 1 - 10 m/d in the mountain areas (Hebron, Jerusalem and Ramallah), 5 - 15 m/d in Tulkarem zone, 85 - 160 in both Timsah and Khudera zones, 300 - 500 m/d around Ras Al Ain spring and 150 - 300 m/d in Beir Al Saba zone. These values comply for wells with typical conductivity values of karstic limestone (Freeze and Cherry, 1979) and with the values achieved in previous studies for the same aquifer (Dafny et. al., 2010).

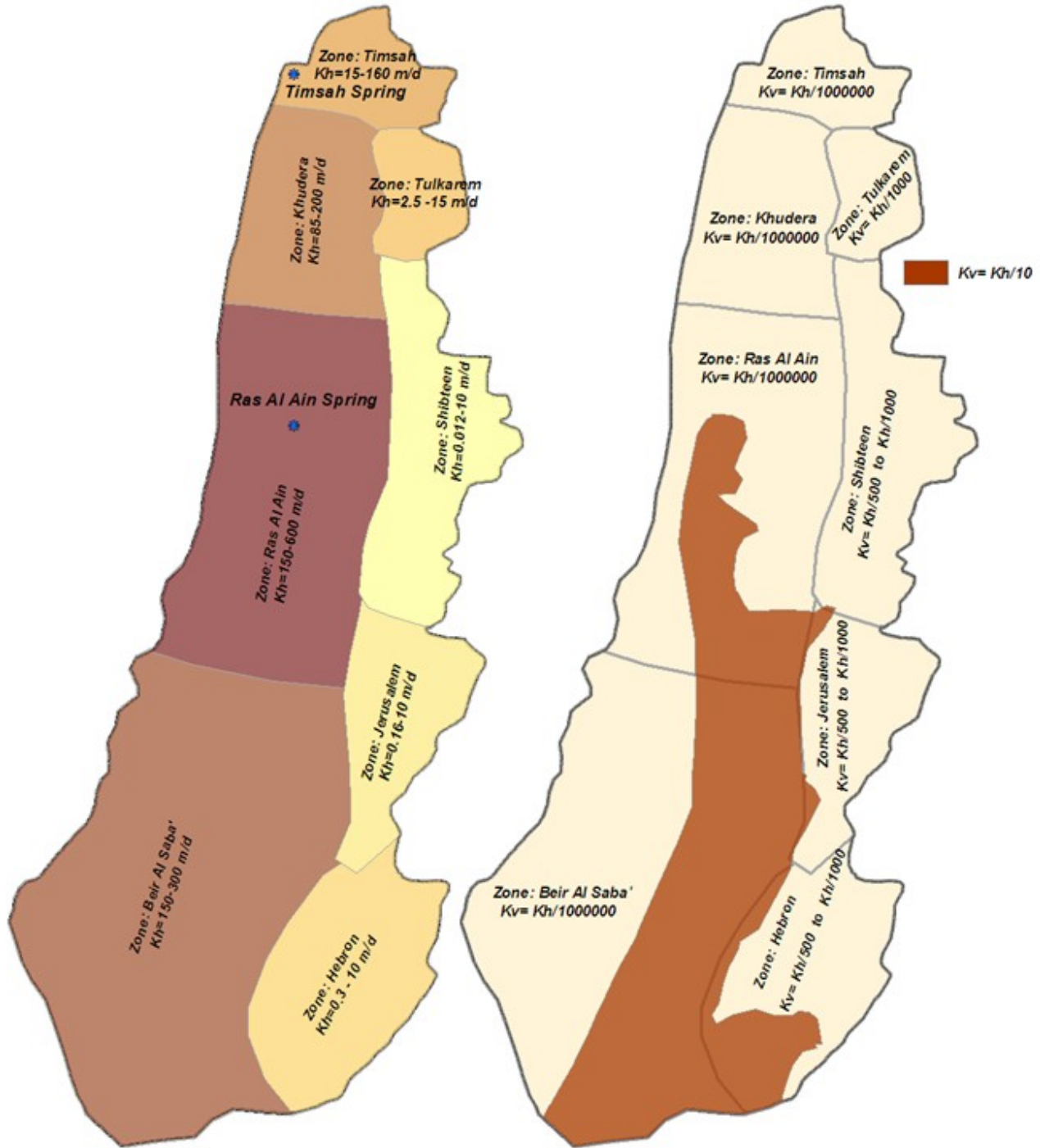


Figure 4.8: Horizontal conductivities and kh/kv ratios for upper and lower sub-aquifers

4.9 SENSITIVITY ANALYSIS

The sensitivity of the model to hydraulic conductivity is carried out using a systematic procedure as described in the following steps:

1. The model domain was divided into 8 zones, Figure 4.8, representing different hydrogeological zones within the WAB.
2. The uncertainty range (i.e. accepted error range) of the 33 well heads was doubled.
3. The hydraulic conductivities were changed for one zone at a time as a percentage of the calibrated values until the heads of any well within the 33 wells reached to any of the new uncertainty limits. Then the resulting heads were recorded.
4. Finally, the ZRMSE was calculated for each zone.

The results of the model sensitivity testing are shown in Figure 4.9. The Figure shows that the model is highly sensitive to hydraulic conductivity in the unconfined part of the Aquifer. It was noticed that slight changes in the horizontal conductivity of the unconfined part of the model domain (-20% - 28% in Tulkarem zone and -5% to 5% in Hebron, Jerusalem and Ramallah mountains) led to high changes in the water levels in the designated unconfined zones. It was also noticed that the head changes occur near the target zone and do not affect the entire model domain.

In contrast, the model shows less sensitivity in the confined part of the WAB. The deviation in hydraulic conductivities ranges between -30% to 325% from the calibrated values for minor changes in water levels, Figure 4.9. The analysis shows that water levels have different levels of changes (in both confined and unconfined) as a result of any change in hydraulic conductivities in any of the confined zones.

The sensitivity analysis of the vertical anisotropy of the Aquifer shows that in confined areas, the aquifer is insensitive to a change in vertical hydraulic conductivities, the water levels change few centimeters as a result of changing the anisotropy coefficient up to 1:1,000. The water levels in the unconfined areas are more sensitive to a change in the vertical conductivity, especially, in both Hebron and Jerusalem zones. It is clear that the vertical conductivities in both zones are significant factors in simulating the water level heads and for determining the dry cells within the two zones.

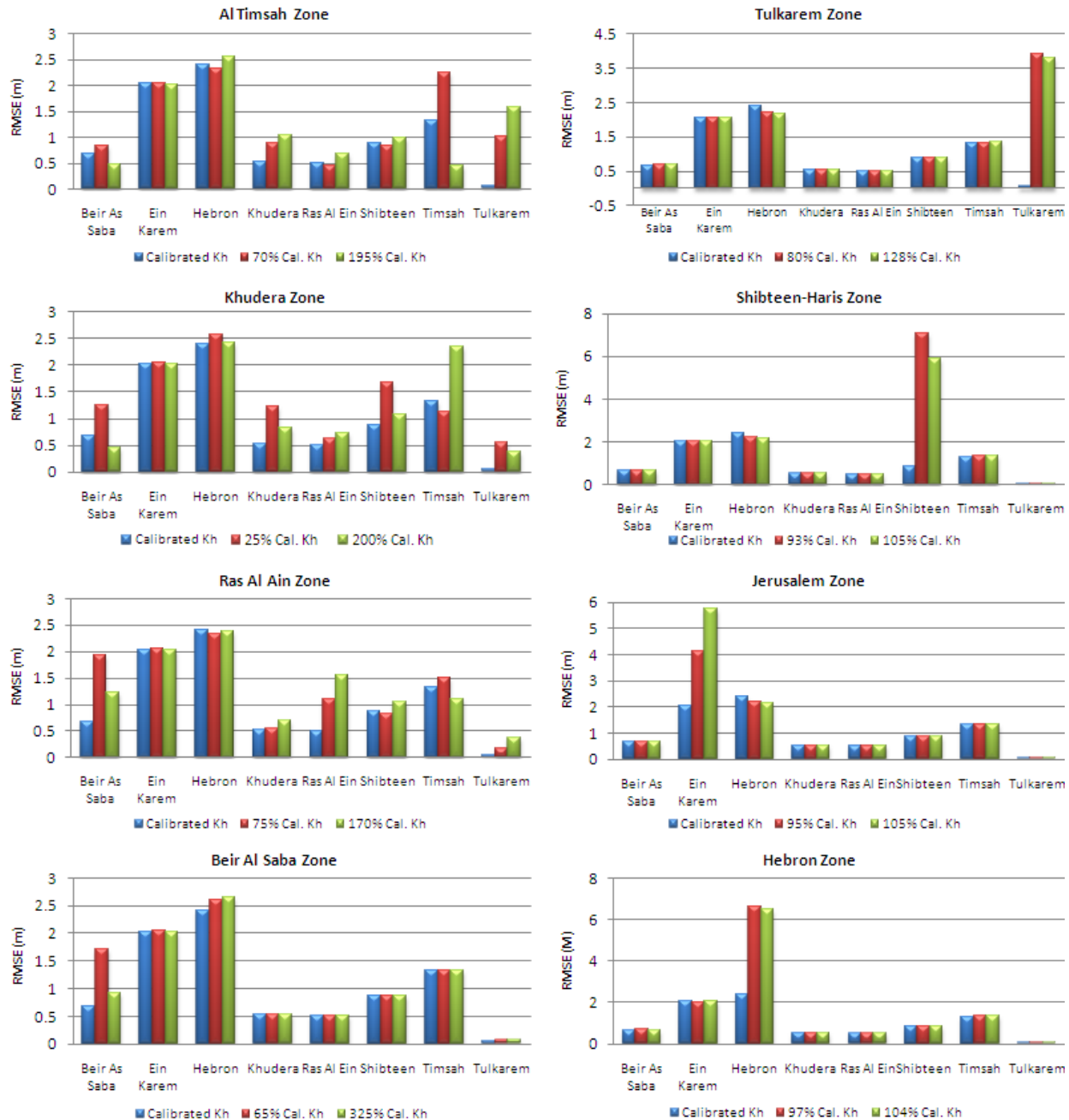


Figure 4.9: Sensitivity analysis to hydraulic conductivities

4.10 CONCLUSION OF THE PRE-DEVELOPMENT MODEL

The geological structure of the WAB has a major influence in controlling the flow within the aquifer. The WAB could be structurally divided into a number of zones, Figure 4.8. In the unconfined zones (Tulkarem and Shibteen zones), the flow is directed towards the northwest. However, in the two other unconfined zones (Hebron Mountains and Jerusalem mountains

zones), the flow generated is towards the southwest, Figure 4.7. At the end, the flow from the unconfined zones accumulates in the confined part of the aquifer and then changes the direction to the north in a narrow channel towards the natural outlet springs.

The pre-development water levels distribution has two types of gradients, the first is flat in the confined part of the Aquifer where water levels range between 5 m in the north close to Al Timsah spring to 27 m in the south in Beir Al Saba' area. The second gradient type is very steep found in the mountain area. For example, the pre-development water level in Hebron zone ranges from 700 m in the upper sub-aquifer and 400 m in the lower sub-aquifer in the eastern side of the zone to 30 m in the foot hills to the east of Beir Al Saba'.

The calibrated hydraulic conductivities as well as the sensitivity analysis reflect the relation of the karstification level and double porosity system within the WAB. This aquifer characteristic was reflected by high conductivity values for the calibrated zones. In high karstic zones (Ras Al Ain zone) the model has the highest hydraulic conductivity, 600 m/d. In less karstified areas, the hydraulic conductivities are also low (i.e. in the order of 10^{-1} m/d in Hebron and Shibteen zones). The mountain areas where the recharge is generated showed that the hydraulic conductivities range between a few meters to a few centimeters per day. In these areas, the calibration and the sensitivity analysis revealed a high influence of hydraulic conductivities on the water heads and the flow quantities.

The water levels in the confined parts of the two sub-aquifers are almost the same, Figure 4.7. However, the water level in the lower sub-aquifer is slightly higher which allows water to flow from the lower sub-aquifer to the upper sub-aquifer.

Chapter 5

CHAPTER 5: GROUNDWATER FLOW DYNAMICS UNDER TRANSIENT CONDITIONS

5.1 INTRODUCTION

Management of groundwater resources in a sustainable manner requires a thorough understanding of its hydrological processes detailed in space and time. This Chapter concentrates on the development of a transient flow model of the WAB in order to understand the flow dynamics of the Basin under different spatial and temporal conditions for both recharge and groundwater exploitation.

Unlike the previous models developed for the WAB (Chapter 1), this model will be more comprehensive in temporal and spatial scales. The transient flow model will be developed for a long-term, monthly time step and refine grid resolution. As a result, the flow dynamics and the aquifer responses under different stresses will be well studied. This model will be used to evaluate the impact of different management options under different climatic and management scenarios on the flow dynamics and on the sustainable yield of the aquifer system. Once the model will be calibrated and validated, it will be transferred to the decision makers in the region to be used for developing an integrated water resources management plan at national and regional scales, it will also be used to predict the future impacts of any scenario that could emerge later.

The development of this transient model is considered as a continuation of the steady state model which was developed in the previous Chapter. Therefore, the boundary conditions, calibrated hydraulic properties (i.e. horizontal and vertical conductivities) and aquifer geometry will be obtained from the pre-development steady state model of the WAB. Other transient parameters including specific storativity and specific yield will be estimated by model calibration.

This system was also be simulated with a three-layer model using MODFLOW-2000 with the same grid size. Time wise, the model covered the period from September 1951 to August 2007 in monthly time steps. The period from September 1951 to August 2000 was used as a

calibration period while the period from September 2000 to August 2007 was used for model validation.

5.2 THE WAB OUTFLOWS

The outflows from the WAB can be divided into two main types: the first is the natural outflow from the two main springs in the Basin (Ras Al Ain and Al Timsah springs). The outflow from these two springs was the dominant outflow during the pre-development period (prior to early 1950s). Afterwards, the second type of outflow emerged as the pumping rate significantly started with 10 Mm^3 in 1951/1952 and then dramatically increased to 300 to 342 Mm^3 by the late 1960s and early 1970s. The pumping outflow then became more dominant than the natural outflow starting from year 1972/73, when the pumping rate was increased to 385 Mm^3 and then kept in the range of $340 - 450 \text{ Mm}^3/\text{yr}$ depending on rainy season. Figure 5.1 shows a comparison between the two types of the WAB outflows. The characteristics of the two types of aquifer outflow were discussed in Chapter 2.

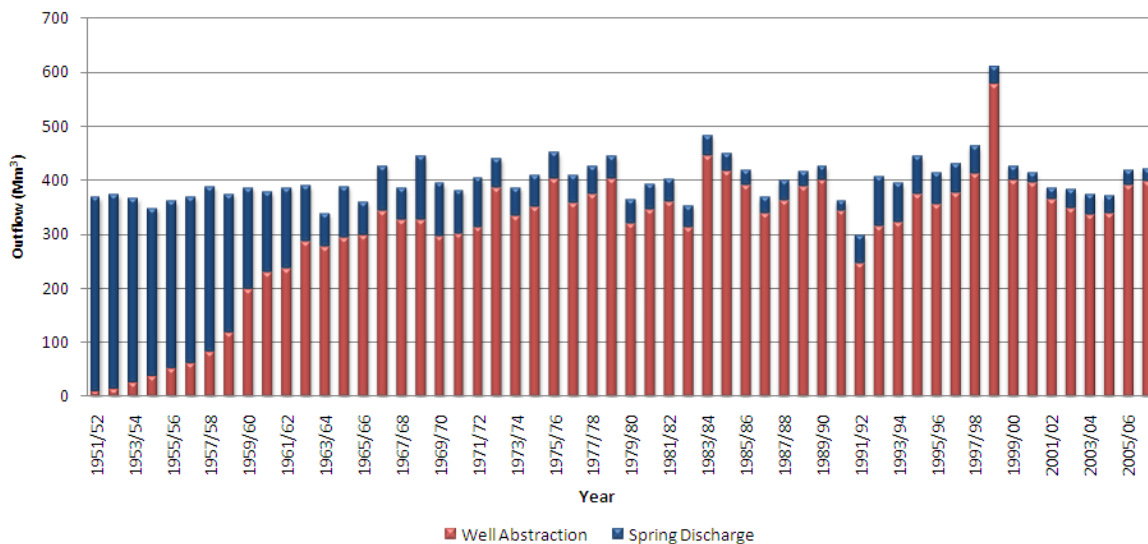


Figure 5.1: Time series of the WAB's outflows

5.3 THE WAB INFLOWS

The main inflow to the WAB is the natural recharge. However, there are other minor components of inflow. These minor inflows are: artificial recharge and sea water intrusion.

5.3.1 Natural Recharge

The estimation of recharge and its distribution were covered in details in Chapters 3 and 4 respectively. To conclude the main recharge features for the development of the transient model, recharge of the WAB is mainly generated from rainfall during winter over the replenishment areas of the Aquifer. The rainfall is characterized by high variation in terms of quantity, temporal and spatial distributions and intensity. The annual rainfall ranges from less than 300 mm/yr up to 1200 mm/yr with a long-term annual average of 550-600 mm/yr (Dafny et al., 2010). The annual recharge has been estimated using the water fluctuation technique taking into consideration the monthly variation of the rainfall (Chapter 3). The long-term average of recharge (i.e. during the model period 1951-2007) was found to be about 373 Mm³/yr. The annual estimated recharge which will be used for the transient model period (1951-2007) is shown in Figure 5.2. The Figure shows that the annual recharge in 26% of the modeled years was 80% less than the average annual recharge considered dry years. Also, 17.2% of the years were found 120% higher than the average recharge (i.e. wet years) meaning that dry years was more frequent than the wet years within the model time domain.

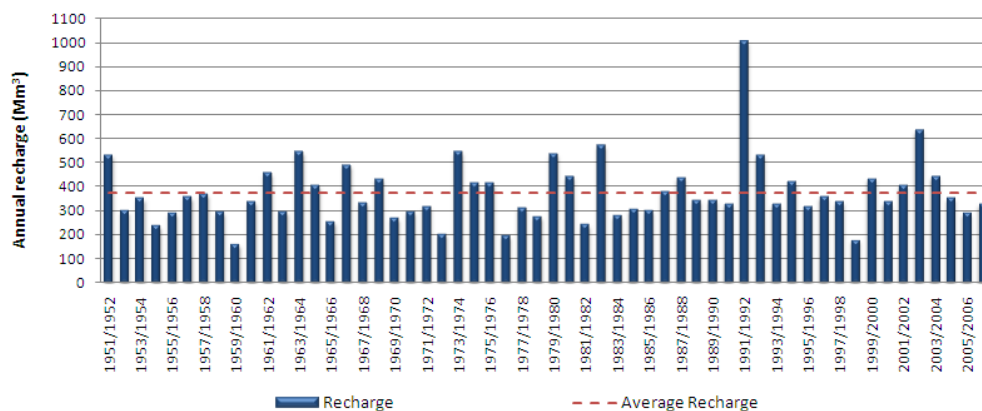


Figure 5.2: Annual estimated recharge during the model period

Initially, the recharged amount was spatially distributed over the replenishment areas based on the rainfall distribution, outcropping formation, slope, land use and surface drainage system as described in Chapter 4. Also, the annual estimated recharge was initially downscaled into monthly amounts using the monthly rainfall values. Both the spatial and

monthly distributions were modified later by trial and error during model calibration in order to match the shape and values of the measured water levels and springs hydrographs.

5.3.2 Artificial recharge and Sea Water Intrusion

Both artificial recharge and sea water intrusion were covered in details in Chapter 2. Figure 5.3 shows the location of the wells used for injecting water and the location of the anticipated aquifer connection with the sea. The Figure also shows that artificial recharge was conducted in the northern and central parts of the Basin where the pumping rate is already high. In this type of use, the Aquifer is used as a storage tank where the excess water during wet months was stored in the Aquifer to be used in drier months.

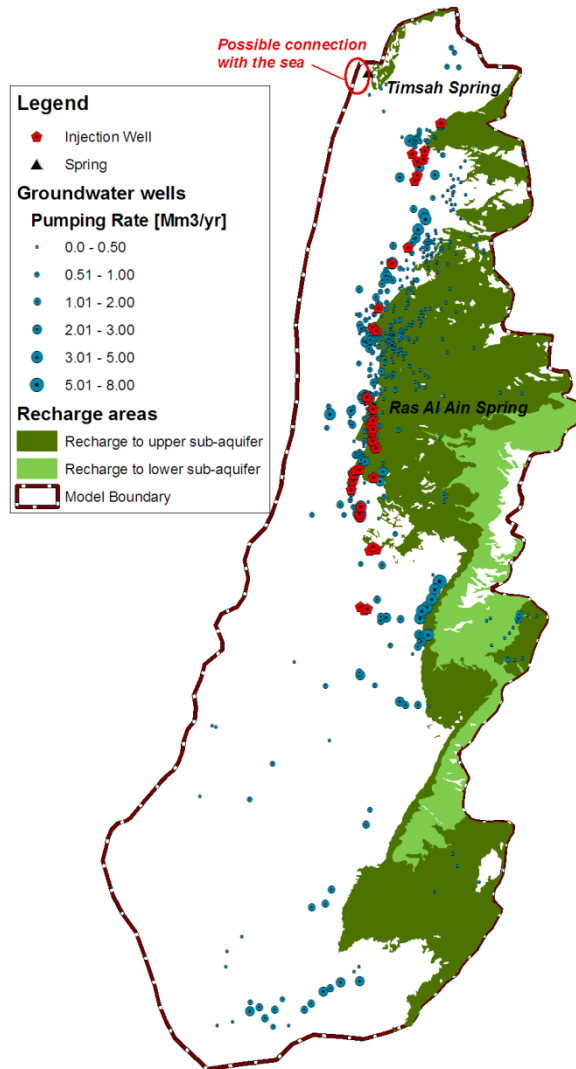


Figure 5.3: Location map of the injected wells

5.4 WATER LEVEL

In total, 19 observation wells were used for the calibration and validation of the numerical flow model, Table 5.1. These wells are uniformly distributed over both the confined and unconfined parts of the Aquifer, Figure 5.4. The water levels during the early 1950s in the confined part of the WAB gently dropped from 25-27 m near Beir Al Saba' in the south to 16 m in the Menashe heights in the north (Rosenthal et. al., 1992 and Dafny et al., 2010). In the unconfined part and for the same period, the water levels stood at 450-500 m in Jerusalem area (Ein Karem), in Hebron Mountains water level was 350-450 m in the lower sub aquifer and 550 - 700m in the upper sub-aquifer and 300-350 m in Salfeet area (Weinberger et al., 1994, Guttman et al., 1988, and Dafny et al., 2010).

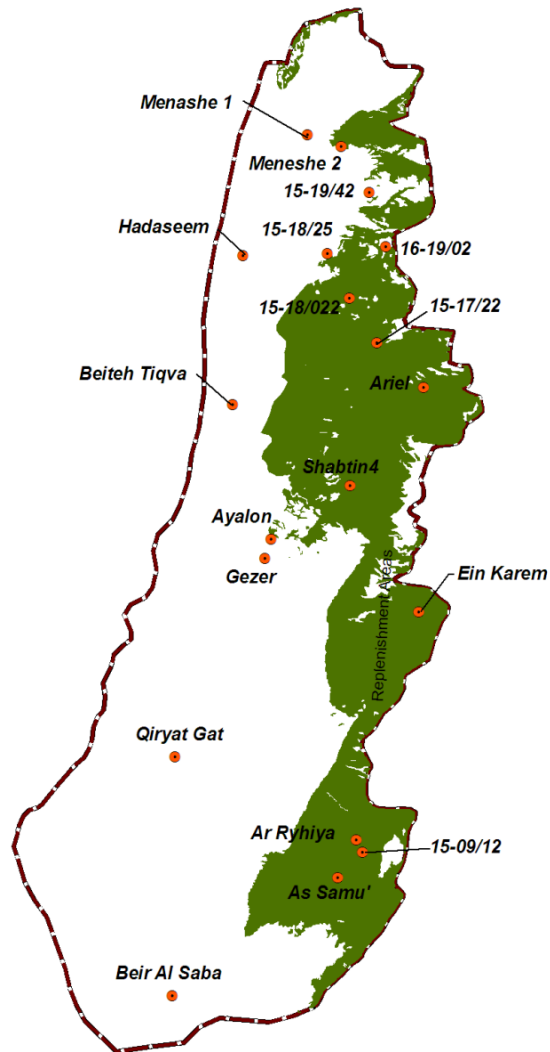


Figure 5.4: Location of observed wells used for model calibration

The water level records were available starting from the late 1960s, and were used for calibration and validation of the transient model. In general, water levels in the entire Aquifer started to decline due to the over exploitation from the Aquifer. Before the wet year 1991/92, the water level in the same areas were stood at 12-13 m near Beir Al Saba' in the south and 8-9 m in the Menashe heights in the north . In the unconfined part and for the same period, the water levels stood at 400-450 m in Jerusalem area (Ein Karem), in Hebron Mountains the water level was 350-450 m in the lower sub- aquifer and 525-650 m in the upper sub-aquifer and 270- 300 m in Salfet area.

The simulated water levels during the 1950-1960 period were accepted whenever the starting point matched with the level during the early 1950s and matched with the available data of the observation wells.

5.5 PHYSICAL PROPERTIES OF THE WAB

The physical properties of the Aquifer (specific storativity, specific yield and conductivities) are required to solve the flow equation. Both horizontal and vertical conductivities for the two sub-aquifers were obtained from the steady state model representing the pre-development period of the Aquifer. The values of conductivities show high spatial variation between confined and unconfined areas, Figure 4.8.

In order to optimize the seasonal fluctuations of the observed and calculated water levels, different values for specific storativity were assigned for the purpose of dynamic conditions calibration. The initial values were obtained from different literatures for similar karstic aquifers (Guttman et al., 1995 and Tsukerman et al., 1999), and then modified during model calibration. As a result, the calibrated specific storativity for confined areas were found in the range of order 10^{-6} to 10^{-5} (1/m). In the unconfined areas, the specific yield ranges between 1% - 7.5%.

5.6 CALIBRATION METHODOLOGY

The transient model calibration efforts focused mainly on the spatial and monthly distributions of recharge and storativity coefficients of the aquifer layers as the main calibrated items. Modifying the hydraulic conductivities (K_h and K_v) and the hydraulic

conductivity of the two springs were achieved during the calibration of the steady state model and set as a secondary target items for the model calibration.

The model domain was divided into different zones based on the confinement line as well as the geological outcropping formations and the main structures within the Aquifer domain. The hydraulic conductivities and the initial storativity coefficients were averaged for each zone and then adjusted during the calibration process. In the same way, the replenishment areas were also divided into a number of recharge zones with initial spatial and temporal (monthly) distribution of recharge.

The main task during the calibration process was to fit the simulation results to the observed data in both spring hydrographs and water levels in the 19 monitoring wells. The calibration efforts also attempted to fit the simulated model to the characteristics of the spring hydrograph and water level records including the monthly variations, trends, values and peaks.

Unfortunately, the full monthly records for the 19 monitoring wells were not available. Some records within the simulated period were missing for some wells and available for others. Therefore, simulated water levels that matched the available measured water levels in all monitoring wells were accepted. In addition, the Root Mean Squared Error (RMSE), Eq. 5.1, was also used to represent the simulation error for each monitoring well.

$$\text{RMSE} = \sqrt{\frac{1}{n} \sum_{i=1}^n (m_i - S_i)^2} \quad \text{Eq 5.1}$$

Where:

n: number of measurement records for each well

m: measured water level at time step *i*

S: simulated water level at time step *i*

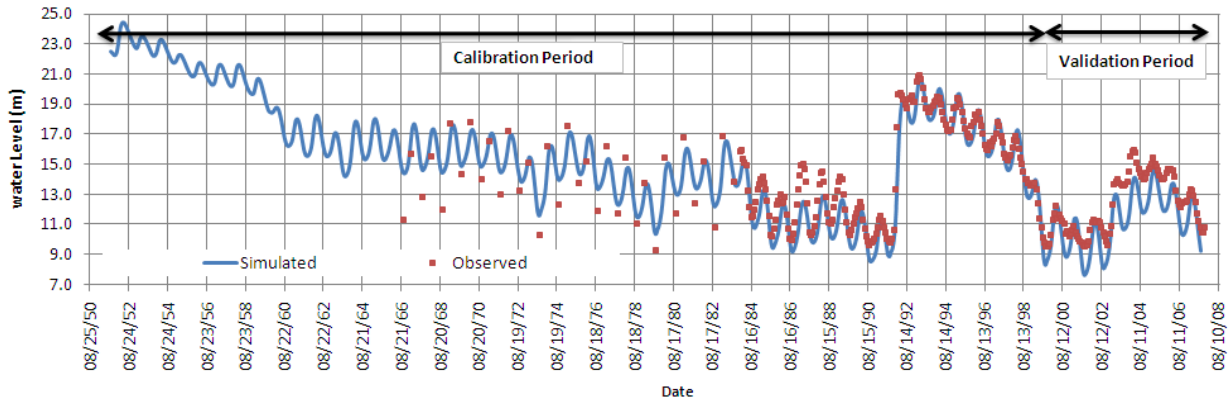
5.7 MODEL VALIDATION

The transient model of the WAB was validated using the data between the period of September 2000 to August 2007. The simulated water levels in the 19 monitoring wells and the hydrograph of the two springs were also used for validating the model. The computed

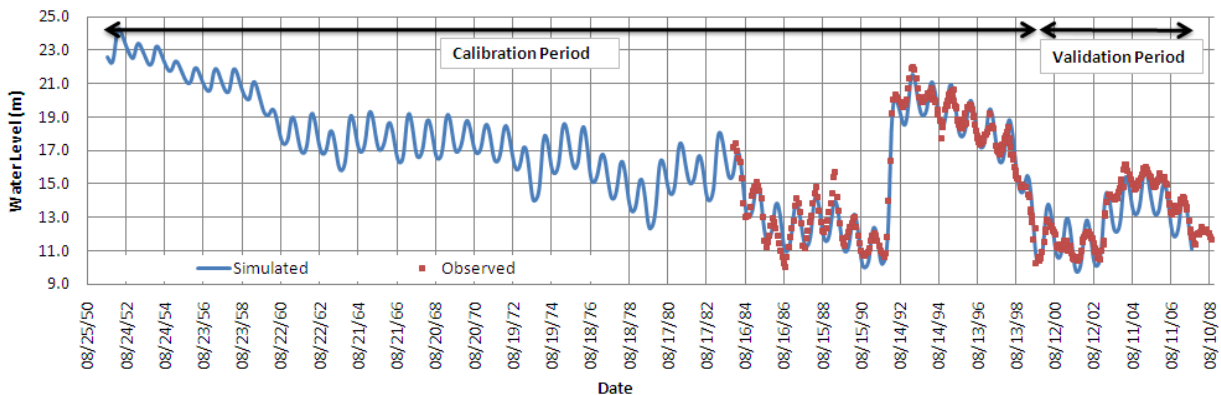
water levels and spring discharges including monthly variations compiled with the measured data in all wells and spring hydrographs for the entire modeling period are shown in Figures 5.5, 5.6 and 5.7.

5.8 MODEL SIMULATION RESULTS

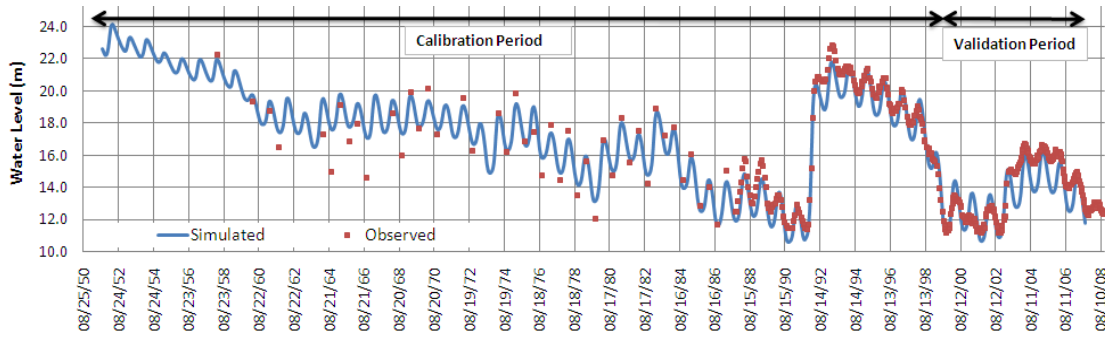
Figures 5.5 and 5.6 show the simulation results for a sample of monitoring wells. The simulated water levels show an excellent match with the available measured water levels in both seasonal variations and head values. The Figures also show the influences of the major events within the modeled period especially the impact of wettest year 1991/1992 and the driest year 1998/1999 which was synchronized with high pumping rates.



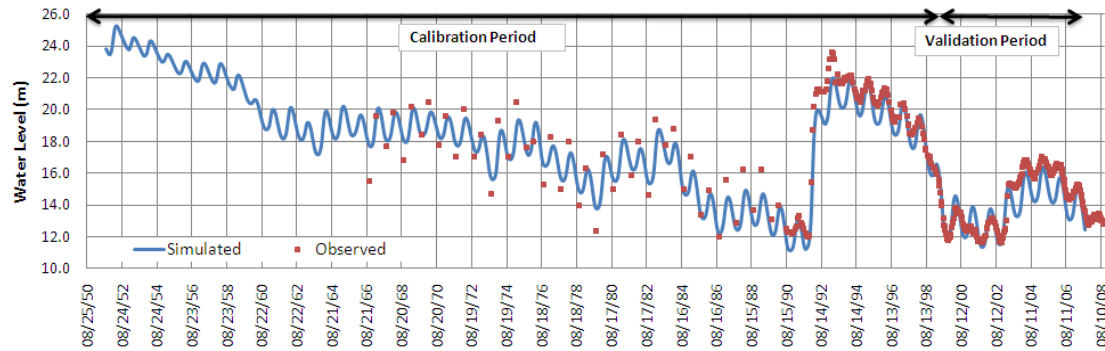
(a) Maneshe #2 well



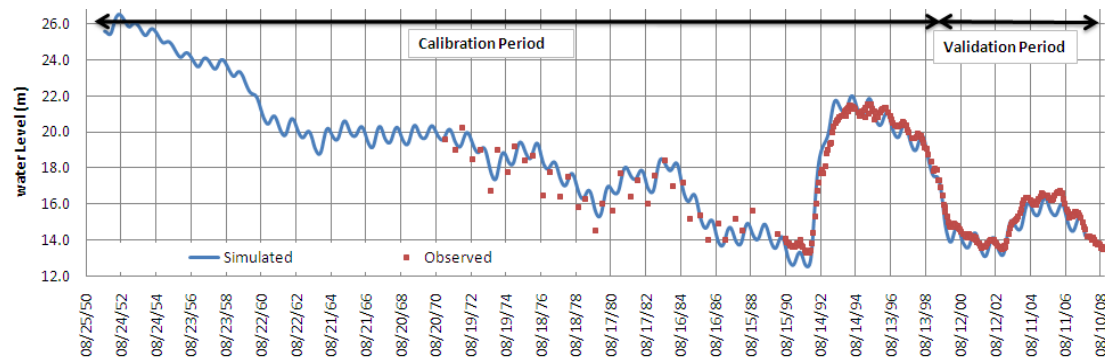
(b) Hadaseem well



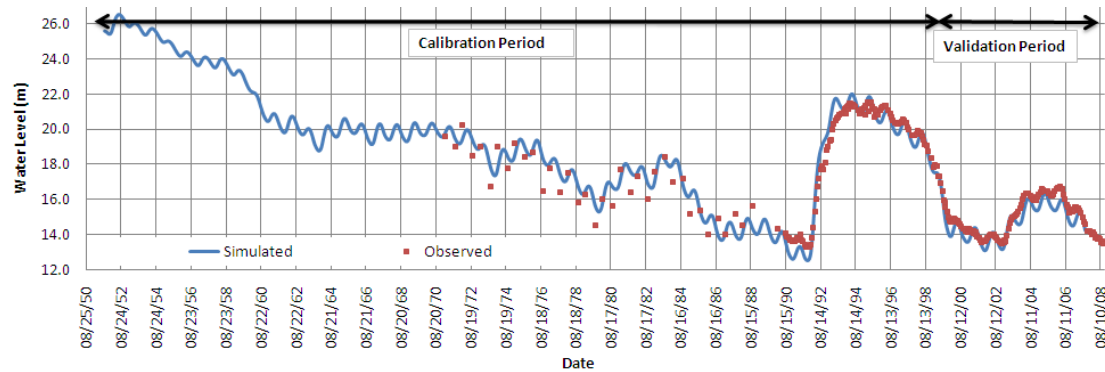
(c) *Beteh Tiqva well*



(d) *Ayalon well*

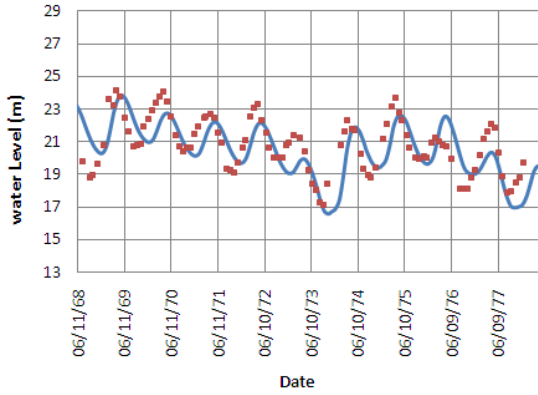


(e) *Qiryat Gat well*

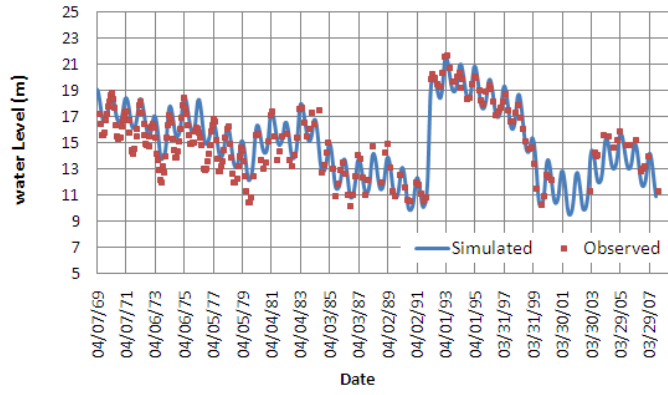


(f) *Beir Al Saba well*

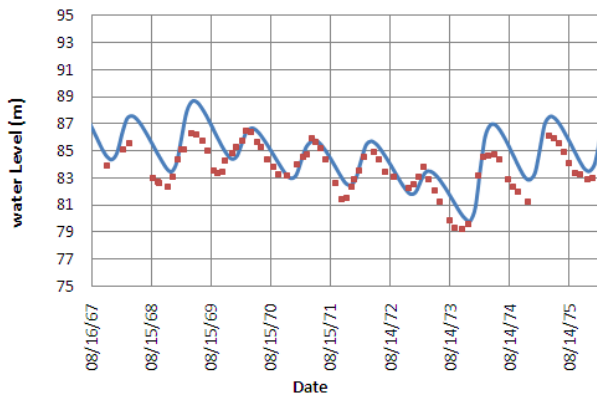
Figure 5.5: Simulated versus observed water levels in the confined part of the WAB



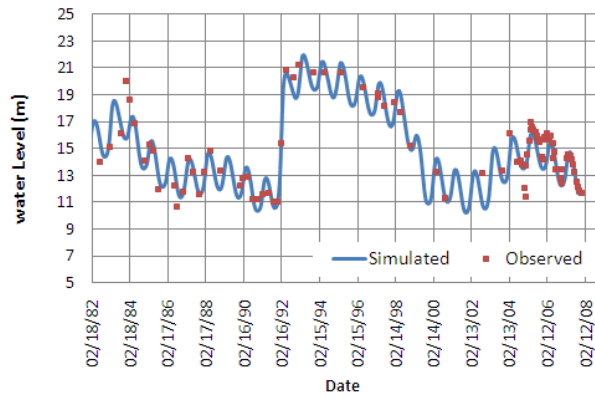
(a) 15-19/42 well



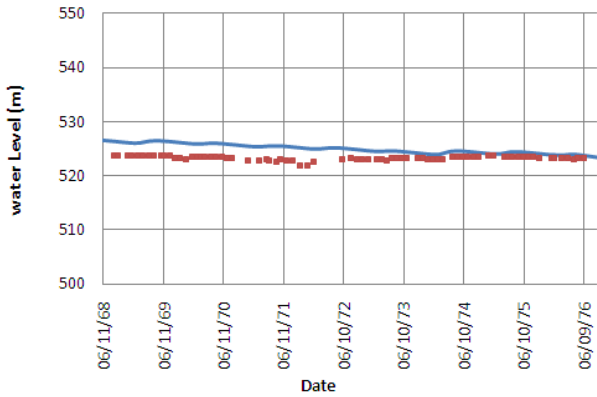
(b) 15-18/025 well



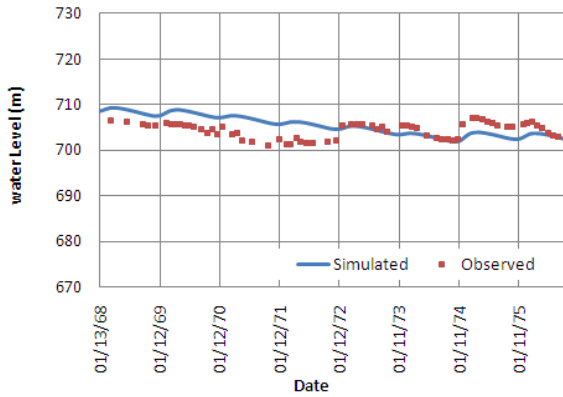
(c) Shabtin well



(d) 15-18/22



(e) As Samu' well

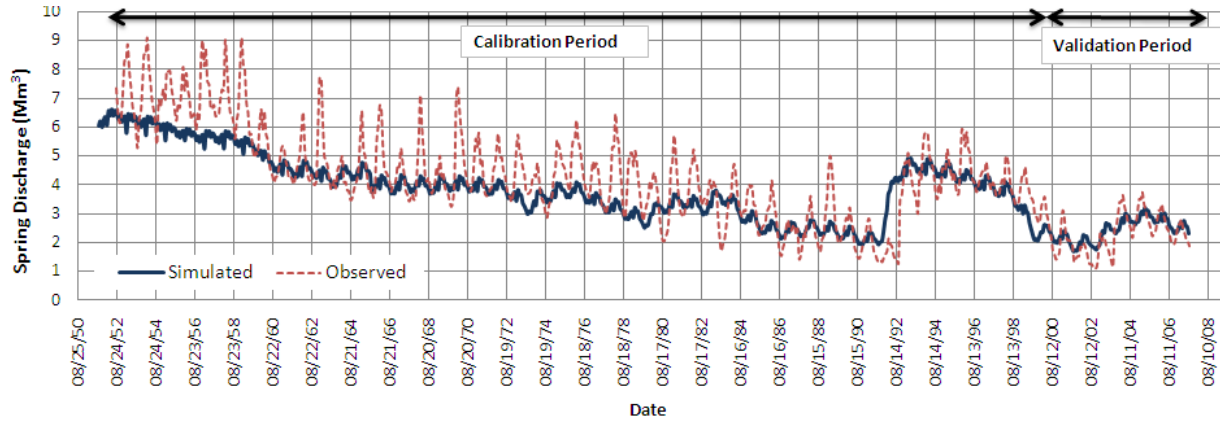


(f) 15-09/12

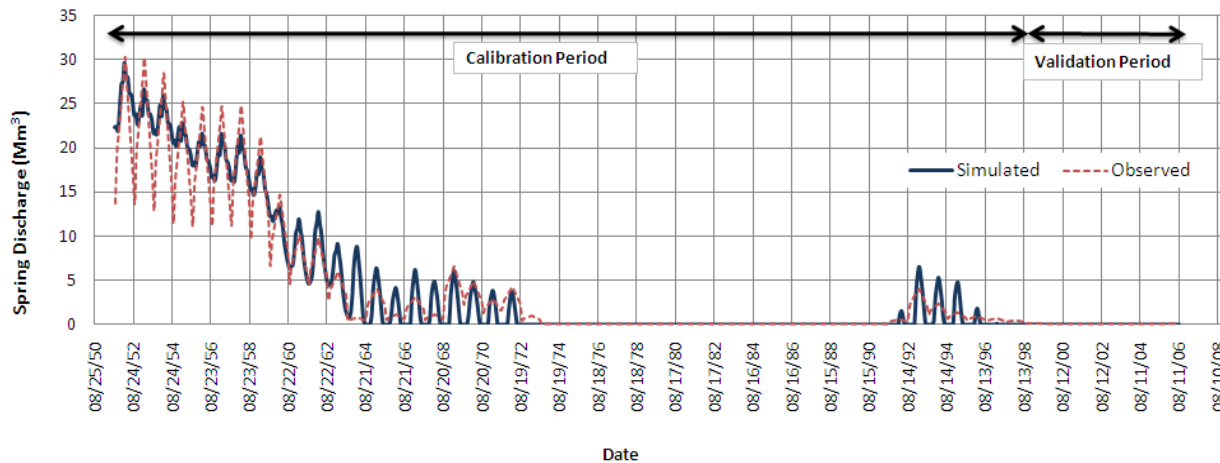
Figure 5.6: Simulated versus observed water levels in the unconfined part of the WAB

Similarly, Figure 5.7 shows the hydrographs of the two spring discharges. The simulated spring hydrograph, especially Al Timsah spring, shows a relatively good match with the measured spring discharge data. However, both seasonal and multi-year variations were simulated by the model; the peaks of discharge were not captured well. The reason for not

simulating the discharge peaks was referred to the double continuity behavior of the aquifer due to the high karstification and existence of underground conduits within the WAB which make springs respond rapidly to recharge events.



(a) *Al Timsah Spring*



(b) *Ras Al Ain Spring*

Figure 5.7: Simulated versus observed spring hydrographs

The overall water levels and springs discharge figures show the best correlation between measured and simulated values. The model succeeded to simulate the water level during the beginning of the modeling period in all wells (i.e. starting from the pre-development water level). The water levels in the WAB started to slightly decline during the first ten years (1951-1961) when the pumping rate was relatively very low (i.e. started with 10 Mm³ in 1951 and increased to a round 200 by Mm³ 1961). Afterwards, the water levels showed a significant decline in all wells as a result of heavy pumping (i.e. more than 300 Mm³).

However, the sum of that simulated annual springs discharge was equal to the sum of measured, the simulated discharge of Al Timsah spring during 1951-1961 was less than the measured discharge, while, the discharge of Ras Al Ain spring was higher. One of the reasons could be the accuracy of data during this period.

The calculated RMSE values showed that measured and simulated water heads very well matched. These values were low in all wells located in the confined area (i.e. around one meter) and relatively high (up to 10 meters) in some wells located in the unconfined area, Table 5.1, due to the geological structure which has a major influence in controlling the flow within the aquifer.

Table 5.1: RMSE for the observed wells

Well Name	Sub-aquifer	RMSE (m)	Type
Hadaseem	Upper	0.85	Confined
Qiryat Gat	Upper	0.54	Confined
Bir Al Saba	Upper	0.63	Confined
Menashe 1	Upper	0.99	Confined
Beiteh Tiqva	Upper	0.97	Confined
Shabtin4	Lower	2.04	Confined
Gezer	Upper	0.89	Confined
Meneshe 2	Upper	1.21	Confined
Ayalon	Upper	0.73	Confined
15-19/42	Upper	1.46	unconfined
16-19/02	Upper	1.26	unconfined
15-18/25	Upper	1.05	unconfined
15-17/22	Lower	3.48	unconfined
As Samu'	Upper	2.78	unconfined
Ariel	Lower	9.8	unconfined
Ar Ryhiya	Lower	8.66	unconfined
15-18/022	Upper	1.15	unconfined
15-09/12	Upper	2.8	unconfined
Ein Karem	Lower	8.98	unconfined

The monthly and spatial distribution of annual recharge was also achieved by model calibration. The downscaling of the annual recharge into monthly recharge was calibrated by comparing the shape of the simulated water levels and measured levels. Initially, the monthly distribution of recharge was set depending on the monthly rainfall then it was adjusted by calibration in order to simulate the same shape of the actual water levels in all monitoring wells. A sample of the obtained best fit monthly distribution curve is shown in Figure 5.8. This curve changes annually according to the monthly distribution of seasonal rainfall.

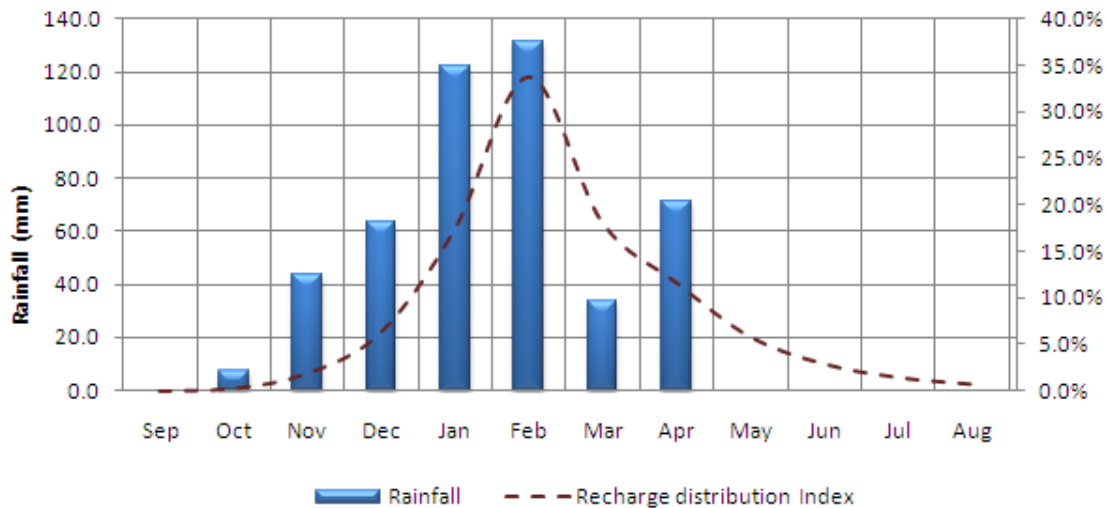


Figure 5.8: Recharge distribution index for year 2005/2006

The spatial distribution of recharge was also calibrated by comparing the value of the simulated water levels with actual water levels. Initially, the spatial distribution of rainfall, outcropping formation, slope, land use and flow accumulation were used to distribute the recharge over space (Chapter 4) which was then slightly modified during the calibration process to match the measured water levels.

5.9 CONCLUSION OF THE TRANSIENT FLOW MODEL

A long-term numerical flow model on a monthly basis was successfully developed for a karstic aquifer (i.e. the WAB). The complexities of the various flow regimes of karstic groundwater were successfully modeled using MODFLOW 2000 by averaging the physical properties of the aquifer formations. The numerical results of the WAB model show good

compliance with the observed curves; particularly including the discharge of the two main springs and the water levels of all wells used for model calibration and validation periods.

The geological structure of the WAB has showed a major influence in controlling the flow pattern within the aquifer. The western hydrological barrier (Talme Yafe Group) prevents groundwater flow seaward and diverts the groundwater northward beneath the Coastal Plain. North to Ramallah Anticline, northeast of the WAB, the natural recharge generated in the replenishment areas in Salfet and Tulkarem regions flows towards the west to be accumulated with the groundwater in the plain areas. In some places, the pumping affects alters the natural flow line distribution and direction of the Upper Aquifer in the WAB. For example, in Ein Karem Region (Jerusalem), the split-off Ramallah Anticline is responsible for a local water level range between 400 and 500 m. Therefore, this part of the aquifer could be considered as a sub-basin within the WAB. In the southern portions of the WAB, the major replenishment area is located in the Hebron Mountains, from there, groundwater is forced to flow south-westward towards Beir Al Saba area by the southwest trending and plunging the split-off anticline of the Hebron anticline. The flow changes its direction to the north towards the natural spring outlets and productive wells once the anticline is buried deep enough.

Recalling the conceptual model of the WAB described in Chapter 2, the transient model of the WAB succeeded in simulating the main responses of the aquifer system during the 56 simulated years. As a result, the model provided significant information about the aquifer's physical properties, flow dynamics, and aquifer responses to different climate and exploitation conditions. As well as validating the special advantage of the WAB that it could be used as both on underground natural carrier and storage reservoir. As another example, the model was able to simulate the high aquifer response after the wettest and the driest years within the model records (i.e. 1991/92 and 1998/99 respectively) as shown in Figures 5.5 and 5.7. Also, the high conductivity area in the central part of the Basin where water level rises faster due to recharge than in other areas which led to a change in the flow direction. Figures 5.9 and 5.10 show the flow pattern of the aquifer at significant periods. These figures reflect the change of the aquifer flow dynamics as a result of aquifer utilization during the last 56 years.

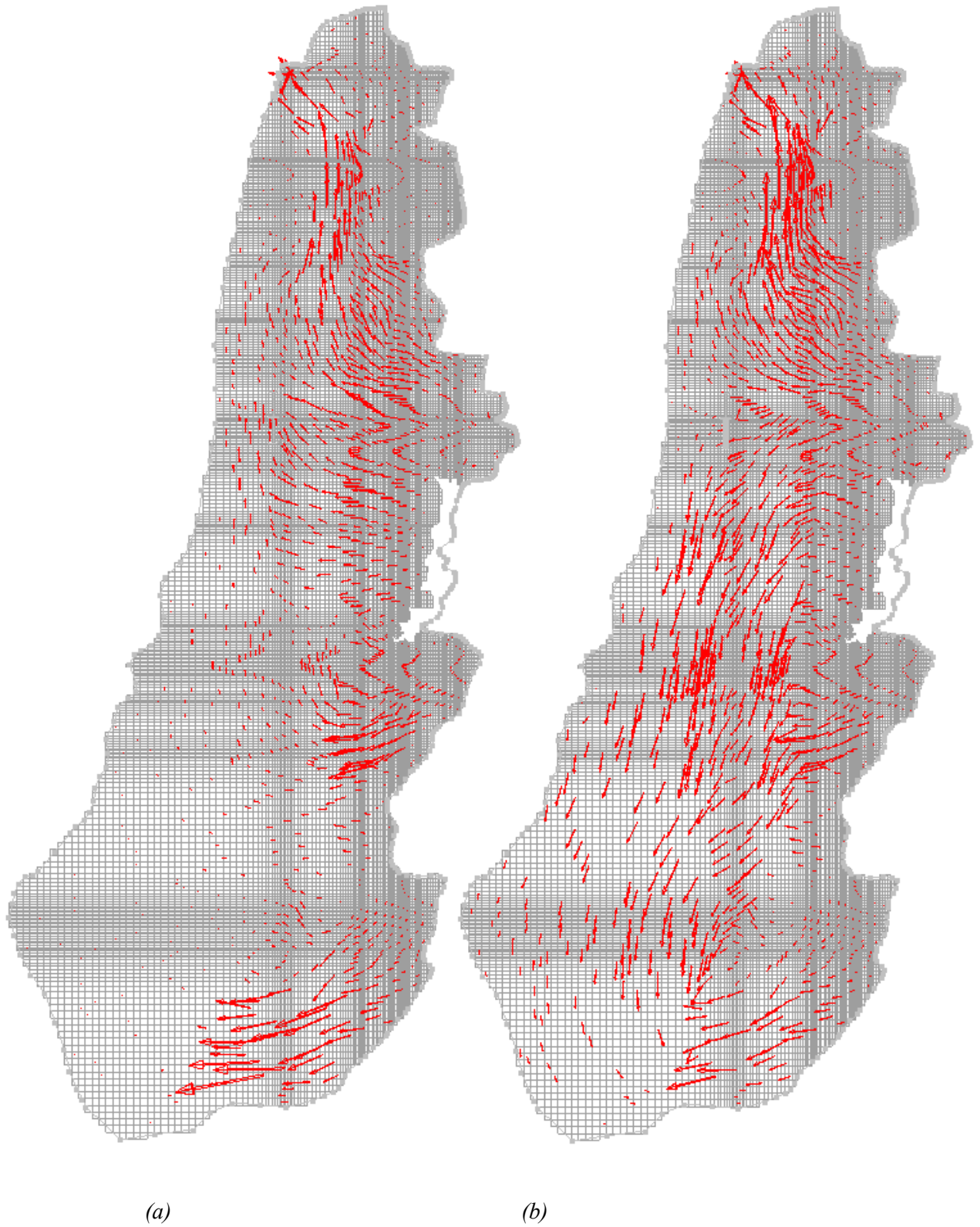


Figure 5.9: Flow direction in the lower sub-aquifer before and after the wettest year (a) April 1991 and (b) April 1992

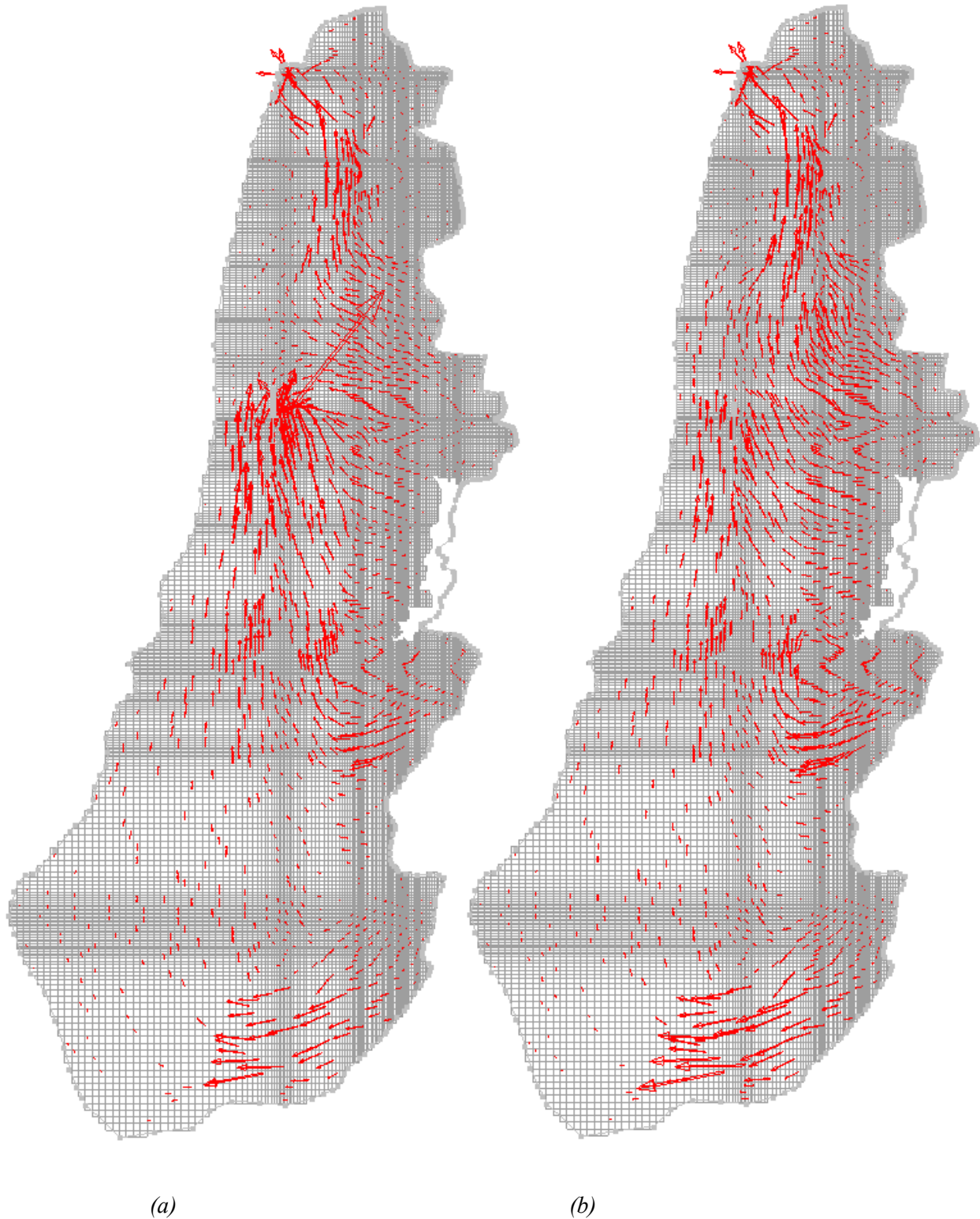


Figure 5.10: Flow direction in the lower sub-aquifer during (a) April 1953 when the outflow was dominated by springs discharge (b) April 1974 when the outflow was dominated by pumping and also after the Ras Al Ain spring was dried out

The water balance of the two sub-aquifers shows that 63% of the natural recharge reaches the upper sub-aquifer. However, 86% from the annual pumping and 37% of the spring discharge are extracted from the upper sub-aquifer. In order to substitute the high outflow from the upper sub-aquifer, the lower sub-aquifer leaks an average of 42.6 Mm³/yr (i.e. 11% of the total aquifer outflow) to the upper aquifer through the interconnection areas between the two sub-aquifers. The water balance of the WAB is shown in Table 5.2.

Table 5.2: Water balance budget for the WAB

	Item		Average	Min	Max
			Mm ³ /yr		
Upper Sub_Aquifer	Flow From Lower Sub-aquifer	Inflow	42.6	-70.9	113.0
	Recharge		235.3	93.7	763.3
	Sea Water Intrusion and Injected water		2.9	2.0	16.9
	Sum of Inflow²		280.8	104.1	759.5
	Drain	OutFlow	-36.8	-3.8	-180.8
	Pumping		-252.7	-9.0	-487.3
	Sum of outflow²		-289.5	-183.4	-494.3
Storage²			-8.7	-255.8	548.7
Lower Sub_Aquifer	Recharge	Inflow	138.1	57.3	475.1
	Sea Water Intrusion and Injected water		2.0	2.0	2.0
	Sum of Lower Inflow²		140.1	49.1	456.5
	Flow To Lower Sub-aquifer	OutFlow	-42.6	70.9	-113.0
	Drain		-62.4	-22.9	-209.2
	Pumping		-40.3	-1.4	-76.6
	Sum of Lower Outflow²		-145.2	-65.4	-210.5
Storage²			-5.2	-142.3	384.1

² The sum of the minimum and maximum values were not calculated by direct addition. It was achieved from the model budget since the minimum and maximum values of the inflow and outflow items may not occur in the same time.

The WAB	Recharge	Inflow	373.4	151.0	1238.4
	Sea Water Intrusion and Injected water		4.9	4.0	18.9
	Total Inflow²		378.3	155.1	1257.2
	Drain	OutFlow	-99.2	-26.7	-389.9
	Pumping		-293.0	-10.3	-563.9
	Total Outflow²		-392.2	-283.3	-605.8
	Total Storage²			-13.9	-401.4

The results also show that the water level started to decline simultaneous to heavy pumping from the Aquifer. As a result, by year 1973 the Ras Al Ain spring dried out, Timsah Spring discharge decreased to a low level where it reached to an average of 30 Mm³/yr and the water level in most of the confined part of the aquifer declined by 10 - 13 m. The Aquifer was partially recovered during a few months almost to its pre-development state after the wettest year within the aquifer records; 1991/1992, where the accumulated annual rainfall was doubles the normal average rainfall. After this wettest year, the water level reached to the pre-development status, the Ras Al Ain spring returned back to the low discharge rate and the discharge rate of Al Timsah spring also increased. The fast response of the Aquifer proves the high karstic level of the WAB as well as the interconnectivity of the aquifer formations in both horizontal and vertical dimensions.

The inflow and outflow from the Aquifer over the 56 years is presented in Figure 5.11. The natural recharge is the dominant inflow to the WAB with an average 98.7% of the total aquifer inflow. The two other minor inflows are the sea water intrusion through the northwestern boundary (3.6-3.9 Mm³/yr) and the injected water during the wet years. The natural recharge as well as the injected water was dependent on the rainy season, therefore, the total annual inflow was highly correlated to the annual rainfall. On the other hand, the types outflow of changed during the model period. Initially, outflow discharged through the two main springs in the aquifer (Ras Al Ain and Al Timsah springs). Afterwards, the springs' outflow decreased by time as a result of increasing the exploitation from the Aquifer through the groundwater wells. As a result, the outflow was mainly from the wells abstraction.

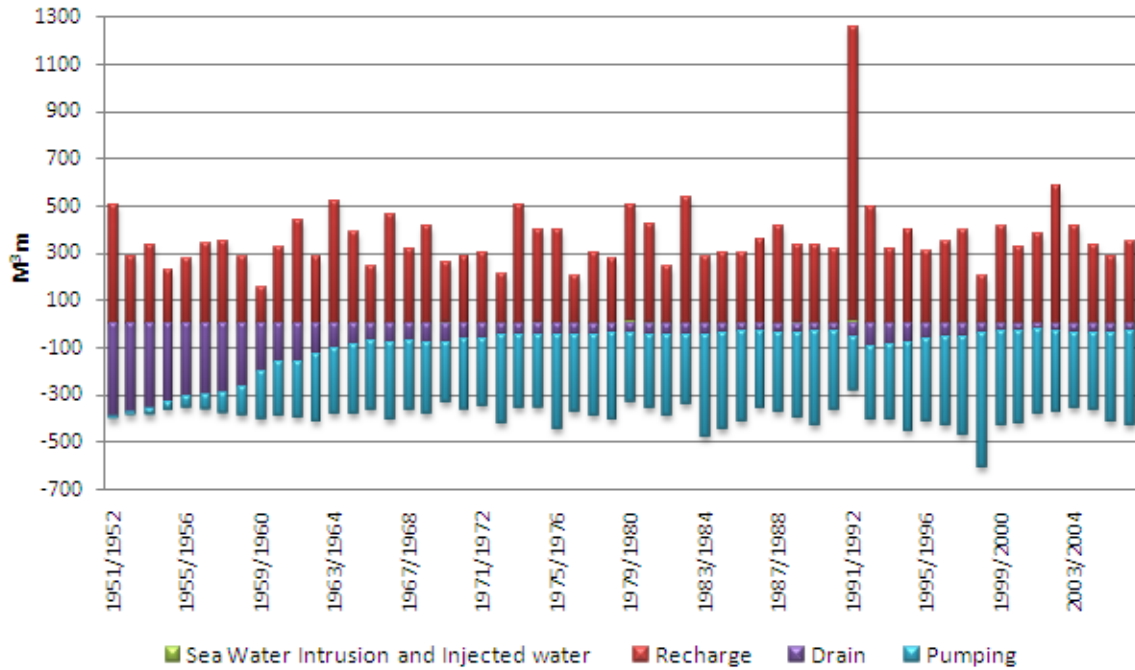


Figure 5.11: Inflow and outflow from the WAB

Chapter 6

CHAPTER 6: SUSTAINABILITY OF THE WAB UNDER DIFFERENT SCENARIOS

6.1 INTRODUCTION

Groundwater is the most important component of the region's water resources. Therefore, understanding the impacts of increasing water demands as a result of population growth and global warming is very essential for the sustainability of these resources. Groundwater sustainability is defined as the development and use of the aquifer system to meet the current and future demands without causing unacceptable consequences (Alley, W.M et al., 1999). For this reason, evaluating the WAB's response under different climate and pumping scenarios is a significant need. As a result, different strategies could be developed in order to maximize the pumping rates without harming the aquifer system.

The numerical transient flow model of the WAB was extended in time to cover the management period of 28 years (i.e. 2007/2008 to 2034/35). This numerical flow model (MODFLOW) was coupled with the Water Evaluation and Planning System (WEAP). The coupled WEAP model can run the MODFLOW model for different defined pumping and recharge alternatives. The WEAP can prepare the input files (i.e. pumping rates and recharge) and then transfer them to MODFLOW model. The MODFLOW is then run accordingly and results (i.e. water levels and water balance) are returned back to the WEAP for presentation and further analysis.

Accordingly, the coupled WEAP-MODFLOW model was run for all defined scenarios, water level distributions and springs' discharges were then used as indicators for the sustainability of the WAB. The results were then analyzed and compared with each other in order to produce the best management scenarios under different climate conditions.

6.2 WATER EVALUATION AND PLANNING SYSTEM (WEAP)

The Water Evaluation and Planning System (WEAP) has been acknowledged by different water planners in the world as an efficient program dealing with the planning and management of water resources. It was developed by the Stockholm Environment Institute.

WEAP is a user friendly software designed to simulate water resources systems and trade-off analysis. It can store a wide range of information characterizing the water system and calculate water demand, supply, runoff, infiltration, crop requirements, flows, storage, and pollution loads, treatment effluent, discharge, cost benefit analysis and stream water quality under different water management alternatives and climate scenarios.

Additionally, WEAP and MODFLOW models can be dynamically coupled. Where, for each time step, outputs of one model will be transferred as input to the other model, Figure 6.1. For example, the required pumping and the total inflow were spatially transferred to the MODFLOW model, the MODFLOW will run based on these inputs and send the results of water levels, springs discharges and aquifer storage to the WEAP model for supply-demand, cost benefit, storage and other calculation and analysis.

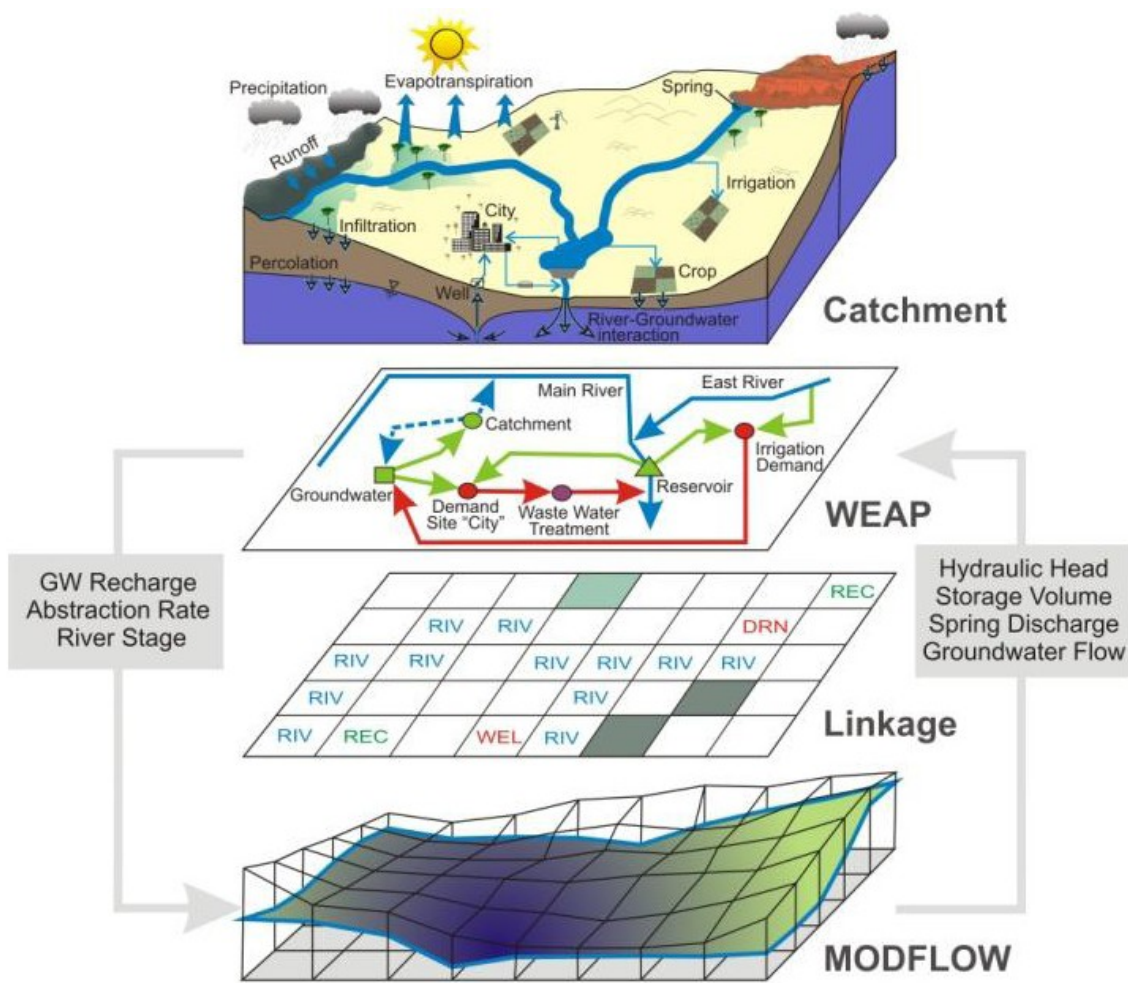


Figure 6.1: Schematic diagram of WEAP-MODFLOW coupling, (Massmann, 2010).

Once the WEAP-MODFLOW model has been coupled into one model, the examination, compare and evaluation different climate, pumping and management scenarios becomes possible. The results may then be visualized as graphs, maps, and tables in different time and spatial scales.

6.3 WEAP-MODFLOW COUPLING

The WAB was basically divided into two management areas; confined and unconfined. The two areas were then divided into smaller zones based on flow directions which were determined based on to the main structure in the aquifer domain, see Chapters 3 and 4. For each zone, demand, groundwater and catchment nodes were defined, Figure 6.2.

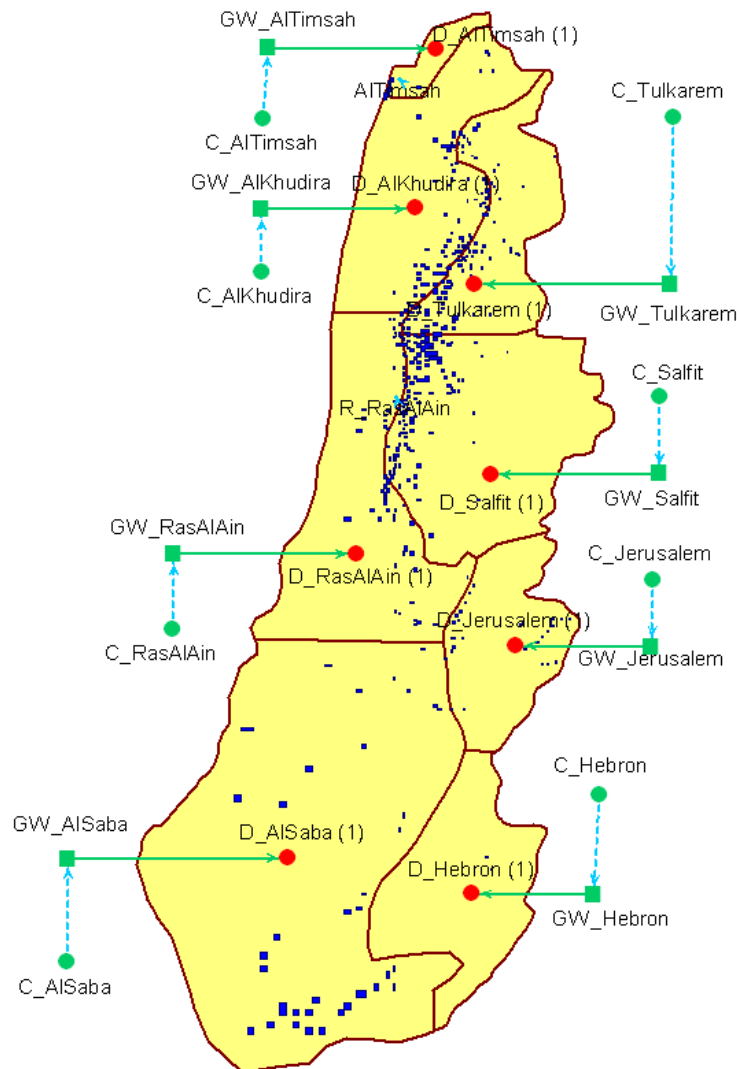


Figure 6.2: Schematic diagram of WEAP-MODFLOW of the WAB

While, there are many functions in WEAP that could be used to estimate recharge, runoff and demand, recharge during the evaluation period was estimated based on the empirical equation developed in Section 3.4. The results were then entered to WEAP as natural recharge quantities for the groundwater nodes. Similarly, pumping rates from different zones were defined as maximum withdrawal using the current spatial distribution of groundwater wells.

6.4 SCENARIOS DEVELOPMENT

The sustainability of the WAB is a function of both the inflow and outflow. The inflow to the WAB is a factor of rainfall, while outflow mainly depends on different human demands (domestic, agriculture, industry and commercial) and the natural status of the water levels which affects the outflow from the springs. In this Section, different rainfall and pumping scenarios in addition to one artificial recharge scenario were evaluated.

6.4.1 Climatic Scenarios

The historical climatic records in the region were showed very high variations in terms temporal and spatial distributions. In addition to these variations, climate change should also be considered. The variation in climate from year to year and the potential of climate change will generally impact the entire ecosystem and the water resources in more specific way. Therefore, the evaluation of the ecosystem under different climatic scenarios will provide an essential foundation to understand the level of impacts and will guide decision makers in the region on how to utilize their ecosystems.

The major climatic parameter in the study area is rainfall which is the main recharge generator. Other parameters such as temperature, humidity, wind have only a minor effect on recharge and were neglected in the evaluation. The rainfall over the replenishment areas of the WAB is considered the main source of recharge. The historic rainfall data for the area showed very high variations in terms of annual quantity as well as monthly distribution. This variation and the potential of climate change were evaluated in order to quantify the impact on the renewable amount of the inflow and the sustainable yield of the aquifer under different climatic scenarios. As a result, the amount of water that could be abstracted from the aquifer

without any adverse impacts (i.e. water levels and springs' discharges) was defined. For this purpose, two climatic scenarios were developed; the first scenario was developed based on the historical rainfall records over the replenishment areas of the WAB and named "**Normal Rainfall Scenario (NRS)**". The second scenario was obtained from a high resolution regional climate change model (i.e. 25 km) achieved by dynamical downscaling of global climate change scenarios with MM5 driven by ECHAM4 and RegCM3 driven by HadCM5. This scenario was called the "**Reduced Rainfall Scenario (RRS)**" since it reduces the amount of rainfall over the management period.

The annual recharge for the two scenarios was calculated based on the empirical equation developed in Chapter 3. The average estimated recharge over the management period was 386 and 277 Mm³/yr for NRS and RRS respectively. The monthly downscaling and spatial distribution over the replenishment areas of the WAB were conducted using the same approach obtained by model calibration (Chapters 4 and 5).

6.4.1.1 Normal Rainfall Scenarios (NRS)

The "Normal Rainfall Scenario" (NRS) did not consider any change in the future rainfall trends, or yearly and monthly distributions. This scenario assumes that the rainfall during the management period (2008-2035) will have the same characteristics of the historical records. Therefore, rainfall data from 1970/71 was to be repeated again from year 2007/08, Figure 6.3.

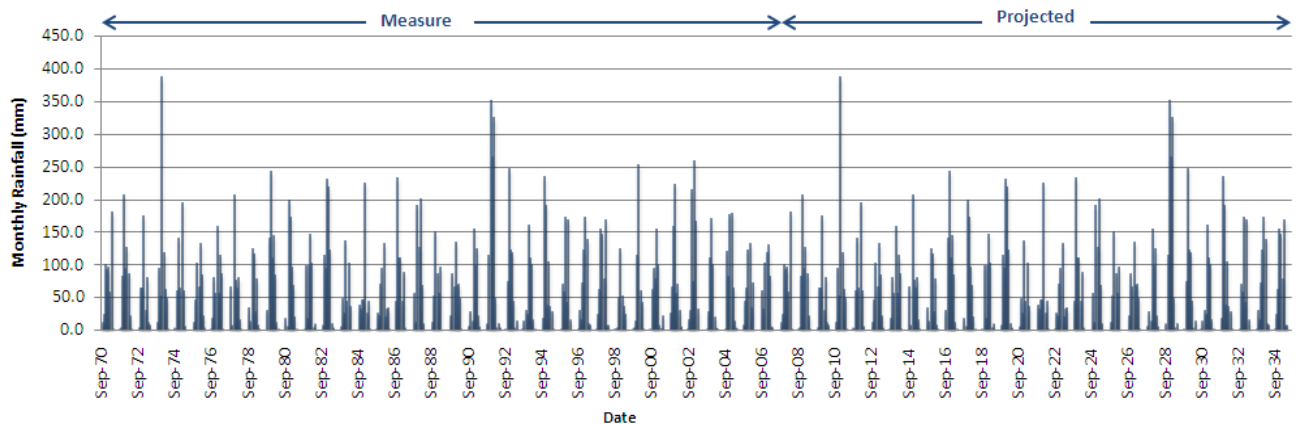


Figure 6.3: Normal rainfall scenario

The NRS showed different rainfall characteristics in terms of annual rainfall quantities and monthly distribution; 2028/29 represents the wettest year within the management period (i.e. which simulates the rainy season 1991/92) where the annual rainfall is almost double the long-term annual average. The minimum rainy year is 2020/21 with annual rainfall 390 mm. The average annual rain was estimated to be 570 mm which is much closer to the normal average (i.e. 560 mm/yr).

6.4.1.2 Reduced Rainfall Scenarios (RRS)

This scenario was obtained from a climate model³ with 25 km resolution achieved by dynamical downscaling of global climate scenarios with MM5 driven by ECHAM4 and RegCM3 driven by HadCM5. This model produced a time series of expected rainfall in daily time steps. The cells overlapping the replenishment areas of the WAB were determined, the average monthly rainfall was then calculated, Figure 6.4.

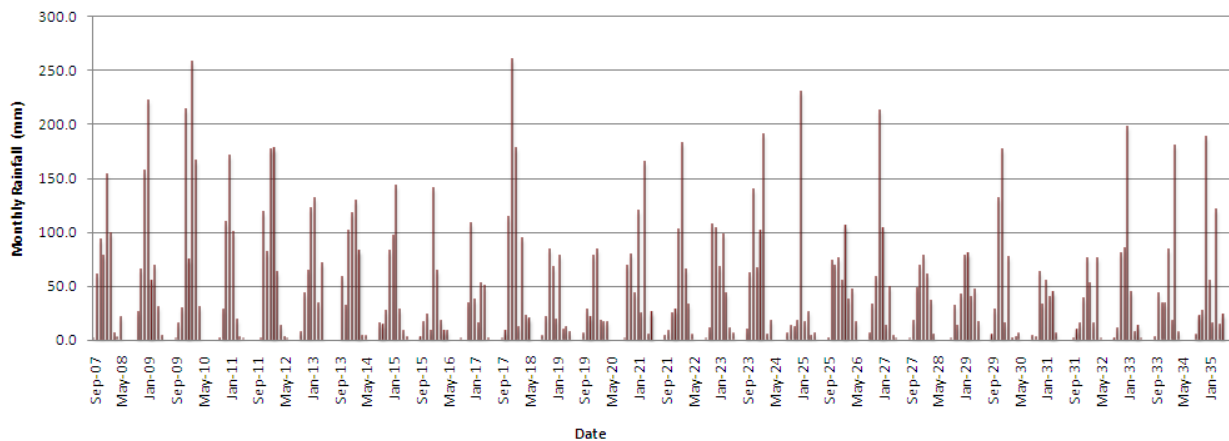


Figure 6.4: Reduced rainfall scenario

This rainfall scenario composed of different types of monthly distribution shows a significant reduction in the total annual amounts. On average, the annual average is 449 mm/yr which is 20% lower than long-term annual average. The lowest rainy season was dated in 2030/31 with an annual amount 249 mm.

³ Climate simulations produced at TAU for the BMBF project GLOWA Jordan River (<http://www.glowa-jordan-river.de>) with RegCM3 in 2009-2010 (Krichak S. O., Alpert P (2010) Projection of climate change during first half of twenty-first century over the Eastern Mediterranean region according to results of a transient RCM experiment with 25 km resolution. Geophysical Research Abstracts, EGU2010)

6.4.2 Pumping Scenarios

The pumping scenarios were developed in the sense of maintaining the sustainability of the aquifer while maximizing the pumping rates in order to meet the growing demands. The water level distribution within the aquifer and the springs' discharges were used as indicators of the sustainability of the aquifer. While the historical pumping rate of the aquifer was used as the maximum amount that could be pumped from the aquifer since it exceeds the average renewable recharge of the aquifer. In light of these criteria, three types of pumping scenarios were developed taking into consideration the type of climate scenario used.

6.4.2.1 Moving Average Scenarios

Generally, the distribution of the rainfall in the region has a cyclic behavior. It meaning that every 7-10 years it repeats its distribution. In each cycle there are one or two wet years and one or two dry years. Accordingly, this scenario was defined with an annual pumping rate equal to 85% of the seven years moving average of the estimated annual recharge. The remaining 15% was kept for the aquifer storage and springs' discharges. Under the two climate scenarios, two pumping scenarios were defined. The first pumping scenario which is related to the NRS called the "*Normal Moving Average Scenario*" and the second the "*Reduced Moving Average Scenario*" which is related to the RRS, Figure 6.5.

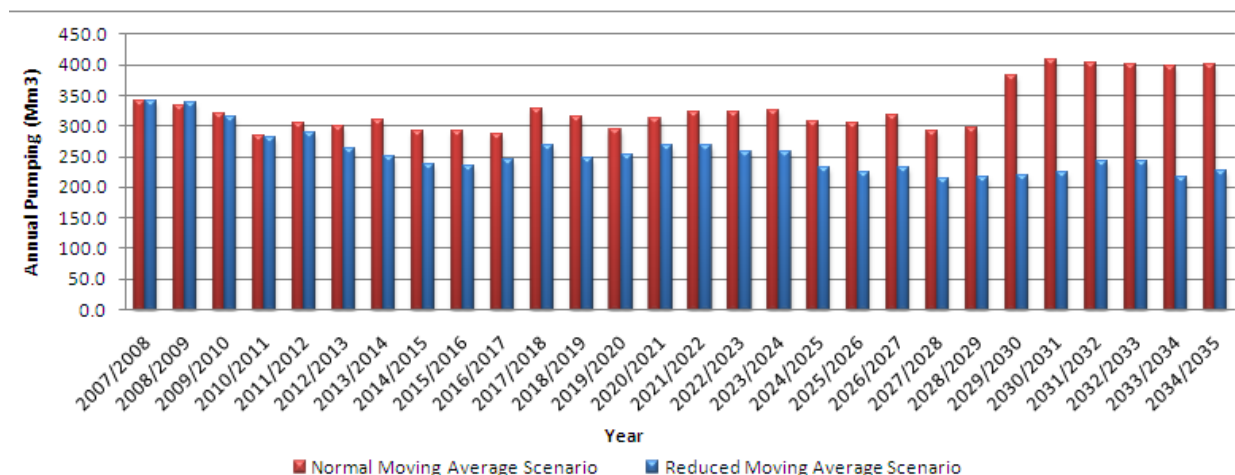


Figure 6.5: Moving average pumping scenarios

The average pumping rate over the management period for the two pumping scenarios was 328 Mm³/yr for the normal moving average scenario and 254 Mm³/yr for the reduced moving average scenario.

6.4.2.2 Aquifer Yield Scenarios

These scenarios were defined according to the long-term annual recharge of the aquifer (i.e. 373 Mm³/yr) and to the annual average of the estimated recharge based on the RRS (2007/08 to 2034/35). In the two scenarios, “*Normal Aquifer Yield Scenario*” and “*Reduced Aquifer Yield Scenario*”, the pumping rates were fixed to 85% of two defined aquifer yields (i.e. 310 Mm³/yr and 221 Mm³/yr).

6.4.2.3 Related Pumping Scenarios

The historical pumping regime showed a high inverse correlation between the annual rainfall and the annual pumping. For example, pumping decreased to 250 Mm³ in the wettest year 1991/92 and extended to 573 Mm³ in the driest year 1998/99. Taking into consideration the historical use of the aquifer, the annual pumping under the two climate scenarios were limited to maximum rates of 450 and 400 Mm³ in the driest years and minimum rates of 280 and 250 Mm³ in both NRS and RRS respectively, Figure 6.6. The average pumping rate was 364 Mm³ under the NRS called the “*Normal Related Pumping Scenario*” while the average pumping rate for the other pumping scenario was 334 Mm³ called the “*Reduced Related Pumping Scenario*”.

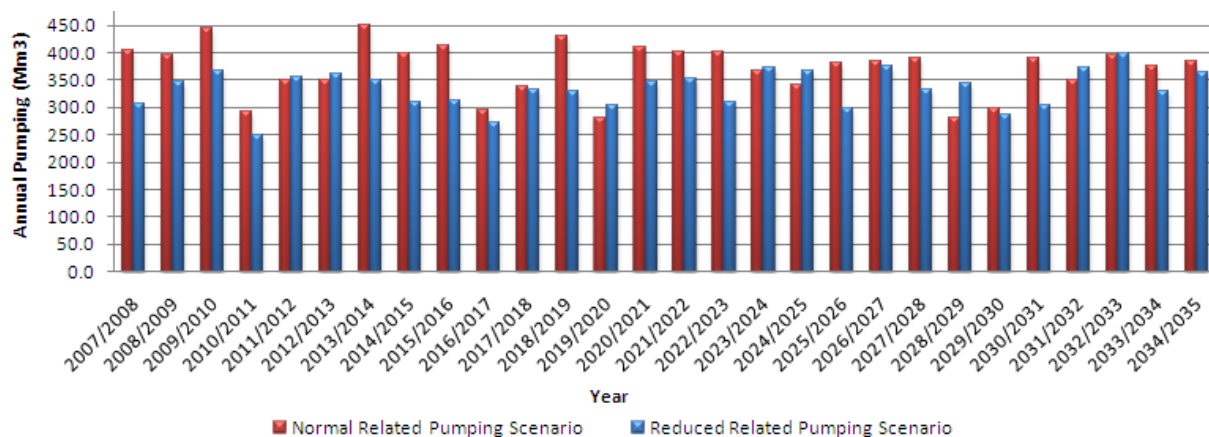


Figure 6.6: Moving average pumping scenarios

6.4.3 Management Scenario

This scenario was developed to check the impact of artificial recharge on the sustainability of the aquifer and quantify the additional water that could be pumped. While, there are many potential sources of water that could be artificially recharged; storm water from the major watersheds has been selected for the purpose of this scenario.

The average runoff to rainfall ratio in the WAB domain was estimated in the range of 2% in dry years to around 10% in wet years (Tal et al., 2007 and SUSMAQ, 2004). Accordingly, three runoff coefficients were used for estimating the potential quantity of storm water could be injected; 2% for dry years, 7% for wet years and 4.5% for years having accumulative rainfall close to the annual average. The watersheds, Figure 6.7, were developed based on 20 x 20 Digital Elevation Model (DEM). Consequently, and based on the average rainfall and the area of each watershed, the minimum, average and maximum potential quantities of storm water that could be collected were calculated, Table 6.1.

Table 6.1: Calculation of potential storm water runoff

Watershed	Area (km ²)	Average Rainfall (mm)	Runoff (Mm ³ /yr)		
			Minimum (2%)	Average (4.5%)	Maximum (7%)
Baqa	563	515	4.6	13.0	33.1
Tulkarem	355	600	3.4	9.6	24.3
Qalqilyia	350	553	3.1	8.7	22.1
Salfeet	374	552	3.3	9.3	23.5
Shibteen	543	598	5.2	14.6	37.0
Jerusalem	395	562	3.5	10.0	25.3
Hebron	1212	333	6.4	18.2	46.0
Sum	3792	488.7	29.6	83.4	211.3

In order to estimate the potential annual storm water under the two climate scenarios, the runoff coefficients (i.e. 2%, 4.5% and 7%) were applied on the two rainfall scenarios. Moreover, to avoid any over estimation, only 50% of the estimated runoff was assumed to be artificially recharged. Figure 6.8 shows the time series of the estimated storm water assumed to be injected to the aquifer.

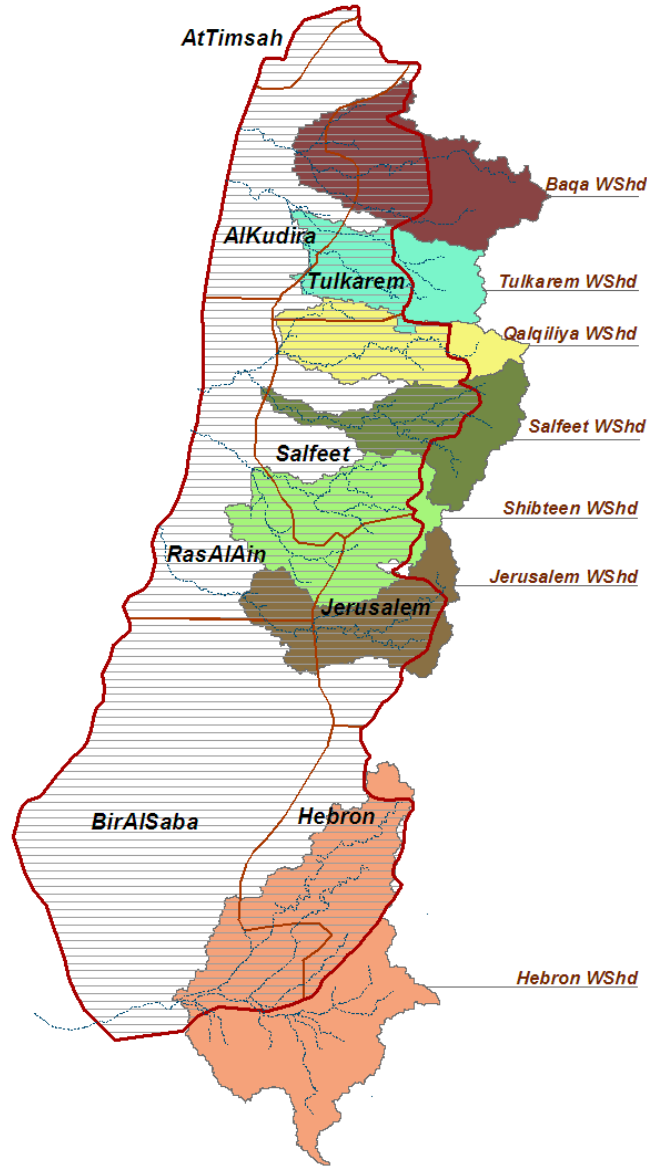


Figure 6.7: Location map of the main watershed within the WAB

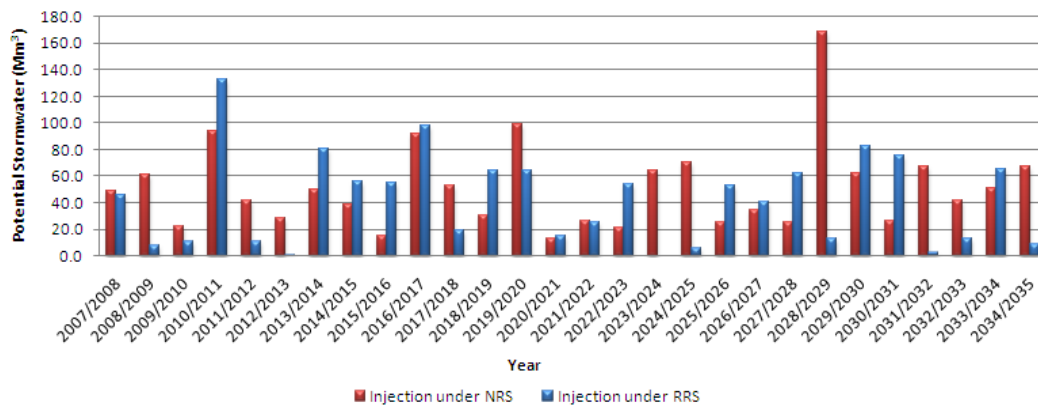


Figure 6.8: Potential quantities for artificial recharge

The spatial distribution of storm water to be injected to the groundwater was assumed to be located during the month of winter and spring months (December, January, February and March) in the downstream areas of each watershed and around the main drainage in each watershed.

6.5 SCENARIOS EVALUATION AND ANALYSIS

In total, 24 scenarios were developed covering different combinations of climate, management and pumping scenarios, Table 6.2. These scenarios varied in terms of the level of climate and demand stresses on the aquifer system.

Table 6.2: List of evaluated scenarios

Code	Name	Sub-code	Sub Name	Average Pumping (Mm ³ /yr)	Average Recharge (Mm ³ /yr)
Sc.1	Normal Recharge-Normal Pumping	Sc.1.1	85% Normal Moving Average	328	386
		Sc.1.2	85% Normal Aquifer Yield (373 Mm ³)	310	
		Sc.1.3	Normal Related Pumping (280-450 Mm ³)	364	
Sc.2	Reduced Recharge-Reduced Pumping	Sc.2.1	85% Reduced Moving Average	254	277
		Sc.2.2	85% Reduced Aquifer Yield (277 Mm ³)	221	
		Sc.2.3	Reduced Related Pumping (250 - 400Mm ³)	334	
Sc.3	Enhancing Normal Recharge-Normal Pumping	Sc.3.1	85% Normal Moving Average	328	437
		Sc.3.2	85% Normal Aquifer Yield (373 Mm ³)	310	
		Sc.3.3	Normal Related Pumping (280 - 450 Mm ³)	364	
Sc.4	Enhancing Normal Recharge-Enhancing	Sc.4.1	85% Normal Moving Average + 50% from the Injected Water	354	437
		Sc.4.2	85% Normal Aquifer Yield (373Mm ³) + 50% from the	333	

	Normal Pumping		Injected Water		
		Sc.4.3	Normal Related Pumping (280 - 450Mm ³)	364	
Sc.5	Enhancing Reduced Recharge- Reduced Pumping	Sc.5.1	85% Reduced Moving Average	254	318
		Sc.5.2	85% Reduced Aquifer Yield (277 Mm ³)	221	
		Sc.5.3	Reduced Related Pumping (250 - 400 Mm ³)	334	
Sc.6	Enhancing Reduced Recharge- Enhancing Reduced Pumping	Sc.6.1	85% Reduced Moving Average + 50% from the Injected Water	275	318
		Sc.6.2	85% Reduced Aquifer Yield (277 Mm ³) + 50% from the Injected Water	242	
		Sc.6.3	Reduced Related Pumping (250 - 400 Mm ³)	334	
Sc.7	Normal Recharge- Reduced Pumping	Sc.7.1	85% Reduced Moving Average	254	386
		Sc.7.2	85% Reduced Aquifer Yield (277 Mm ³)	221	
		Sc.7.3	Reduced Related Pumping (250 - 400 Mm ³)	334	
Sc.8	Reduced Recharge- Normal Pumping	Sc.8.1	85% Normal Moving Average	328	277
		Sc.8.2	85% Normal Aquifer Yield (373 Mm ³)	310	
		Sc.8.3	Normal Related Pumping (280 - 450 Mm ³)	364	

In all the evaluated scenarios, the spatial distribution of the natural recharge and pumping rate were kept unchanged. One of the main and primary results was the validation of the level of continuity of the aquifer system. The water level distributions in all defined zones show the same trend in rising or declining as a result of the evaluated scenario. This phenomenon confirms that the WAB is a one entity system.

In order to analyze the evaluated scenarios, 15 cells representing the location of existing monitoring wells in both upper and lower sub-aquifers were used for evaluation, Figure 6.9. In the coming sections, the analysis show the water levels in four representative cells (wells) were uniformly distributed within the aquifer; Menasheh , Beteh Tiqva, Qiryat Gat and Beir Al Saba' wells.



Figure 6.9: Location map of the observed cells

6.5.1 Results under Normal Rainfall Scenario

The six scenarios evaluated under the NRS show high variations in the level of impacts on the two criteria used for evaluation (i.e. water level and spring discharge). These impacts could be classified into three types:

The first type of impact will maintain the aquifer state to the same level as that of the base line year (i.e. 2007) with a low decline in water levels. The scenarios giving this type of impact are Sc1.1 and Sc1.2, where 85% of the moving average (i.e. 328 Mm³/yr) or the aquifer yield (310 Mm³/yr) respectively was pumped during the management period, Figure 6.10.

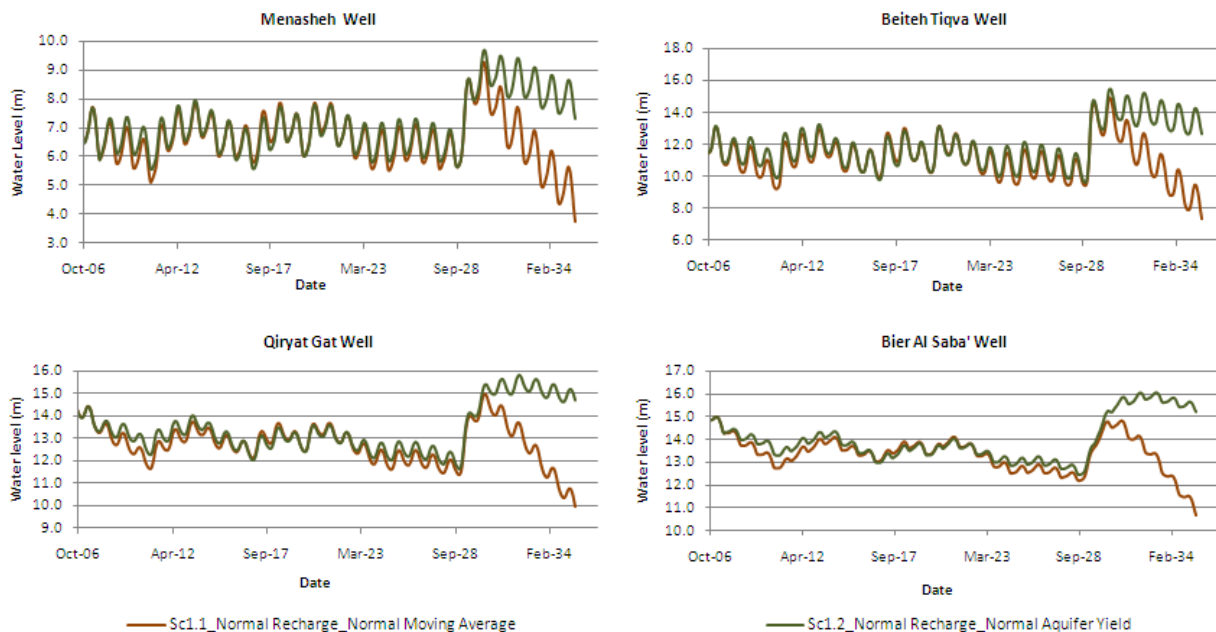


Figure 6.10: Water levels under Sc1.1 and Sc1.2 sub-scenarios

However, the water levels in the two scenarios look the same except in the year after 2029/30 where they completely diverged. The reason for this diversion was due to the existence of a very wet year within the evaluated period, this allows the increase in the pumping rate in scenario “Sc1.1” to around 400 Mm³/yr starting from year 2029 continuing for seven years later including the wet years within its pumping calculations. In addition to the increase in pumping rate, the springs increased their discharge rates, Figure 6.11, as a result of the temporary increase in water levels due to increase of annual recharge during the wet year.

Therefore, the increase in pumping rate and springs discharges will double the impact on the water level. On the contrary, “Sc1.2” which fixed the pumping rate according to the historical yield of the aquifer will benefit from the wet year by increasing the amount of water stored in the aquifer which increasing the water levels to higher state, the aquifer become more stable with a higher storage reservation for drier years.

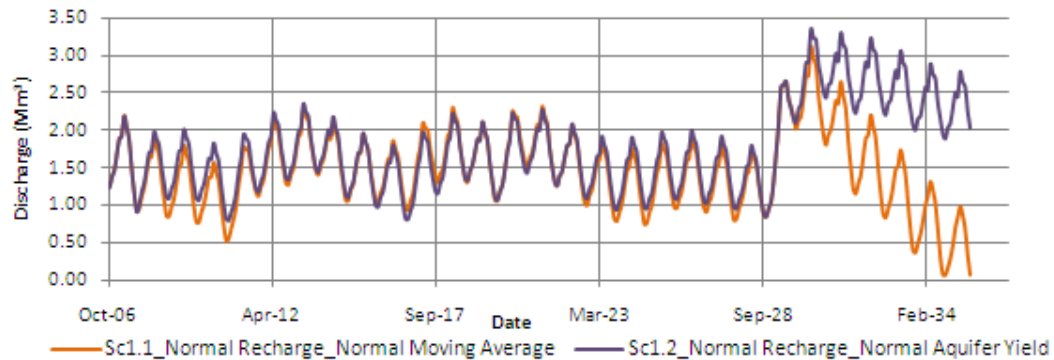


Figure 6.11: Al Timsah spring discharge under Sc1.1 and Sc1.2 sub-scenarios

The second type of impacts reflected the danger of the current aquifer utilization, since the annual pumping rate is related to the annual rainfall (Sc1.3 and Sc7.3) where annual pumping reached in some dry years to 400 - 450 Mm³, much higher than the average recharge, Figure 6.12. The water levels in both scenarios continued to deteriorate throughout the entire the aquifer.

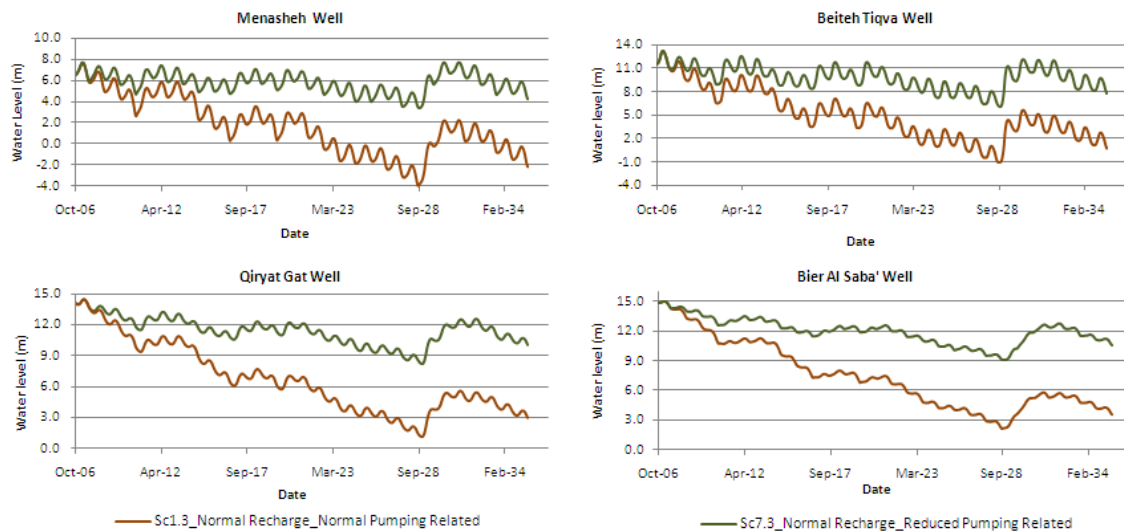


Figure 6.12: Water levels under Sc1.3 and Sc7.3 sub-scenarios

In addition to the water level impacts, the spring's discharge declined with time to very minor rates; the discharge rate will be reduced from 1.5 - 2 Mm³/month at the beginning of the evaluated period to less than 0.05 Mm³/month after 6 - 7 years, Figure 6.13.

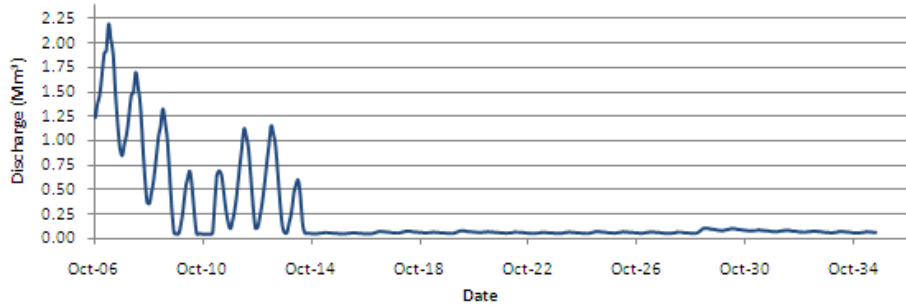


Figure 6.13: Al Timsah spring discharge under Sc1.3 sub-scenarios

In sub-scenario “Sc7.3”, the water levels at the end of the evaluation period were almost the same of those achieved by sub-scenario “Sc1.1”, Figure 6.14. This implies that if the WAB will be stressed in order to fulfill the demand, then “Sc7.3” could be selected under the assumption that an exceptional wet years will come within the management period that substitute the over exploitation from the aquifer. This sub-scenario will increase the pumping rate to an additional 5.6 Mm³/yr with a minor decrease in spring's discharges. In addition to this benefit, the pumping rate increase during dry years up to 400 Mm³.

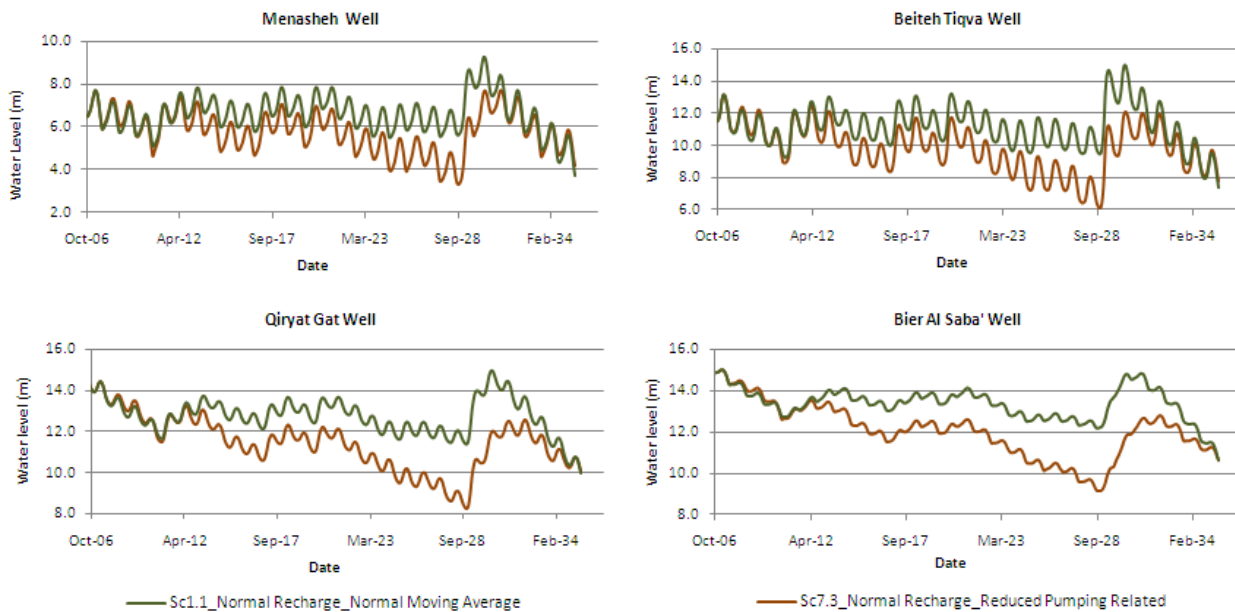


Figure 6.14: Water levels under Sc1.1 and Sc7.3 sub-scenarios

Thirdly, the aquifer could be recovered by reducing the pumping rate to 220 - 254 Mm³/yr as shown in sub-scenarios “Sc7.1” and Sc7.2”. Accordingly, water levels will start to rise and could reach relatively to levels close to the pre-development period, Figure 6.15

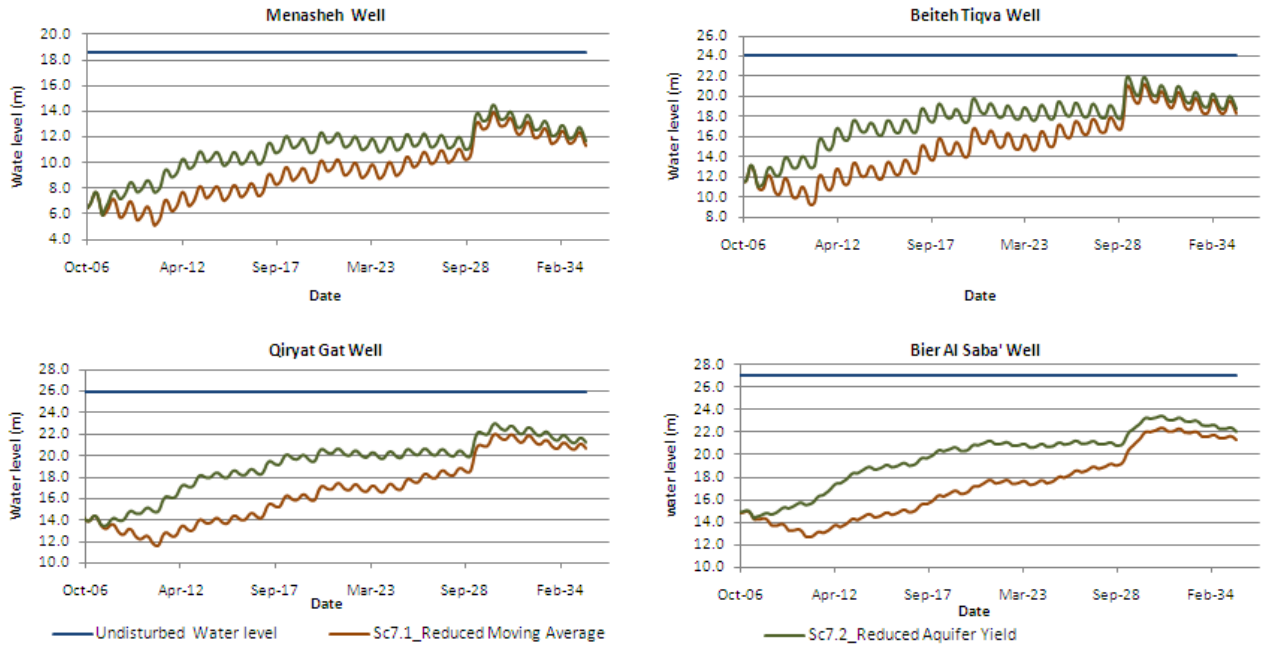


Figure 6.15: Water levels under Sc7.1 and Sc7.2 sub-scenarios

In addition, the springs will also start to increase their discharge; Ras Al Ain spring will start once again to discharge a significant amount which could reach in the wettest year during the evaluation period around 50% of its historical discharge. Al Timash spring will also increase its discharge with time to reach 70 - 75% of its pre-development discharge by the end of the evaluation period, 6.16.

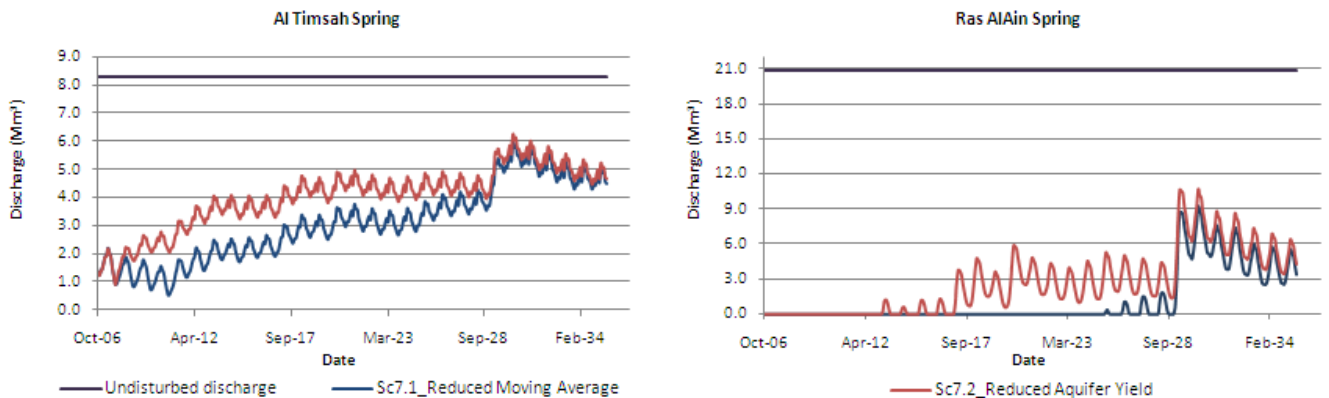


Figure 6.16: Springs discharges under Sc7.1 and Sc7.2 sub-scenarios

Consequently, the aquifer system of the WAB has proved its high response to any expected change in inflow or outflow. Figures 6.12 and 6.13 show the high response of the aquifer in the very wet year expected in 2028/29 in terms of sudden increase of water levels and springs discharges. As a result, regardless of the growing demand for water, the continued deterioration of the aquifer could be easily stopped by reducing the pumping rate.

6.5.2 Results under Reduction Rainfall Scenario

The reduction of natural recharge amounts as a result of the reduction of rainfall due to global climate change will maximize the stress in the WAB. The regional climate model showed a significant reduction in the annual rainfall and accordingly the annual recharge (i.e. Section 6.4.1.2). In order to evaluate this possible climatic scenario, managed and unmanaged pumping scenarios were evaluated; sub-scenarios Sc2.1 and Sc2.2 represent the managed pumping scenarios (i.e. pumping rate were reduced) and sub-scenarios Sc8.1 and Sc8.3 represent the un-managed scenarios (i.e. pumping rates were kept high).

Despite the impact of reducing in pumping rates on the water supply to the demand sites, the aquifer could at least be kept of the same status of the base year of evaluation (i.e. 2007). In this context, two scenarios were introduced; the first scenario suggests that an immediate action should be taken by reducing the annual pumping rate to 221 Mm³/yr (i.e. 85% of the expected average recharge over the evaluation period). However, this scenario will also reduce the pumping rates by at least 120 Mm³/yr, alternative sources will then have to be introduced. Taking this intermediate action will allow the aquifer to increase its storage during the wet years to be used in the very dry years. Accordingly, water level and springs discharge will increase during the first half of the evaluation period before starting to decline as a result of climate change. The second scenario which is seemed more practical, states that actions should be gradually taken by decreasing the pumping rate by using the moving average of the estimated recharge. In this scenario, water levels and the springs' discharges will continue in almost the same level as the base year.

On the other hand, keeping the pumping rate at high levels will to severely deteriorate the aquifer as follows, Figure 6.17:

- Additional 17 - 20 m draws down by the end of the evaluation period.
- Minimize the spring discharges to less the $0.05 \text{ Mm}^3/\text{yr}$.
- Increase the number of dry cells in the unconfined part of the aquifer.
- Increase the possibility of salt water intrusion from the Sea and from the deep aquifer.

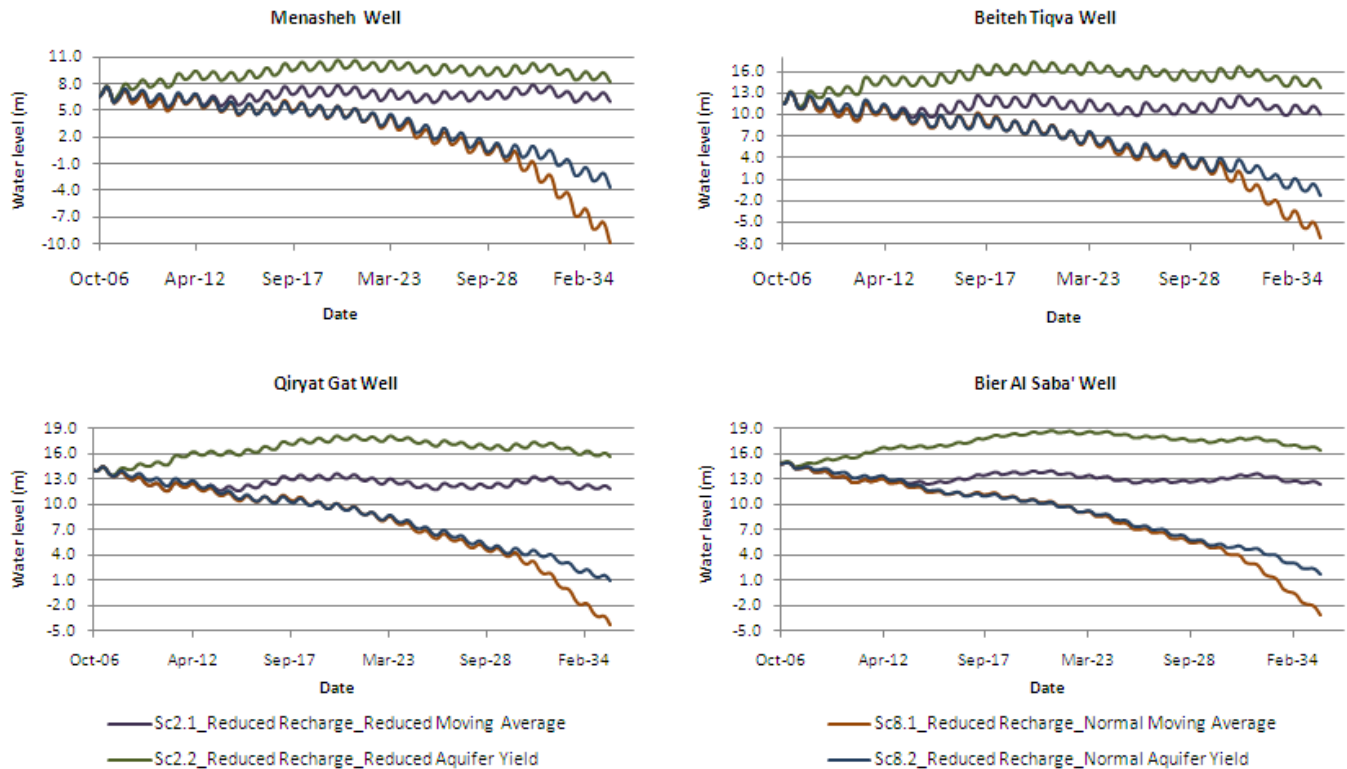


Figure 6.17: Water levels under Sc2.1, Sc2.2, Sc8.1 and Sc8.2 sub-scenarios

6.5.3 Results under Management Scenario

This scenario proved that the aquifer could be used as a storage reservoir. Excess water such as storm water during winter months could be artificially recharged to the aquifer to be used later during summer months when the demand is usually high. The sub-scenarios “Sc4.2” and “Sc6.2” show an example of the impacts on water level distributions under the two rainfall scenarios and with increase pumping rates, Figure 6.18.

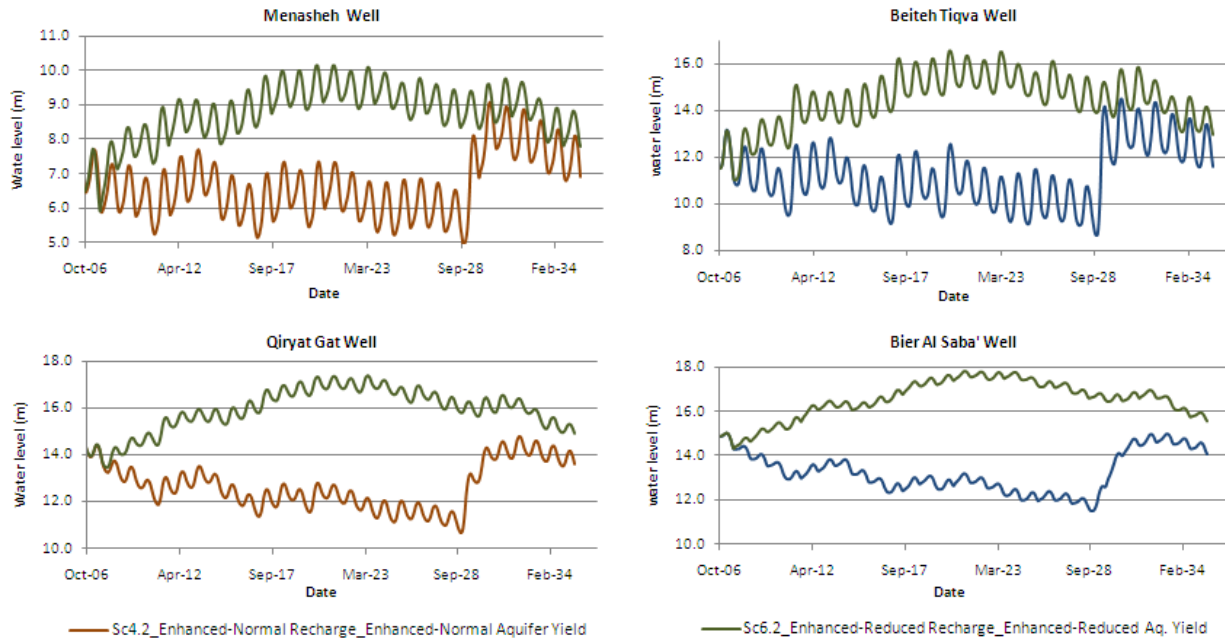


Figure 6.18: Water levels under Sc4.2 and Sc6.2 sub-scenarios

6.6 CONCLUSIONS

The numerical model of the WAB confirmed its ability to evaluate different types of scenarios expected to happen in the future. This could validate the numerical model of the WAB and give decision makers the confidence to evaluate any scenario that could emerge during the coming future.

The response of the WAB over different rainfall and pumping scenario was proved the high level of influence on the sustainability of the aquifer system. The main conclusions of the scenarios evaluation are:

1. The aquifer seemed to behave as one aquifer system under different conditions.
2. The pumping rates during the last forty years stressed the aquifer; the water levels and the springs' discharges deteriorated from year to year. This deterioration was due to the pumping rate which was inversely correlated to the amount of annual recharge.
3. Accordingly, the optimized pumping rates from the WAB were found to be 310 and 254 Mm^3/yr under NRS and RRS respectively. These amounts will maintain the water levels and springs' discharges from further deterioration.

4. Decision makers should take into consideration global changes in terms of climate (temperature and rainfall), demand growth, and urban expansion. Therefore, aquifer utilization should be annually reviewed.
5. Using storm water generated in the main watershed within the WAB region for artificial recharge to the WAB will increase the optimized annual pumping rate by 15 - 20 Mm³/yr.
6. While, the water levels in the unconfined part of the aquifer are less affected by different pumping scenarios, the impact of the reduction in annual recharge as a result of climate change will influence the unconfined part of the aquifer, Figure 6.19. Therefore, more attention should be given in order to avoid more stress in the demand sites in this part due to the possible decrease in groundwater supply. Based on that, enhancing aquifer recharge in these areas by water harvesting, land terracing in steep lands and land rehabilitation as well as using treated wastewater for artificial recharge will be possible actions to be taken.

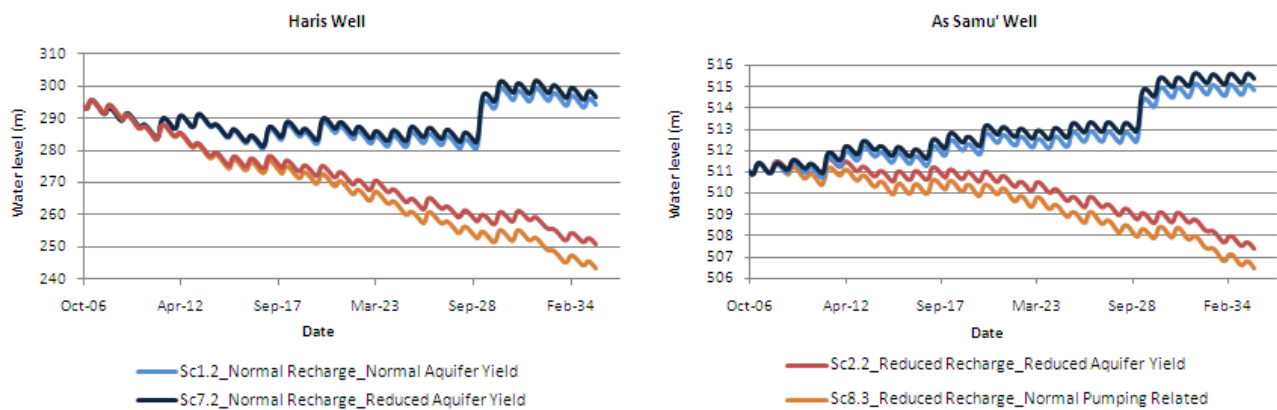


Figure 6.19: Water levels in the unconfined part of WAB under different scenarios

Chapter 7

CHAPTER 7: SUMMARY AND FUTURE OUTLOOK

7.1 INTRODUCTION

Scarcity of fresh water in the Middle East is considered one of the largest challenges facing socio-economic development of the region. The stresses on natural sources are increasing day by day as a result of rapid global change (i.e. population growth, climate change, etc.). Therefore, the management of trans-boundary water resources is an urgent need not only for protecting these resources but also for the stability and development of the entire region. The Western Aquifer Basin (WAB) as one of the main trans-boundary groundwater resources was depicted for a case study. It extends from the mountains of the West Bank in the east to the Mediterranean Sea in the west and from the Carmel Mountains in the north to the Egyptian border in the south. The Aquifer is utilized by both Palestinians and Israelis with a sustainable yield estimated to be around 373 Mm³/yr. During the pre-development period, this yield was naturally discharged through the two main springs in the Aquifer; Al Timsah spring (Tananim spring) in the north with a discharge of 90 - 120 Mm³/yr and Ras Al Ain spring (Yarkon Spring) in the middle of the Aquifer with a discharge of 220 - 280 Mm³/yr. In the early 1950s, significant pumping from the Aquifer started and increased with time to reach 400 Mm³/yr during the 1970s. The pumping rates were kept in this range with some variation depending on the rainy season. The highest pumping rate, 573 Mm³, was recorded in the driest year in the record, 1998/99, while the lowest pumping rate, 250 Mm³, was recorded in the wet year 1991/92. Due to the high pumping rates which most of the time exceed the annual renewable recharge, the water level and the discharge of the two main springs deteriorated; Ras Al Ain spring dried out in 1973, Al Timsah spring currently discharges around 20-40 Mm³/yr and the drawdown in the Aquifer has reached 10-16 m compared to the water level during the pre-development period.

The WAB is composed of two permeable limestone and dolomitic limestone layers with signs of high karstification separated by a less permeable layer (i.e. Yatta formation). These two layers are called the upper and lower sub-aquifers. The WAB is also divided into two zones; the first zone is the confined area within the Aquifer in the eastern part and the second

is the confined part on the western side. The dominant inflow of the Aquifer (i.e. 98%) is the natural recharge from the rainfall over the outcropping formations in the replenishment areas of the WAB.

The main objective of this research was to investigate the flow dynamics and responses of the highly karstified aquifer of the WAB under different levels of variations in both inflow and outflow conditions and also to assess the sustainable yield of the Aquifer under different global changes. To achieve the intended goal, an intensive analysis has been conducted starting from studying the inflow mechanisms and its relation to the rainfall variation, the boundaries, the steady state conditions of the Aquifer, development of a refined transient flow model and ending with the development of different future scenarios and their impacts on the flow dynamics of the aquifer system. The summary of the conclusions obtained from the overall analysis and how this conclusion contributed in achieving the main objective of this study is shown below.

7.2 RAINFALL-RECHARGE VARIATIONS

The rainfall over the replenishment areas showed a high level of variation in terms of accumulative annual amounts, monthly distribution, intensity and spatial distribution. Therefore, the estimated annual recharge proved that recharge is affected by the monthly rainfall distribution in addition to the annual amount of rainfall. The water level fluctuation technique over a certain period of time was successfully used. It provided a new storage coefficient of the WAB which could be used to estimate the annual recharge by measuring the annual change in the water levels in specific monitoring wells. The storage coefficient of the WAB indicates that for one meter drop/rise in the water level in the confined part of the WAB, the aquifer could lose/gain 102 Mm^3 of water.

The long-term annual recharge was found to be $373 \text{ Mm}^3/\text{yr}$ with high variation from year to year. Accordingly, the relation between annual recharge and the distribution of annual rainfall as well as the accumulative annual rainfall confirmed that the high variations of annual recharge volumes are directly linked to monthly rainfall variation. High statistical correlation was found between the annual recharge and the rainfall during the months of November, December, January and February. The highest annual recharge will be achieved

whenever the monthly distribution of the rainfall took the shape of log normal distribution and more than 70% of the annual rainfall accumulates during four consecutive months (i.e. November - February).

On the basis of understanding the influences of rainfall variations on generating recharge, a multi-regression equation has been developed to consider the monthly distribution of rainfall as a chief factor in forecasting annual recharge within the Aquifer. The equation shows that recharge is highly dependent on rainfall amounts during four main rainy months: November, December, January and February. The equation also concludes that the monthly rainfall in the months March to October is not effective for generating recharge; where the generated recharge from rainfall in these months and other minor recharge components was estimated at 39.6 Mm³/yr during the analyzed period (1970/71-2005/06).

7.3 THE WAB RESPONSES UNDER INFLOW AND OUTFLOW VARIATIONS

The responses of the WAB under different recharge and pumping variations have been studied by developing a groundwater flow model of the WAB. The WAB was simulated by a three-layer model using MODFLOW-2000. The active model area encompasses about 6250 square kilometers discretized into non-uniform cell sizes with dimensions ranging from 200 to 750 m. There were two models developed; the first was the steady state model representing the pre-development state of the WAB. As a result, the model provided detailed information about boundary conditions, flow patterns, horizontal and vertical hydraulic properties, water level distributions, layer interaction, spring outflows, aquifer geometry and recharge distributions (i.e. space and time). The second model was the transient flow model. This model was developed to study the flow dynamics in space and time. Time wise, the model covers the period from September 1951 to August 2007 in monthly time steps. The period from September 1951 to August 2000 was used as a calibration period while the period from September 2000 to August 2007 was used for model validation.

From the transient model, the specific storativity and specific yield were estimated; the specific storativity was found to range from 10^{-6} to 10^{-5} while the specific yield ranged between 1% and 7.5%. Also, the results showed the change of aquifer flow patterns, water levels and spring discharges as a result of extensive exploitation.

The water balance of the two sub-aquifers shows that 62% of the natural recharge reaches the upper sub-aquifer. However, 86% of the annual pumping rate and 37% of the spring discharge are extracted from the upper sub-aquifer. In order to substitute the high outflow from the upper sub-aquifer, the lower sub-aquifer leaks an average of 42.6 Mm³/yr (i.e. 11% of the total aquifer outflow) to the upper aquifer through the interconnection areas between the two sub-aquifers.

The main outcomes obtained from the numerical flow model of the WAB are summarized in the following points:

1. Both water levels and springs rapidly respond to recharge and pumping events which referred to the double continuity behavior of the Aquifer due to the high karstification and existence of underground conduits within the WAB.
2. Due to the high level of karstification and heterogeneity of the Aquifer formations, the WAB is well connected in vertical and horizontal dimensions. Accordingly, the WAB behaves as one entity system.
3. The geological structure of the WAB has showed a major influence in controlling the flow pattern within the aquifer. The western hydrological barrier (Talme Yafe Group) prevents groundwater flow seaward and diverts the groundwater northward beneath the Coastal Plain. North of the Ramallah Anticline, northeast of the WAB, the natural recharge generated in the replenishment areas in Salfet and Tulkarem regions flows towards the west to be accumulated with the groundwater in the plain areas.
4. The WAB could be used as underground natural carrier (from South to North)
5. The WAB could be used as an underground reservoir with a storage capacity of 373 Mm³.
6. In the confined areas, the water levels are more sensitive to recharge and pumping variations.
7. The replenishment areas of the WAB could be classified as a high risk to pollution due to the urbanization and agricultural practices.
8. The WAB is surrounded by saline water bodies from top, bottom, south and west; therefore, un-managed exploitation will increase the potential risk for aquifer salinization.

7.4 SUSTAINABILITY OF THE WAB UNDER DIFFERENT FUTURE MANAGEMENT OPTIONS

The responses of the WAB under a combination of different rainfall and pumping scenarios were studied by extending the transient flow model of the WAB to year 2034/35. Two rainfall scenarios were defined representing both reduction in rainfall trend as a result of climate change and no change in rainfall trend. The pumping scenarios were defined based on the existing aquifer use which was related to the annual amount of rainfall and two other scenarios related to the aquifer yield and moving average of the aquifer recharge. The results showed a comparison between different climate and pumping scenarios in terms of water levels distribution and springs' discharges, which reflect the status of the WAB under different conditions. Accordingly, two pumping scenarios were recommended to maintain the water level and the springs' ability to continuously discharge. These scenarios are:

1. Pumping 85% from the historical aquifer yield under the no change in rainfall scenario (i.e. 310 Mm³/yr)
2. Pumping 85% of the 7 year moving average of the aquifer recharge (254 Mm³/yr) under the reduction of the expected rainfall scenarios.
3. The pumping rates in the two recommended scenarios could be extended to an additional 15 - 20 Mm³/yr by injecting some of the available storm water generated in the main western watershed.

7.5 SUGGESTIONS FOR FURTHER RESEARCH

The WAB still requires further investigations in order to improve the model results. Additional research efforts would also be required for the quality of the water and recharge mechanizes.

- Monitoring Program: Continuous and refine measurements for meteorological parameters, springs discharges, well abstractions and groundwater heads are still required. The measured data used in this study was discrete, with many missing and out range data; in many cases data was measured once or twice a year. Therefore, an integrated monitoring network to measure meteorological data, water levels, pumping

and discharge rates should be installed in the WAB with more focus on the unconfined part of the Basin.

- Recharge Estimation: An alternative recharge estimation technique that includes all meteorological and physical parameters would be very necessary better understanding the recharge mechanisms. By including refine data for rainfall and evapotranspiration as well as land use, soil, geology and structural characteristics for the replenishment areas of the WAB, this proposed technique will be more powerful for estimating the impact of management options under different expected global change (i.e. climatic change, land use change, etc.)
- Modeling Efforts: The modeling and study results show the high level of karstification of the WAB. Therefore, double continuity modeling is needed to simulate the interaction between the matrix and conduit flows.
- Water quality: It was shown that the WAB is relatively surrounded by saltwater bodies from the west, bottom and in some locations from the top. In the east, where the aquifer is replenished, intensive agriculture and urban areas were considered as high potential in terms of aquifer contamination. Therefore, developing a pollutant transport model for sources in the WAB is highly recommended.

References

LIST OF REFERENCES

- Abusaada, M.J., Aliawi, A.S, and P. E. O'Connell.. 2006. *Assessment of Sustainable Yield of Aquifers Using Groundwater Flow Modeling and Decision Support Systems: Western Aquifer Basin as a Case Study*. Second International Conference on Water Resources and Arid Environment, Al Riyadh, Saudi Arabia.
- Alley, W.M, T.E. Reilly, and O.L Franke. 1999, *Sustainability of ground-water resources*. U.S. Geology Survey Circular 1186.
- Avisar, D., Rosenthala, E., Flexera A., Shulmana, Ben-Avrahama Z. and Guttman, J. 2002. *Salinity sources of Kefar Uriya wells in the Judea Group aquifer of Israel. Part 1- conceptual hydrogeological model*. Journal of Hydrology 270, 27–38 pp.
- Baida, U., Gutman, Y., Gotlieb, M. and Kahanowicz, Y., 1989. *Water supply to the Dan district: hydrogeology and mathematic models*. TAHAL, Water Planning for Israel, Tel Aviv, Rep. 0t/89/45 (in Hebrew), 65 pp.
- Berger D., 1999. *Hydrological model for the Yarqon-Tananim aquifer*. Mekorot Ltd., 50p.
- Bar Yosef, Y., 1978. *The Tananim Deep borehole: a further investigation of the salinization processes in the Yarkon Tananim aquifer*. Tahal, Water Planning for Israel, Rep. 01/78/29, Tel Aviv, 27 pp.
- Blake, G. S. and Goldschmidt, M. J., 1947. *Geology and Water Resources of Palestine*. Government Printer, Jerusalem, 413 pp.
- CDM, 1997. *Study of the sustainable yield of the Eastern Aquifer Basin*. Palestinian Water Authority and USAID. Deliverable number 18.02.
- CH2MHILL, 2001. *Physical Setting and Reference Data for the Eastern and Northeastern Basins*. Updated Version. CH2M HILL International Services Inc., Vol. I. Jerusalem.

- Dafny, E., Burg, A. and Gvirtzman, H., *Effects of Karst and geological structure on groundwater flow: The case of Yarqon-Taninim Aquifer*, Israel, Journal of Hydrology (2010), doi: 10.1016/j.jhydrol.2010.05.038
- Ecker, A., 1995. *Contribution of Brackish Water in Avedat and Mt Scopus Groups Aquitard to the Judea Group Aquifer in Yarqon-Be'er Sheva Basin*. Geological Survey of Israel, Jerusalem p. 55.
- Fleischer, L., 2003. *Structural Map on Judea Group*, Ministry of National Infrastructure, (Maps).
- Flexer, A., 1968, *Stratigraphy and facies development of Mt. Scopus Group (Senonian–Paleogene) in Israel and adjacent countries*. Isr J Earth Sci 17 :85–114
- Ford, D., and Williams, P., 2007. *Karst hydrogeology and geomorphology*. Wiley, England , 562 pp.
- Freeze, R.A. and Cherry J.A., 1979. *Groundwater*. Prentice Hall Inc., New Jersey, 604 pp.
- Frumkin, A. and Gvirtzman, H., 2005. *Cross-formational rising groundwater at an artesiankarstic basin: the Ayalon Saline Anomaly*, Israel. Journal of Hydrology 318 (2006) 316–333
- Gieske, A.S.M., 1992. *Dynamics of groundwater recharge: a case study in semi - arid Eastern Botswana*. Enschede, Febo, 1992. 289 p.
- Goldschtoff, Y. and Schachnai, E., 1980. *The Yarkon Taninim aquifer in the Beer Sheva area: outline and calibration of the flow model*. Tahal, Water Planning for Israel, Rep. 01/80/58, Tel Aviv.
- Gunn, J., 1985, *a conceptual model for conduit flow dominated karst aquifers*. Karst Water Resources (Proceedings of the Ankara - Antalya Symposium, July 1985). IAHS, Publ. no. 161

- Guttman, J., Goldschtof, Y., Baida, U. and Mercado, A., 1988b. *A two-layer model of flow regime and salinity in the Yarkon- Taninim aquifer*. TAHAL, Tel Aviv, Rep. 01/88/23.
- Guttman, J., 1991. *Feasibility of increased groundwater exploitation in the Beer Sheva basin*. Tahal, Water Planning for Israel, Tel-Aviv. Tahal Rep 01/91/08 .
- Guttman, J. and Zukerman, H., 1995. *Yarkon-Taninim-Beer Sheva basin-setting and calibration of a model for flow and salinity*. TAHAL, Tel Aviv, Rep. 01/95/72.
- Hydrological Service of Israel (HSI), 2008. *Development of utilization and status of water resources in Israel (annual hydrological report) 2007*. Jerusalem, Israel: Hydrological Service of Israel.
- Kroitoru, L., 1987. *The characterization of flow systems in carbonatic rocks defined by groundwater parameters: Central Israel*. Ph.D. Thesis, Feinberg Graduate School, Weizmann Institute of Science, Rehovot 124 pp.
- Katz, A., 2001. *Identification of Salinity Sources of the Yarkon–Taninim Aquifer Using Modern Geochemical Criteria*. The Hebrew University, Jerusalem p. 15.
- Kruseman, G., 1997. *Recharge from intermittent flow*. In: *Recharge of phreatic aquifers in (semi- arid areas)*, Simmers, I. (ed.), International Association of Hydrogeologists, 19, Balkema, Rotterdam.
- Lerner, D.N, Issar, A.S. and Simmers, I., 1990. *Groundwater recharge: A guide to understanding and estimating natural recharge*. International Contributions to Hydrogeology, 8, Heise, Germany.
- Lewy, Z., 1991, *Periodicity of Cretaceous epirogenic pulses and the disappearance of carbonate platform facies in the Late-Cretaceous time (Israel)*. Isr J Earth Sci 40 : 51–58
- Mandel, S., 1961. *Properties and genesis of the Turonian Cenomanian aquifer in western Israel as an example of a large limestone aquifer*. Ph.D. Thesis, Technion, Haifa.

- Mandell A., Zeitoun D., and Dagan G., 2002. *Salinity sources of Kefar Uria wells in the Judea group aquifer of Israel. Part 2- quantitative identification model*. Journal of Hydrology 270 (2003) 39–48
- Massmann J., Wolfer J., Huber M., Schelkes K., Hennings V., Droubi A. and Al-Sibai M., 2010. *WEAP-MODFLOW as a Decision Support System (DSS) for integrated water resources management: Design of the coupled model and results from a pilot study in Syria, Groundwater Quality Sustainability*, Krakow, 12–17, XXXVIII IAH Congress, University of Silesia
- McDonald M. and Harbaugh A., 1988, *A modular threedimensional finitedifference groundwater flow model: U.S. Geological Survey Techniques of WaterResources Investigations*, Book 6, Chapter A1, 548 p.
- Mercado, A., 1980a. *Groundwater salinity in the Yarkon-Taninim Beer Sheva basin: statistical models for the simulation of the salinity regime in the Taninim springs*. TAHAL, Tel Aviv, Rep. 01/80/37 (in Hebrew) 47 pp.
- Mercado, A., 1980b. *Groundwater salinity in the Yarkon Taninim Beer Sheva basin: a conceptual model of the salinity regime and its source*. TAHAL, Water Planning for Israel, Tel Aviv, Rep. 01/80/60 (in Hebrew) 65 pp.
- Miro, D., 1979. *Summary of pumpage testing in the Nir-Am 11 and Gan Yavne 4 oil boreholes*. TAHAL. Water Planning for Israel, Tel Aviv, Internal Report 01/79/62 (in Hebrew) 11 pp.
- Paster, A., Dagan, D. and Guttman J., 2005. *The salt-water body in the Northern part of Yarkon-Taninim aquifer: Field data analysis, conceptual model and prediction*, Journal of Hydrology 323 (2006), 154–167 pp.
- Peleg, N. and Gvirtzman, H., 2010. *Groundwater flow modeling of two-levels perched karstic leaking aquifers as a tool for estimating recharge and hydraulic parameters*. Journal of Hydrology 388, 13–27 pp.

- PHG, 2010, *The Inequitable Abstraction, Allocation and Consumption of Water Resources in the occupied Palestinian territory*, The Water and Sanitation Hygiene Monitoring Program, Report (2007-2008).
- Rani, F.M. and Chen, Z. H., 2010, *Numerical Modeling of Groundwater Flow in Karst Aquifer, Makeng Mining Area*. American Journal of Environmental Sciences 6 (1): 78-82, 2010
- Rosenthal, E., Weinberger, G., Berkowitz, B., Flexer, A. and Kronfeld, J., 1992. *The Nubian sandstone aquifer in the central and northern Negev, Israel: delineation of the hydrogeological model under conditions of scarce data*. Journal of Hydrology, 132: 107-135 pp.
- Ronen, D. and Kanfi, Y., 1978. *Groundwater Quality in the Yarkon-Tanninim*. Ministry of Agriculture Water Commission, Tel Aviv p. 129.
- Sauter, M., 1992. *Quantification and forecasting of regional groundwater flow and transport in a karst aquifer (Gallusquelle, SW Germany)*, Tübingen, 151 pp.
- Tsukerman, H., et al., 1999. *Flow and salinity regime in Yarqon-Taninim-Beer Sheba basin*. Tel Aviv, Water Planning of Israel, p. 24.
- SUSMAQ, 2003. *Conceptual flow model of the Western Aquifer Basin, sustainable management of the West Bank and Gaza aquifers*, Working Report SUSMAQ-MOD #06 VO.03. Ramallah: Water Resources and Planning Department, Palestinian Water Authority.
- SUSMAQ, 2004. *Boundaries of the Western Aquifer Basin and the Eocene Aquifer in the Northeastern Aquifer Basin*, Working Report SUSMAQ-MOD #06.1 V1.0, Ramallah: Water Resources and Planning Department, Palestinian Water Authority.
- Weinberger, G. and Rosenthal, E., 1993. *The fault pattern in the northern Negev and southern Coastal Plain of Israel and its hydrogeological implications for groundwater flow in the Judea Group aquifer*. Journal of Hydrology 155, 103–124pp.

- Tal, A., Al Khateeb, N., Asaf, L., Assi, A., Nassar, A., Abusaada M., Gasith, A., Laronne, J., Ronen, Z., Hirshkowitz, Y., Halawani, D., Nagouker, N., Angell, R., Akerman, H., Diabat, M. and Abramson, A., 2007. *Watershed Modeling: BioMonitoring and Economic Analysis to Determine Optimal Restoration Strategies for Transboundary Streams*. Final Report MERC project -M23-019
- Weinberger, G., Rosenthal, E., Ben-Zvi, A. and Zeitoun, D.G., 1994. The *Yarkon-Taninim groundwater basin, Israel: hydrogeology; case study and critical review*. Journal of Hydrology 161, 227–255 pp.
- Weiss, M. and Gvirtzman, H., 2007. *Estimating Ground Water Recharge using Flow Models of Perched Karstic Aquifers*. Ground water 45, 761-773PP.
- Zeitouni, N. and Dinar, A., 1996. *Mitigating Negative Water Quality and Quality Externalities by Joint Mangement of Adjacent Aquifers*. Environmental and Resource Economics 9: 1-20, 1997
- Zukerman, H. and Shachnai, E., 1999. *Yarkon-Taninim-Beer Sheva basin, flow model update*. TAHAL, Tel Aviv, Rep. 6759-00.133

CURRICULUM VITAE

Name **Abu Saada, Muath J.**

Profession Hydroinformatics/ Modeling and GIS Expert

Date of birth 1971, 8 March

Nationality Palestinian

Telephone 00972 (or 00970) 599 858249

Email muath@phg.org or muathas@gmail.com

Education

1996 BSc. Electrical & Computer Engineering, Birzeit university, Birziet, West Bank, Palestine

2004 M.Sc. Sustainable Management of the Water Environment, Newcastle University upon Tyne, Newcastle, U.K
Thesis: **Development of an Integrated Management Tool for the Western Aquifer Basin.**

2008 Starting PhD program entitled “**Flow Dynamics and Management Options in a Stressed Carbonate Aquifer System, The Western Aquifer Basin, Palestine**”, **University of Gottingen, Germany.**

Experience record

2009-2011 Environmental Master Plan for Jericho City.

2009-Ongoing An Integrated Approach to Sustainable Management of water resources under Global Change, GLOWA JORDAN RIVER, Phase III

2008- 2010 Watershed Model for Marj Sanour, IUCN

2006-2008 An Integrated Approach to Sustainable Management of water resources under Global Change, GLOWA JORDAN RIVER, Phase II

2005-2008 Developing Decision Support System on Wastewater Treatment Technologies, Regional Data Base IV, EXACT

2006-2009 Artificial recharge study, North Gaza. Gabardine project (Groundwater Artificial recharge Based on Alternative sources of water: aDvanced INtegrated technologies and managEment).

2007 Developing Social-Economical-Environmental Impact Assessment Tool for Solid waste Management, UNESCO

2005-2007 Watershed Modeling, Bio-monitoring, and Economic Analysis to Determine Optimal Restoration Strategies for Tranboundary Streams, (The Arava Institute, Israel; Water and Environmental Development Organization, , Palestine and funded by MERC).

2005 Assessment of the Supply/Demand Gap and the Evaluation of the suitable

	Conservation Measures towards Sustainable Water Resources in Palestine. Develop Management Tool to evaluate these management options.
1999-2005	Sustainable Management of the West Bank and Gaza Aquifers. (Newcastle University and Palestinian Water Authority).
2001-2002	Water Recourses Program, Phase III (CH2MHILL & Palestinian Water Authority). Development of Conceptual as well as Steady State models for the Northeastern and Eastern Tip basins.
1996-2005	PHG Database, Development of GIS Database department for the Palestinian Hydrology Group, PHG.

Training Activities

- Lecturer on Applied GIS in Environmental Science and Introduction to GIS, Al Quds University, Abu Dees, Palestine.
- Lecturer on Applied GIS for the Water Environment (AGWA) program, Palestinian Water Training Institute (PWTI), Ramallah, Palestine.
- Lecturer on IWRM course, Birzeit University, Birzeit, Palestine.
- Lecturer on GIS Applications in a training course entitled, "GIS Applications in Municipal Management" organized by Palestinian Hydrology Group, Ramallah, Palestine.
- Lecturer on GIS Applications in a training course entitled, "GIS Applications in Wastewater Management" organized by Birzeit University, Birzeit, Palestine.
- Lecturer on Environmental Information Technology, Water Studies Institute, Birzeit University, Birzeit, Palestine.
- Lecturer on sustainability management of water resources in urban areas in a training course entitled, "Management of Groundwater Wells in the North Governorates of the West Bank" organized by House of Water and Environment, Ramallah, Palestine.

Publications

- Abusaada, M., Sauter M. and Massmann J., 2011, Evaluating the Sustainability of Groundwater Aquifers under Different Management and Climate Scenarios Using WEAP as a Tool, Case Study: The Western Aquifer Basin. 2nd WEAP Regional Conference, Amman, Jordan.
- Abusaada M. 2009. Geographical Information System for Undergraduate Students (Text Book for Birzeit and Al Quds universities)
- Abusadah M., Wishahi S., Rabi A., Ghanam S., and Assi A., 2009, Modeling Water cycle of Marj Sanour Watershed Using WEAP. 1st WEAP Regional Conference, Damascus, Syria.
- Abusaada M., Rabi A., Ghannam S., Tamimi. A., 2009. Impact of the “Do-nothing” Approach at the Gaza Strip – Palestine, GABARDINE Deliverables – D 71.

- Abusaada M., Rabi A., Ghannam S., Tamimi. A., 2009. Economic analysis and feasibility of AR at Gaza-Strip, Palestine, GABARDINE Deliverables – D 72.
- Abusaada M., Rabi A., Ghannam S., Tamimi. A., 2009. Environmental Impacts of suggested AR response strategies, at Gaza-Strip, Palestine, GABARDINE Deliverables – D 73.
- Abusaada M., Rabi A., Ghannam S., Tamimi. A., 2009. Social Considerations Regarding the Use of Brackish Water and Recovered effluent for Agricultural Purposes, GABARDINE Deliverables – D 74.
- Tal A., Abusaada M., Khateeb N. and Assi A. 2007. Watershed Modeling: BioMonitoring and Economic Analysis to Determine Optimal Restoration Strategies for Transboundary Streams. Final Report MERC project -M23-019.
- Abusaada M., Ghannam S. and Aliewi, A., 2007. Evaluation of the suitable measures towards sustainable water resources in Palestine. International Conference: Sustainable Development & Management of Water in Palestine, Amman, Jordan.
- Abusaada, M.J., Aliewi, A.S, and P. E. O'Connell.2006, Assessment of Sustainable Yield of Aquifers Using Groundwater Flow Modeling and Decision Support Systems: Western Aquifer Basin as a Case Study. Second International Conference on Water Resources and Arid Environment,Al Riyadh, Saudi Arabia.
- Parkin G., Abusaada M., Aliewi A. and Kilsby C. 2005, Evaluation of Environmental Sustainability Indicators for Water Resources Management Options in Palestine. Report No. SUSMAQ - SUS #51 V1.1, Sustainable Management of the West Bank and Gaza Aquifers, Palestinian Water Authority (Palestine) and University of Newcastle upon Tyne (UK).
- Aliewi A., Abusaada M., Ghannam S., Yaqubi A., Mimi Z., Jayyousi A. 2005. Assessment of the Supply/Demand Gap and Evaluation of the Sustainable Measures towards Sustainable Water Resources in Palestine. House of Water and Environment (HWE), Palestinian Water Authority (PWA), Birzeit University and An Najah University.
- Aliewi A., Abusaada M. and Jayyousi A. 2004. Sustainable Yield of Palestinian Aquifers. Report No.: SUSMAQ-SUS #70 V 0.1. Sustainable Management for the West Bank and Gaza Aquifers, Palestinian Water Authority (Palestine) and University of Newcastle upon Tyne (UK).
- Aliewi A., Abusaada M., Kalbounh A. And Messerschmid C. 2003. Steady State and Transient Flow Models of the Western Aquifer Basin. Report No.: SUSMAQ-MOD #49 V0.1. Sustainable Management for the West Bank and Gaza Aquifers, Palestinian Water Authority (Palestine) and University of Newcastle upon Tyne (UK).
- Aliewi A., Abusaada M., Kalbounh A. And Messerschmid C. 2003. Steady State Flow Model of the Western Aquifer Basin. Report No.: SUSMAQ-MOD #23 V0.2. Sustainable Management for the West Bank and Gaza Aquifers, Palestinian Water Authority (Palestine) and University of Newcastle upon Tyne (UK).
- Abusaada M., Aliewi A., Kalbounh A. and Messerschmid C. 2003: Monthly Recharge Estimation in Wadi Natuf, Palestine. Proceedings of the Second International Conference on Wadi Hydrology 1-4 July 2003, Amman, Jordan. Local Groundwater Pollution Model for Wadi Zeimar, Palestine.

